BIOREMEDIATION OF SITES CO-CONTAMINATED WITH BENZENE OR TOLUENE AND HEAVY METALS

By

BRICE ALLEN FIDDLER

Bachelor of Science in Civil Engineering

Oklahoma State University

Stillwater, Oklahoma

2014

Submitted to the Faculty of the
Graduate College of the
Oklahoma State University
in partial fulfillment of
the requirements for
the Degree of
MASTER OF SCIENCE
July, 2016

BIOREMEDIATION OF SITES CO-CONTAMINATED

WITH BENZENE OR TOLUENE AND HEAVY

METALS

Thesis Approved:

Mark Krzmarzick

Thesis Adviser

Babu Fathepure

Gregory G. Wilber

ACKNOWLEDGEMENTS

I would like to thank Dr. Mark Krzmarzick and Mr. Xiang Fu. This paper would not be possible without their help and advice. I really appreciate Dr. Krzmarzick always being available to discuss my research. I would definitely be lost without his wisdom. Mr. Fu was always willing to help out with lab work. No matter if I was out of town or was going to be in the lab all day and night, Xiang was willing to help out. Without their support and help, all of this would be impossible and I would like to thank them one more time.

Name: Brice Allen Fiddler

Date of Degree: JULY, 2016

Title of Study: BIOREMEDIATION OF SITES CO-CONTAMINATED WITH BENZENE OR TOLUENE AND HEAVY METALS

Major Field: Environmental Engineering

Abstract: Co-contamination of both organics and heavy metals are a common occurrence in hazardous waste sites. The contaminants enter the environment due to human activity and can leech through the soil, entering groundwater sources used for irrigation and drinking water. This can lead to many health concerns for humans and the ecosystem. These sites are difficult to remediate due to the combined toxic effects heavy metals and the hazardous organics have on the microbes of the soil community. Little is known about the effects toxic heavy metals have on the bioremediation of organics. One solution is to characterize the ability of naturally occurring micro-organisms in the soil that are resistant to the heavy metal toxicity and have the ability to degrade the organic compounds. The study's goal is to identify naturally occurring bacteria in soil that are able to degrade benzene and toluene while in presence of heavy metals. Microcosms were created with a range of two heavy metals (lead and cadmium) and 0.4488 mM of benzene or 0.1888 mM of toluene. Sterile controls were made to ensure only biological activity was the cause of the degradation in the microcosms. The results found that there were naturally occurring bacteria in the soil with the ability to degrade benzene or toluene, and resist heavy metal toxicity. Heavy metal concentrations had little to no effect on the degradation of the benzene and toluene. Toluene was degraded fastest by the microbes, likely due to its methyl group. With this information, further research will be performed to better identify the microbes responsible for the degradation of benzene and toluene in co-contaminated sites. These microbes can potentially be used for the bioremediation of benzene or toluene in water and soils co-contaminated with heavy metals.

TABLE OF CONTENTS

Chapter Page

LIST OF TABLES

Table Page

LIST OF FIGURES

Figure Page

Figure Page

Figure Page

CHAPTER I

INTRODUCTION

Background

Benzene, toluene, ethylbenzene, and xylene, better known as BTEX, are volatile organics that cause many health issues to communities living near contaminated sites. Heavy metals, such as lead and cadmium, affect many microbial physiological systems. This can cause problems when trying to remediate sites contaminated with both benzene or toluene and heavy metals. Research into co-contaminated sites is important for improving public health and advancing remediation efforts. Many bacteria that have the ability to degrade benzene and toluene are also sensitive to heavy metals.

Benzene is one of the most widely produced chemicals in the United States. It is used in the production of other chemicals, rubber, pesticides, dyes, detergents, and it is used as a fuel additive (Boberg et al., 2011; Stams et al., 2010; and Barker et al., 2012). Elevated levels of benzene or toluene and VOCs are typical in industrial areas and places associated with heavy traffic. The increasing use of ethanol for fuel has decreased the amount of benzene and toluene released to the environment due to transportation (Alvarez et al., 2015). Tobacco smoking is a common source of benzene exposure. Auto exhaust and industrial emissions account for about

20% of total nationwide exposure to benzene while 50% of exposure comes from smoking tobacco (Mitra et al., 2011).

Lead and cadmium are some of the most common toxic pollutants in the environment and can be found in high concentrations at many hazardous waste sites. Heavy metal exposure can also come from household items such as paints and linoleum. Children are especially susceptible to the heavy metal toxicity, due to increase likelihood of ingestion and still developing organ systems. General signs of heavy metal toxicity are: gastrointestinal disorders, diarrhea, tremors, paralysis, vomiting and convulsion, depression, and pneumonia (Duruibe et al., 2007). Long term health affects due to heavy metals exposure, and accumulation in the body, include: cancer, cardiovascular, pulmonary, endocrine, reproductive, and immune system problems (Abd-Allah et al., 2013).

Heavy metals can affect many proteins and genes in the body that can leave the population even more susceptible to disease. The mRNA (used to detoxify compounds), certain metabolizing genes, and DNA repair genes were also shown to be affected by heavy metals (Abd-Allah et al., 2013). Cadmium specifically causes kidney, bone, and lung complications. Lead has been shown to cause blood, kidney, joint, reproductive, heart, gastrointestinal, urinary, and nervous system damage. These effects are due to interference with the body's metabolic processes. Once inside the body they are oxidized and form stable toxic compounds disrupting protein and enzyme functions (Duruibe et al., 2007). These health concerns can occur even at low contamination concentrations. The reasons Pb and Cd were the heavy metals chosen for the experiment, were that they are toxic at very low concentrations and they are a commonly found pollutant at hazardous waste sites.

Pollutants in surface and ground water sources affect both drinking and recreational water. Contact with both forms of contaminated media can result in benzene, toluene, or heavy metal poisoning. The pollutants can accumulate in the organisms living in the water and organisms drinking the water. The contaminants are then transported through the ecosystem into the food chain. There is little knowledge on the remediation methods of these co-contaminated sites. Many current methods are inefficient, time consuming, and not cost effective. Microbial degradation is a long-term and efficient treatment option because of the reusability of the microbial populations and the environmentally friendly by-products (Escher et al., 2006). The remediation of heavy metals typically focuses on immobilization of the metal, due to their inability to be degraded.

Bacteria are affected by heavy metal contamination, with their populations being typically smaller and less diverse (An et al., 2012). Soil microbes are very important to agriculture as they play an important role for nutrient cycling and soil fertility (Oliveira et al., 2006). When the soil microbes are negatively affected, it negatively affects plant life and eventually human health (An et al., 2012 and Oliveira et al., 2006). Different toxic effects occur to microbial populations at different concentrations of the heavy metals. Higher concentrations of heavy metals can reduce the amount of microbes able to resist the heavy metals toxic effects. The microbial community can be affected by heavy metals due to many different factors including: metal type, concentration, and the various microbes in the affected environment. Microbial communities also will react differently to co-contaminated sites, with heavy metals and organics, than they react to a single type of contamination (An et al., 2012).

Discovery of new bacteria and/or new biological treatment methods for sites contaminated with both organics and heavy metals is critical to finally cleaning up many of co-contaminated sites. Many micro-organisms, such as the symbiotic bacteria *Rhizobium*, are sensitive to heavy metal concentrations as low as 3 (mg Cd)/(kg soil) (Giller et al., 2009). This causes a severe reduction in microbial activity (Arjoon et al., 2015 and Alisi et al., 2012). The metal/organic complexion can also reduce the bio-availability of the organics, making the organics less available to the microbes for degradation (Arjoon et al., 2015). Soil microbes and enzymes activity can be negatively affected by heavy metal concentrations in the soil. The lack of dehydrogenase enzyme activity is an indicator of the effect heavy metal toxicity has on microorganism activity (Oliveira et al., 2006).

There have been many different types of bacteria that have shown the ability to degrade benzene and toluene. The micro-organisms use the organic compounds for their carbon and energy source, removing the contaminant from the system (Hendrickx et al., 2006 and Haquea et al., 2012). Degradation can occur down two different pathways: either activation of the aromatic ring or by processing the side chains (Lin et al., 2010). Anaerobic bacteria cannot use pathways with mono- or dioxygenases, they instead must use nitrate or sulfate as their electron acceptor (Stams et al., 2010 and Barker et al., 2012). In aerobic conditions, oxygen can be the terminal electron acceptor of aromatic compound degradation (Stams et al., 2010).

The remediation of benzene and toluene can be enhanced through the addition of microorganisms and/or by adding nutrients, Bio-augmentation and biostimulation respectively (Kasi et al., 2013). Adding other organic compounds can improve hydrocarbon degradation by sulfate reducing bacteria (Stasik et al., 2015). The compounds can also be degraded under

methanogenic conditions and through respiration. To enhance degradation, multiple electron acceptors can be added to the system to increase microbial diversity; a single electron accepter may not improve degradation greatly (Stasik et al., 2015). In groundwater, sulfate and nitrate are the most common electron acceptor for microbial degradation. Benzene and toluene in most cases can be the sole carbon and energy source for these microbes. Benzene and toluene typically degrades linearly based on initial concentration of the pollutant (Stasik et al., 2015 and Kasi et al., 2013). This linear pattern of degradation is not affected by depth of soil. High benzene and toluene concentrations are toxic to microbial communities, this can inhibit degradation rates. Anaerobic bioremediation of these compounds have a low operating cost and have environmentally friendly by-products.

Bacteria shown to degrade benzene and toluene belong to the phyla *Actinobacteria*, *Proteobacteria*, and the genus *Pseudomonas*, which can use benzene as its only carbon source in aerobic conditions (Hendrickx et al., 2006; Haquea et al., 2012; and Stams et al., 2010). Benzene degradation was the most common BTEX degradation trait among bacteria and was related to tmoA-like genotype (Hendrickx et al., 2006). However, only a few anaerobic species have been observed to degrade benzene, including *Dechloromonas* and *Azoarcus* strains (Stams et al., 2010). The bacteria with these traits would most likely be found in a in a pre-existing co-contaminated soil.

Bacteria native to contaminated soils will have adapted to the toxic conditions of the soil (Giller et al., 2009). These naturally occurring bacteria would also have an advantage over inoculates due to physicochemical pollutant characteristics, microbial ecology, and methodology of inoculation (Alisi et al., 2012).

Regulations and maximum permissible limits have been established by various organizations, including the World Health Organization (WHO) and the EPA(EPA), in order to prevent toxic levels of benzene, toluene, and heavy metals from entering the environment. Discovery of micro-organisms with the ability to degrade benzene and toluene while under the influence of heavy metals is vital to the remediation of co-contaminated hazardous waste sites.

CHAPTER II

REVIEW OF LITERATURE

Environmental Problem

Many hazardous waste sites are heterogeneous in that there are diverse contaminants (Escher et al., 2006). Contaminant mixtures such as lead (Pb) or cadmium (Cd), and benzene, toluene, ethylbenzene, and/or xylene (BTEX) are common pollutant combinations at these sites. Benzene, toluene, and heavy metals are very stable in their environment and can pollute a system for many years. These contaminations are often the result of spills, leaks, and mishandling of the waste (Gidarakos et al., 2015). Landfills are also a major source of benzene, toluene, and heavy metals into the environment (Klimiuk et al., 2008). Leachate, from the landfills, seeps through soil and into groundwater. Heavy metals, benzene, and toluene are mobile pollutants; they travel through different media and over long distances if not properly contained. Heavy metals can quickly travel through the leachate; this is due to a low pH raising the metals solubility. At high enough concentrations, these pollutants can be hazardous to the surface and groundwater microbial communities and the organisms that come in contact with the contaminated media. These pollutants accumulate in the tissues of organisms and can travel through the food chain, affecting multiple species.

Benzene, toluene, and heavy metal toxicity can be a severe human health hazard. The toxic effects of these pollutants are very serious and can cause neurological damage and cancer. The EPA's Integrated Risk Information System (IRIS) states that benzene is a human carcinogen, can cause genetic changes, and can cause proliferation of bone marrow cells (Miller et al., 2016). Toluene health effects are irritation of the respiratory system and eyes and central nervous system damage due to exposure. These compounds are also shown to effect the growth of the fetus in pregnant women. Exposure to these compounds can occur through numerous pathways such as skin contact, inhalation, and ingestion.

Heavy metals are another set of toxic pollutants that can travel great distances from their sources. Heavy metals can contaminate the air (through dust particles), soil, and water. These complex contaminations can lead to severe consequences to the environment and public health. Heavy metal toxicity can lead to reduced microbial growth in soil, disruption of metabolic activity in microbes, cancer in humans, and organ system problems.

Benzene and toluene are naturally occurring chemicals found in petroleum products. These compound account for 90% of the water soluble compounds in petroleum (Mitra et al., 2011). A major source of benzene and toluene contamination is the leaking of underground storage tanks used for petroleum (Conley et al., 2011 and Stams et al., 2010). These leaks are the result of corrosion, cracks, and spills while refilling the tank (Guignet, 2014). Leaks from these tanks can seep into the soil and into groundwater. From the groundwater the benzene and toluene can travel to other bodies of water such as surface and groundwater, irrigation water, and even drinking water. This can be devastating to local environments and human populations. Benzene and toluene from these sources typical come in contact with humans through inhalation of vapors or ingestion of contaminated water (Guignet, 2014 and Mitra et al., 2011).

Problems occur in the remediation of organics in water systems such as aquifers; specifically the contaminants benzene and toluene, which are difficult to degrade due to their large negative resonance energy (the stability of the compound) (Stams et al., 2010). This difficulty is compounded by the oftentimes high concentrations of heavy metals in water and soil. The biodegradation of organics, such as benzene or toluene, have been well studied aerobically and anaerobically; reports show heavy metals having adverse effects to the biodegradation of these chemicals (Hong et al., 2007). Most research however, is performed on a single contaminant which rarely occurs in actual field cases (Haquea et al., 2012).

Around 40% of hazardous waste sites are co-contaminated with both heavy metals and organic compounds (Dang et al., 2009 and Arjoon et al., 2015). This co-mingling of organics and heavy metals makes treatment options for these sites difficult for the micro-organisms degrading the organics because of the toxic effects of the heavy metals (Arjoon et al., 2015). The impact the metals have on the biodegradation of organic pollutants is not only due to the metal concentrations and type, but also the type organic pollutants (Dang et al., 2009 and Hong et al., 2007). Different types of heavy metals at various concentrations affect the soil micro-organisms differently and must be tested independently (Arjoon et al., 2015and Giller et al., 2009). The increased concentration of heavy metals reduces the chance of microbial resistance to the metals' toxic effects.

Benzene, Toluene, and Heavy Metal Information

Benzene and Toluene Information

Benzene and toluene are volatile organic compounds (VOCs) retrieved during fossil fuel extraction that are used globally as solvents in many manufacturing and refining processes (Bolden et al., 2015; Berry et al., 2006; and Stams et al., 2010). Benzene and toluene are some of the most common and hazardous industrial VOC emissions (Haquea et al., 2012; Lin et al., 2010; and Stams et al., 2010). These compounds cause public health and ecological issues due to their toxicity and ability to bio-accumulate in the food chain. Benzene and toluene are also soluble and can seep through soil and enter groundwater.

Accidental spills of oil and gasoline is a major source of benzene and toluene contamination in the environment. This is due to benzene and toluene being highly mobile in the soil (Boberg et al., 2011; Bae et al., 2014; Stams et al., 2010; and Berry et al., 2006). Even at low concentrations, both benzene and toluene can be very toxic and are difficult to remediate in complex mixtures. Benzene and toluene are environmental priority pollutants that the EPA regulates. All BTEX compounds are volatile mono-aromatic hydrocarbons (Figure 1) that make up around 18% of petroleum products by weight (Berry et al., 2006).

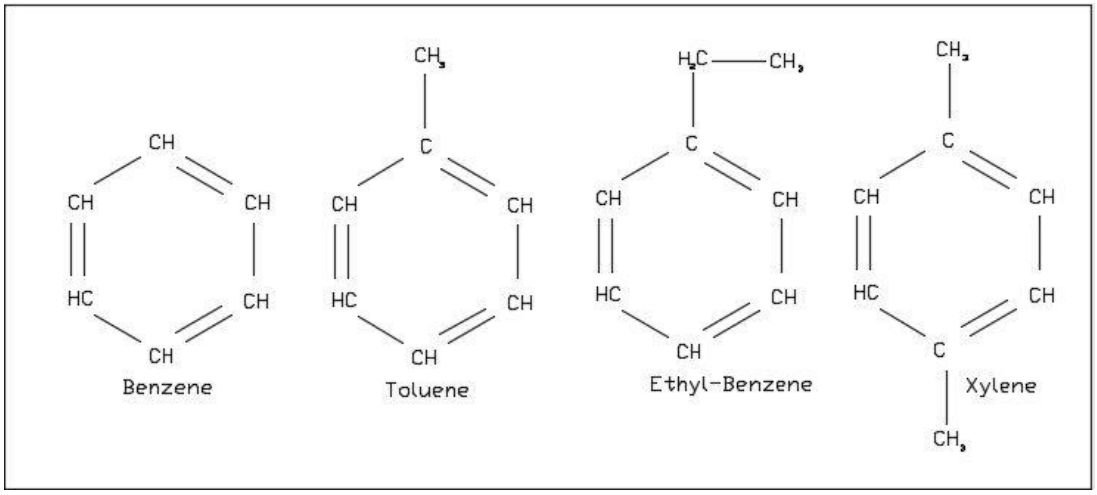

Figure 1: BTEX compound are four volatile organic compounds (VOCs) that are found in petroleum and petroleum products. These hydrocarbons contain a central benzene that makes the compounds very strong and difficult to degrade. Toluene is the easiest of the compounds to degrade and benzene is the most difficult to degrade.

Benzene has been known as a human carcinogen and been linked to leukemia, especially in children (Bulsara et al., 2007). Continuous exposure to toluene is associated with nervous system, liver, and kidney damage (Guignet, 2014 and Mitra et al., 2011). There are many occupations that have an increased chance of exposure to benzene and toluene; examples are the petroleum and motor vehicle industry. Many household products emit benzene and toluene such as paints, varnish, rubber cements, adhesives, and degreasing agents (Bulsara et al., 2007).

Bioremediation is an environmentally friendly solution to remove benzene and toluene from both soil and groundwater. In this process, microbes degrade organics to CO_2 and water. Bioremediation of benzene and toluene can take place in both aerobic and anaerobic environments. Many different types of microbes can perform bioremediation such as bacteria and fungi. Fungi, while able to survive in harsher environments, were shown to be unable to degrade benzene and toluene when the compounds were the sole carbon source (Mitra et al., 2011).

Benzene and Toluene Effects on Humans

Benzene and toluene cause nervous system damage, endocrine system damage, and can also cause birth defects when contact with the contaminant occurs (Bolden et al., 2015). Benzene and toluene can enter the body though inhalation, ingestion, and dermal contact (Conley et al., 2011). Benzene is a known human carcinogen and can cause brain, heart, lung, and liver damage (Conley et al., 2011; Stams et al., 2010; and Barker et al., 2012). Benzene and toluene can spread to the groundwater, affecting irrigation and drinking water if not properly controlled (Barker et al., 2012 and Gidarakos et al., 2015). The majority of contaminated sites with benzene or toluene and heavy metals are located on industrial areas and the populations that live near them are now typically small. Communities living near superfund sites have experienced higher levels of these contaminants in drinking water and soil.

Heavy Metal Information

Heavy metals are typical contaminants found at hazardous waste sites. Heavy metals cannot be degraded and must be remove by another remediation method, such as phytoremediation. Lead and cadmium are some of the most common heavy metal contaminants at hazardous sites (Dang et al., 2009 and Hong et al., 2007). Cadmium is the second most common metal found at EPA Superfund sites and is a high-priority pollutant (Dang et al., 2009).

Microbes have developed a few metabolic mechanisms in order to avoid the toxic effects of heavy metals. One method is to convert the ion to a less toxic form. Then the metal is sent to the periplasm, near the outer edge of the cell, and reduced to a lower oxidation state in order to lower solubility. Finally, the ion is expelled from the cell (Barua et al., 2010). The genes that enable this are plasmid-borne and are easily transferred between different bacteria. Heavy metals can be devastating to a microbial community resulting in lack of diversity in microbial life.

Heavy Metal Effects on Humans

Heavy metals are high density metallic elements that are toxic at low concentrations (Duruibe et al., 2007). Most of the toxic effects on organisms affect growth and development. Some heavy metals are important for biological activity but many, such as lead and cadmium, have no biological role, are toxic to humans at low concentrations, and cause great health concerns (Duruibe et al., 2007 and Begonia et al., 2008). A typical symptom of heavy metal toxicity is severe nervous system problems (Junjib et al., 2006). The toxicity of the heavy metals depends on factors such as concentration and oxidation state. Oxidation state is important to the solubility of the heavy metal.

Heavy metal contamination can come from many human sources such as foundries, manufacturing, and mining sites. The major sources are industrial sources and traffic (Junjib et al., 2006). Dust is a common vector for heavy metals to come into contact with human

populations. During mining processes, heavy metals in soil and rock can be eroded and picked up by wind in the form of dust. Lead is the third most common heavy metal found in urban dust (Junjib et al., 2006). Dust can dramatically affect human health through inhalation. If contaminated soils or waters are used for agriculture, the metals can be taken up and accumulate in crops and livestock. The contaminant is then passed onto humans through the food chain.

Important issues concerning heavy metals in the environment are sources, leaching, and modes of deposition (Duruibe et al., 2007). Though heavy metals sources can be both natural and man-made, the major sources are due to human activity. Cadmium is a by-product of zinc and lead refinement, while lead is emitted from mining activities and fuel combustion in automobiles. The contamination of these pollutants can last hundreds of years after their initial deposition (Duruibe et al., 2007). The metals then leach through the groundwater and into aquifers. Surface runoff is another transportation method for the pollutants.

Microbial Effect

Both lead and cadmium can disrupt the metabolic activity of microbes at low concentrations. Lead and cadmium are found in the environment typically as a result of mining waste, industrial wastewater discharges, and fly ash (Chen et al., 2010; Drake et al., 2009; Kang et al., 2007; Agency for Toxic Substances and Disease Registry, 2007; and Agency for Toxic Substances and Disease Registry, 2008). The waste disposal sites of these industries can seep through the soil and into the groundwater causing contamination of both surface and groundwater (Chen et al., 2010; Drake et al., 2009; Chen et al., 2008; and Kang et al., 2007). This mobility is influenced by pH and organic content; a low pH and a low organic content increase the mobility of these heavy metals (Agency for Toxic Substances and Disease Registry, 2008 and Oliveira et al., 2006). The amount of heavy metals released into the environment increases due to industrial activities and technological development (Arjoon et al., 2015).

Lead is one of the most commonly found heavy metals in soil. Lead has no biological role and is hazardous to the environment. It has been shown that microbial diversity changes even with small changes in heavy metal concentration, from 0 to 2000 ppm of lead (Begonia et al., 2008). Lead can cause microbes to reduce biomass, have impaired respiration, have reduced activities, and can alter the microbial community in the soil (Chen et al., 2007; Oliveira et al., 2006; and Duarte et al., 2016). Cadmium is one of the most hazardous heavy metals. The bacteria strain *Pseudomonas* has shown resistance to cadmium. Ways the bacteria resist heavy metal toxicity are binding the metal to the cell wall, extracellular polymers, and causing the metal to become less soluble.

Microorganisms can change and adapt to higher concentrations of heavy metals by becoming more resistant to the pollutant (Begonia et al., 2008). Over time, heavy metals become less soluble in soils. This can reduce the chance of contact with the human population but does

not affect the toxicity of the metal to the microbial community in the soil. Inoculation of specific bacteria into a soil can reduce heavy metal toxicity in plants. The microbes immobilize the metals reducing plant uptake. Heavy metals from a single source can remain in an environment for hundreds of years, resulting in long term damage to the environment and local public health. Small changes in heavy metal concentrations can have drastic effects on the microbial community. Two common ways microbes have adapted to survive in a heavy metal contaminated environment are a trans membrane metal pump (that removes the metal from inside the cell before it damages any organelles) and an enzyme that is resistant to metals (predominantly found in denitrifying bacteria) (Begonia et al., 2008).

A group of decomposers that is negatively affected by heavy metal toxicity is the fungi group *Hyphomycetes* (Duarte et al., 2016). The toxic effects include impaired reproductive activity and reduced growth. Some *Hyphomycete* do tolerate the heavy metals by producing a metal binding protein (Duarte et al., 2016). Contaminated communities are less diverse due to the toxic effects of the heavy metals. Many contaminated sites are not just dealing with one problem; mine drainage not only has toxic heavy metals but also has a lower pH (Duarte et al., 2016). Lower pH negatively impacts degrading enzymes and increases solubility of heavy metals. Certain strains of rhizosphere bacteria, such as the genus *Methylobacterium*, have been shown to be highly resistant to heavy metals (Madhaiyan et al., 2007). This resistance is the result of binding the metals to the microbe's cell wall (removing the metal from the cells vital areas), extracellular polymers, or making the metal insoluble by changing the oxidation state.

Benzene and toluene can also become inhibitory compounds if the concentration becomes too high, around 20–80 mg/L (Lin et al., 2010). These effects pose a problem for remediation projects that contain both organic compound and heavy metals. The diversity of the environment, difficulty to degrade, and higher heavy metal concentrations inhibit the growth and degradation rate of the microbes in the co-contaminated sites (Hong et al., 2007 and Arjoon et al.,

2015). At low enough concentrations, microbes both aerobically and anaerobically can degrade benzene and toluene as their carbon source: *Desulfosporosinus sp., Syntrophaceae, Desulfovibrionales* and some strains of *Chloroflexi* are all examples of anaerobic toluene degraders. The conditions observed for the naturally occurring microorganisms in the study are a fully saturated soil, co-contaminated with both benzene or toluene and heavy metals (Pb and Cd), at 30 ºC.

Aerobic & Anaerobic Degradation

Remediation

The remediation of co-contaminated sites is difficult due to the toxic effect the heavy metals have on the microbial community. Bioremediation is the most widely used remediation technique and is an effective way to remove harmful organics from contaminated sites due to the ability to restore the soil and preserves its quality (Hong et al., 2007; Alisi et al., 2012; and Lin et al., 2010). Bioremediation is reliable, simple, and cost effective when compare to other forms of remediation (Haquea et al., 2012 and Lin et al., 2010). Common forms of bioremediation include phytoremediation, bio-stimulation, and bio-augmentation.

Benzene and toluene typically enter the environment through spills and leaks of petroleum products. These compounds have a high solubility in water and can migrate to groundwater quite easily. Benzene and toluene can pollute soils and drinking water far away from the initial source due to this high mobility. These compounds are a serious public health concern, leading to neurological damage and hematological effects (Dou et al., 2008). There are many different paths to remove benzene and toluene from the environment, such as physical, chemical, and biological methods. Of these methods, biological is the most efficient. Microbes can degrade and use benzene and toluene as a carbon source in both aerobic and anaerobic conditions. Aerobic conditions make it much easier for bacteria to degrade the organics. Aerobic degradation uses oxygen as the terminal electron acceptor and produce high amounts of energy. Oxygen is the most effective electron acceptor due to its high electronegativity. Many benzene and toluene contaminated sites are anaerobic however. Anaerobic degradation typically uses sulfate or nitrate as the terminal electron acceptor and produce low amounts of energy. Benzene and toluene have been known to be biodegraded in anaerobic conditions; however, the process is

very slow compared to aerobic biodegradation. High biochemical oxygen demand from fuel causes aquifers to develop anaerobic conditions.

Bio-augmentation is adding specific microbes to improve biodegradation by increasing the degrading population's numbers and diversity. Bio-augmentation can be an effective remediation strategy for anaerobic benzene and toluene contaminated sites. Microbes transferred are typically nitrate-reducing bacteria that oxidize the toxic organics to CO_2 (Dou et al., 2008). These bacteria have the ability to completely degrade benzene and toluene. Toluene is one of the easiest BTEX compounds to degrade due to its methyl group, while benzene is one of the more difficult BTEX compounds to degrade (Dou et al., 2008). Naturally occurring bacteria in the soil can enhance the degradation process of the bio augmented microbes.

Bio-stimulation modifies the environment to promote the growth of specific microorganisms in a system. The modifications are typically the addition of nutrient limiting factors to increase microbial population. Different compounds and nutrients are added to the system to improve the growth of native bacteria and promote the degradation of benzene or toluene. In bio-stimulation, compounds can be introduced to stimulate microbial growth or change the conditions of the environment.

Phytoremediation, the uptake of pollutants by plants, is another remediation option for removing benzene and toluene from the environment (Burken et al., 2009). At a typical hazardous waste site however, the microbes in the aerobic rhizosphere degrade more VOCs than the plants take up. Phytoremediation has been shown to aid bioremediation of benzene and toluene by moving contaminants to a more microbial active area of the soil and by providing oxygen to the soil. There can be hundreds of different species of microbes capable of degrading benzene and toluene in the plant's rhizosphere alone. The microbes responsible for the biodegradation of benzene and toluene in the rhizosphere are denitrifiers, *Pseudomonads*, and

mono-aromatic hydrocarbon degraders (Burken et al., 2009). It is common to find benzene and toluene degraders in soils, no matter the contamination history. Oxygen is the limiting factor in most soil aerobic biodegradations of benzene and toluene, other factors include water content, temperature, pH, nutrients, and salinity (Burken et al., 2009).

Aerobic and anaerobic remediation applications must be investigated because benzene and toluene can contaminate surface water and then leech into the ground water, an anoxic environment (Hendrickx et al., 2006). There are many different electron acceptors microbes can use during metabolism of organic compounds; because of this, it has been shown that benzene and toluene can be remediated in anaerobic and aerobic conditions (Fowler et al., 2014 and Barker et al., 2012). Both conditions must be studied because differences exist between benzene and toluene degradation under aerobic and anaerobic conditions (Figure 2 and Figure 3) (Stams et al., 2010). Aerobic biodegradation is a faster process that requires oxygen as the electron acceptor and releases more energy throughout the oxidation process. Anaerobic degradation however is a longer process, in the absence of oxygen, uses SO_4^{2-}, NO_3^-, or CO_3^{2-} as the electron acceptor, and releases less energy through oxidation. Both processes have no toxic by-products (Gidarakos et al., 2015).

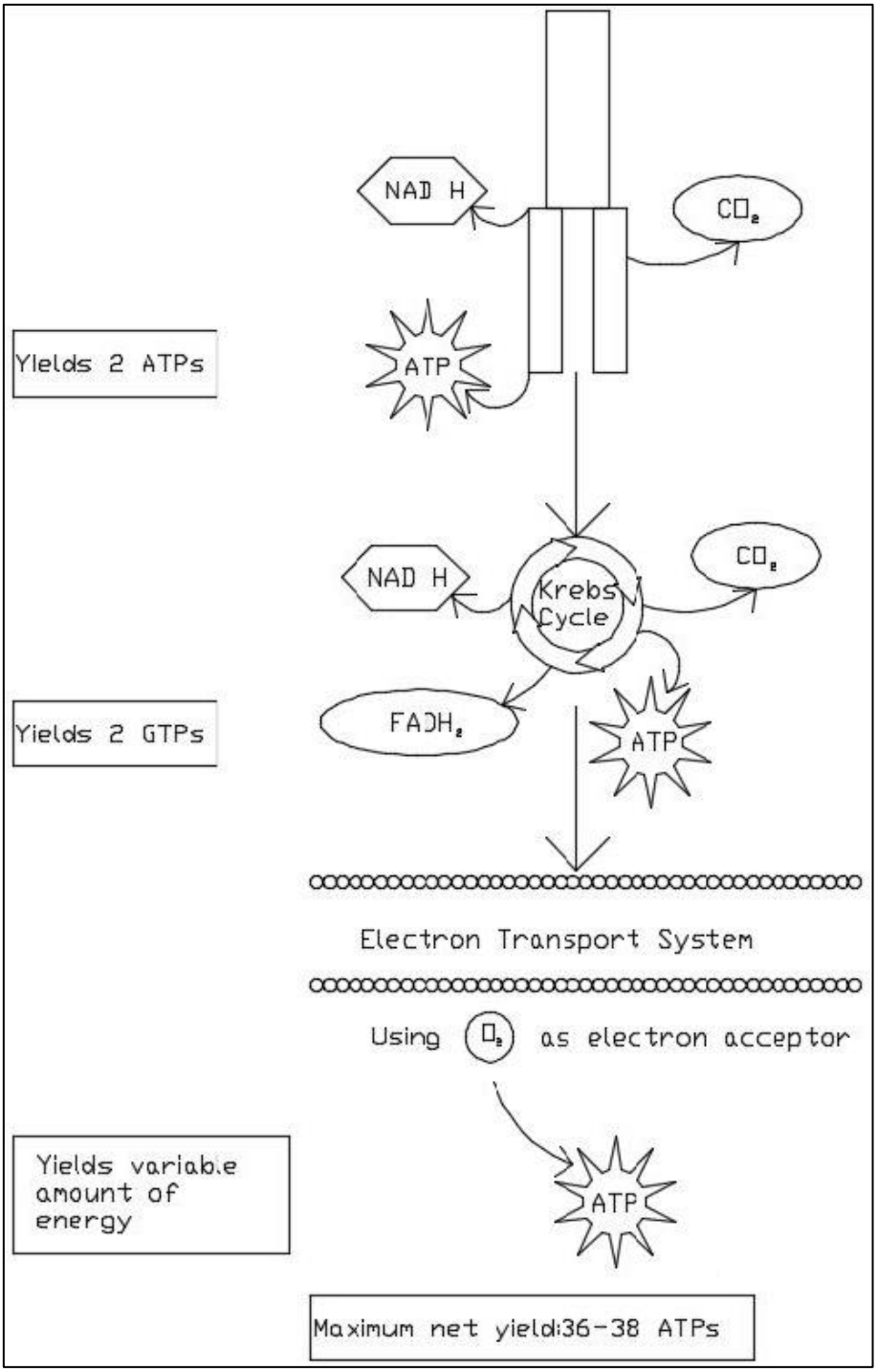

Figure 2: The aerobic pathway is the process that the microbes use to obtain energy and nutrients in the presence of oxygen. This process uses oxygen as a terminal electron acceptor. Oxygen is the most effective electron acceptor due to its high electronegativity. The pathway yields high energy and is a very efficient process to obtain energy.

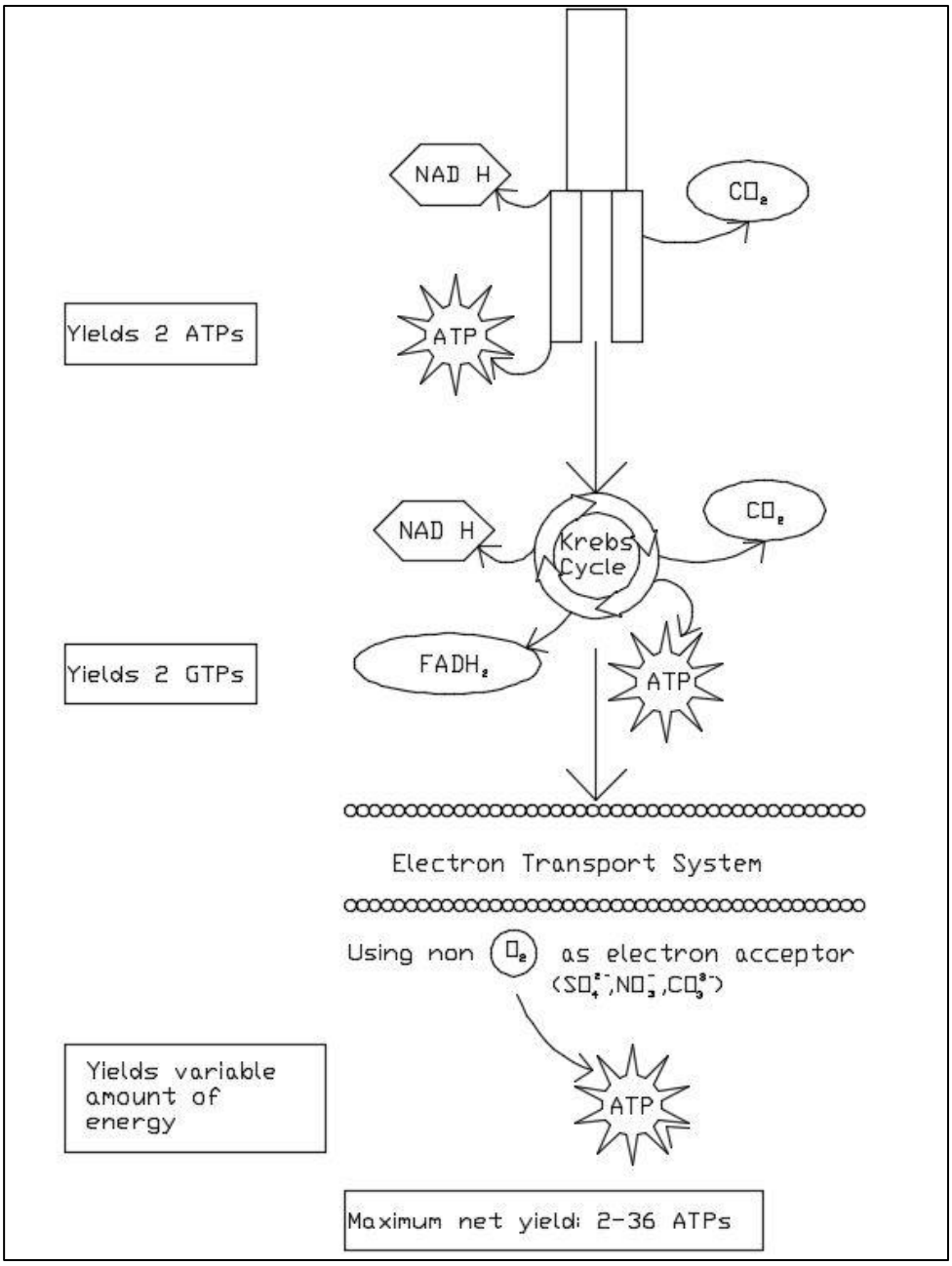

Figure 3: The anaerobic pathway is the process that the microbes use to obtain energy and nutrients in the absence of oxygen. This process uses sulfate and nitrate as a terminal electron acceptor. The pathway yields less energy than the aerobic process and takes more time to break down carbon sources.

Factors affecting bioremediation are related to microbial distribution and growth conditions: such as relationships among the contaminants, environmental factors, and the microbial communities (Lin et al., 2010). For optimum biodegradation, certain conditions must be met. It has been shown in benzene and toluene biodegradation that the best degradation results came at a pH range of 7.5-8 for bacteria, 6 for fungi, and a temperature range of 20-30ºC (Haquea et al., 2012).

Aerobic Degradation

Fossil fuel leaks and spills are a major source of benzene and toluene contamination to the environment. Both aerobic and anaerobic microbes possessing the genes capable of degrading benzene and toluene can be found naturally occurring in soils and aquifers (Alvarez et al., 2015). Major factors effecting biodegradation are dissolved oxygen and pH, while toxicity from waste and temperature of the medium are minor factors (Alvarez et al., 2015).

The degradation of benzene and toluene is an important area of interest for many waste treatment systems. Aerobic bacteria have been shown to degrade benzene and toluene, examples are *Achromobacter xylosoxidans Y234* (Daugulis et al., 2006). These bacteria have been used in bio scrubbers to remove VOCs from wastewater and gas. For many aerobic bacteria, oxygen can be a limiting factor for aerobic bio-degradation. The catechol 2,3-dioxygenase genes are present in microbes able to aerobically degrade aromatic compounds, including benzene and toluene (Alfreider et al., 2007).

Anaerobic Degradation

Benzene and toluene are hazardous compounds that are very volatile, soluble in water, and are carcinogens. The major contamination sources of benzene and toluene in soil and groundwater are underground storage leaks or accidental spills of petroleum products (Kasi et al., 2013 and Alfreider et al., 2007). Benzene and toluene are highly mobile and can contaminate

mediums, such as groundwater, over great distances (Kasi et al., 2013). Bio-remediation is the most efficient way to treat contaminated anaerobic groundwater (Deng et al., 2008). However, anaerobic degradation takes more time than the aerobic process (Deng et al., 2008).

Benzene and toluene are toxic and are resistant to bio-degradation. Benzene and toluene are very stable due to their ring structure. Benzene is the most difficult BTEX compound to degrade due to its stability (Stams et al., 2010; Deng et al., 2008; and Kasi et al., 2013). The reason for this is the benzene's structure is more stable, requiring higher activation energy to break the ring. In a co-contaminated environment, microbes will typically break down the other BTEX compounds first. Toluene is the easier BTEX compound to degrade anaerobically due to its methyl group. Anaerobic biodegradation does have some issues; volatile fatty acids (produced during fermentation of organics) can inhibit benzene and toluene bioremediation.

Many bacteria species with the capability to degrade one BTEX compound can degrade all of the BTEX compounds (Kasi et al., 2013). The common electron-accepting physiologies to bio-degrade benzene and toluene anaerobically are de-nitrification, iron reduction, and sulfate reduction (Kasi et al., 2013). Benzene is then broken down three pathways: hydroxylation (producing phenol), methylation (producing toluene), or carboxylation (producing benzoate) (Kasi et al., 2013) that can then be more easily metabolized.

There are a few bacteria strains able to degrade benzene under denitrifying conditions, such as *Dechloromonas aromatica* RCB, *Dechloromonas* sp. JJ, *Azoarcus* sp. DN11: toluene is degraded in denitrifying conditions by *Thauera aromatica* strain K172 (Kasi et al., 2013). Co-contaminated BTEX sites can be an issue for anaerobic bacteria degrading benzene (Kasi et al., 2013). This is due to the microbes degrading the other BTEX compounds first, taking longer to begin degrading the benzene. Some bacteria commonly found to be aromatic degraders in anaerobic benzene contaminated sites are of the phylum *Proteobacteria* and *Firmicutes* and the

genus *Geobacter* (Alfreider et al., 2007). In groundwater, sulfate and nitrate are the most common electron acceptor for microbial degradation. Benzene and toluene in most cases can be the sole carbon and energy source for these microbes.

Identifying Micro-organisms

There are numerous methods for identifying the micro-organisms that can be used for the remediation of co-contaminated sites. Some micro-organisms have already shown the ability to degrade benzene and toluene. These bacteria contain specific genes that allow the degradation of the organics. The genes shown to aid in the degradation of benzene and toluene have been the tmoA-like gene and the xylM gene (Hendrickx et al., 2006). Gene sequences are typically identified using the PCR gel electrophoresis method (Alisi et al., 2012 and Lin et al., 2010).

Using RT-qPCR and RNA stable isotope probing, to help identify and quantify the bacteria community, researchers have found many bacteria associated with toluene degradation including: in aerobic conditions *Desulfosporosinus sp*, species belonging to the *Azoarcus* or *Thauera* genus, and in anaerobic conditions *Syntrophaceae*, *Desulfovibrionales* and *Chloroflexi* (Fowler et al., 2014 and Stams et al., 2010). Sulfate-reducing bacteria and *Geobacter* spp. have been shown to be benzene and toluene degraders in the absence of sulfate. The anaerobic pathway to toluene catabolism is the addition of toluene to the double bond of fumarate. The compound is eventually oxidized via reductive ring cleavage to carbon dioxide (Stams et al., 2010). Methanogenic toluene degrading bacteria, such as *Firmicutes, Chloroflexi, Spirochaetes,* and *Deltaproteobacteria*, have been shown to mineralize toluene to methane (Fowler et al., 2014).

It has been reported that the addition of some metals at low levels increase biodegradation and microbial activity because they are required for certain physiological processes (Dang et al., 2009; Hong et al., 2007; and Arjoon et al., 2015). There are types of

bacteria that exhibit resistance to heavy metal toxicity such as *Sphingmonas wittichii* RW1 (Hong et al., 2007). The growth and population of these microbes are unaffected by the contamination of heavy metals, such as lead. The discovery of a micro-organisms that are resistant to heavy metal toxicity can potentially be used to bio-remediate benzene- and toluene-contaminated soils and water sources.

Unknowns

The research project is trying to answer if there are microbes that are able to biodegrade benzene or toluene in the presence of heavy metals. By discovering the identities of these microbes, engineers would be able to inoculate treatment processes with these bacteria in order to remove the benzene and toluene efficiently without any dangerous byproducts. The degradation rate of these benzene and toluene degrading bacteria is an important detail to find. The degradation rate would provide a time frame for remediation projects based on how long the contaminated medium needs to be treated in specific units. The tolerance of these microbes to lead and cadmium are important to learn as well. The information would be used to determine what site (based on lead and cadmium concentration) would be able to be remediated with the microbes. The lag time is also very important to microbial degradation research. Finding the different effects heavy metals have on how quickly the microbial community starts to biodegrade benzene and toluene is a key component in bioremediation. All of these unknowns are essential in providing a bio-remediation solution to co-contaminated hazardous waste sites.

Summary

Hazardous waste sites co-contaminated with benzene or toluene and heavy metals are a severe public health and environmental issue. These compounds stay in the environment for long periods of time and are very mobile. Benzene or toluene and heavy metals can affect soil, surface water, and ground water. These compounds have negative effects on the microbial communities of their medium and can cause serious medical issues in higher level organisms. The microbial community's population can be less diverse and microbial activity is reduced are typical results of heavy metal toxicity. These effects are due to lead and cadmium serving no biological role and their affect metabolic activity. These pollutants can accumulate in biological tissues and can be passed on to other organisms through the food chain. Benzene, toluene, and heavy metals can enter the body through inhalation and ingestion.

Some microbes can develop resistance to heavy metal toxicity. These microbes would be essential to remediation efforts at co-contaminated sites. Bioremediation is an efficient and environmentally safe remediation process to remove benzene and toluene from co-contaminated sites. Microbes, both aerobic and anaerobic, can use benzene and toluene as a carbon source. There are many types of remediation; bioremediation is one of the most efficient and environmentally conscious methods of removing pollutants from hazardous waste sites. The aerobic process is much faster than the anaerobic process due to effectiveness of oxygen as an electron acceptor. Toluene is also the easier BTEX compound to degrade (because of its methyl group) and benzene is the more difficult BTEX compound to bio-degrade. The genes shown to allow microbes to degrade of benzene and toluene are the tmoA-like gene and the xylM gene. This research's goal is to identify the microbes able to biodegrade benzene and toluene in co-contaminated sites, typical degradation process values (such as degradation rate and lag time), and the effects heavy metals have on the degradation process.

CHAPTER III

METHODOLOGY

Microcosms

Soil samples were collected from a parking lot runoff catch basin in Stillwater, Oklahoma. The microbes in the soil would hypothetically be adjusted to benzene and toluene from the storm water running off the parking lot. Around 1 L of soil was collected for both aerobic and anaerobic tests. The aerobic soil was taking from the top soil and stored in a Norlake Scientific incubator (Figure 95) at 30 ºC, while the anaerobic soil was taken from a depth of 0.5 ft in water-saturated soil. It was assumed that the majority of soil voids would be saturated with water and contain lower redox values. The anaerobic soil was then sealed with tin foil to preserve moisture content and transported to an anaerobic glove box upon arrival in the laboratory.

Mineral media was then made in order for the microbes to receive proper nutrients. There were two types of mineral media created, one set for aerobic microbes (Table 1) and one for anaerobic microbes (Table 2). Both media contain trace elements required by organisms for growth (Table 3 and Table 4). The trace elements addition for the anaerobic media was added in the Coy Laboratories anaerobic glove box (Figure 96). The mineral media was created in 1 L and 2 L flasks. The aerobic media's pH was then adjusted, using a 1 M solution of the base, sodium hydroxide (NaOH), and 1 M solution of the acid, phosphoric acid (H_2PO_3). The aerobic media's pH was adjusted before autoclaving in a Primus Sterilizer Co. Inc. autoclave (Figure 97). The

autoclave sterilizes media by raising the temperature to high temperatures (to kill microbes) and pressures (to prevent volatilization). The temperature the autoclave raises the chamber to be is 250 ºF and the pressure is raised to 18 psig. After autoclaving, the anaerobic media's pH was then adjusted using 1 M NaOH and 1 M H_2PO_3 in the glove box.

The mineral media was then divided into 160 mL silanized serum bottles, at 100 mL per bottle. The salinization processed was perform by placing 3 mL of 10% dichlorodimethylsilane ($Si(CH_3)_2Cl_2$) with toluene as a solvent for one hour in a fume hood. The bottles were then rinsed in hexane, methanol, and water. The $Si(CH_3)_2Cl_2$ forms a covalent bond between the glass in order to prevent compound adsorption to the glass. There were 92 bottles used for the initial aerobic tests (54 standard microcosms and 38 sterile controls) and 54 bottles for the anaerobic tests (42 standard microcosm and 12 sterile controls, Figure 98).

Table 1: The aerobic mineral media recipe is formulated to provide necessary elements and a buffer to sustain biological life.

Aerobic Mineral Media		
Compound Name	Chemical Symbol	Concentration
Sodium Chloride	NaCl	1,000 mg/L
Magnesium Chloride Hexahydrate	$MgCl_2*6H_2O$	500 mg/L
Potassium Phosphate	KH_2PO_4	200 mg/L
Ammonium Chloride	NH_4Cl	300 mg/L
Potassium Chloride	KCl	300 mg/L
Calcium Chloride	$CaCl_2$	15 mg/L
Trace Elements A	-	1 mL/L
Trace Elements B	-	1 mL/L
Yeast Extract	-	100 mg/L

Table 2: The anaerobic mineral media contains many different limiting minerals to support high microbial physiology.

Anaerobic Mineral Media		
Compound Name	Chemical Symbol	Concentration
Sodium Chloride	NaCl	1,000 mg/L
Magnesium Chloride Hexahydrate	$MgCl_2*6H_2O$	500 mg/L
Potassium Phosphate	KH_2PO_4	200 mg/L
Ammonium Chloride	NH_4Cl	300 mg/L
Potassium Chloride	KCl	300 mg/L
Calcium Chloride	$CaCl_2$	15 mg/L
Trace Elements A	-	1 mL/L
Trace Elements B	-	1 mL/L
Yeast Extract	-	10 mg/L
Resazurin (0.1% w/v)	$C_{12}H_7NO_4$	0.25 mL/L
After Autoclave		
Sodium Bicarbonte	$NaHCO_3$	1.2 g/L
Cysteine	C3H7NO2S	24.2 mg/L
Sodium sulfide nonahydrate	Na_2S*9H_2O	48 mg/L

Table 3: The trace elements solutions contain the elements that are only required in minute quantities for biological activity.

Trace Elements Solution A		
Compound	Concentration	Units
$FeCl_2*4H_2O$	1.5	g/L
$CoCl_2*6H_2O$	0.19	g/L
$MnCl_2*4H_2O$	0.1	g/L
$ZnCl_2$	70	mg/L
H_3BO_3	6	mg/L
Na_2MoO_4	36	mg/L
$NiCl_2*6H_2O$	24	mg/L
$CuCl_2*2H_2O$	2	mg/L
25% HCl	10	ml/L

Table 4: The trace elements solutions contain the elements that are only required in minute quantities for biological activity.

Trace Elements Solution B		
Compound	Concentration	Units
$Na_2Wo_4*2H_2O$	8	mg/L
NaOH	0.5	g/L
$Na_2SeO_3*5H_2O$	6	mg/L

Heavy metal stock was created using cadmium chloride ($CdCl_2$) and lead acetate ($Pb(CH_3COO)_2$). The heavy metal solutions were made at a concentration of 5,000 ppm (5,000 mg/L) and then added to the microcosms at increasing concentrations of 50 µg/L, 500 µg/L, 5,000 µg/L, and 50 mg/L. Triplicates were made for each different heavy metal concentration microcosm set and duplicates were made for each varied heavy metal concentration for the sterile controls. Then, 2 g of soil was added to the microcosms. The anaerobic soil was stored in the anaerobic glove bag for one day, to insure a completely anaerobic medium, before being added to the microcosms. The 42 microcosms used for controls were then autoclaved once a day for three straight days to insure complete sterilization of the microcosms.

Stock solutions of benzene or toluene were created by filling and sealing 160 mL serum bottle with deionized (DI) water from a Labconco Water Pro PS, then injecting 1.8 mmol of benzene to create an 11.22 mM stock solution of benzene and injecting 0.755 mmol of toluene to create 4.72 mM stock solution of toluene. The rubber stoppers used to seal the serum bottles were Teflon-coated in order to prevent benzene or toluene adsorption to the stopper. Concentrations of the stock solution were determined by the solubility of both benzene and toluene. The aerobic stock solutions were place in an incubator for three days until complete mixing, while the anaerobic solutions were left in the anaerobic glove box until the benzene or toluene had completely dispersed throughout the water. After complete mixing of the benzene or toluene stock solutions, 2 mL of benzene stock and 4 mL of toluene stock were added to the 100 mL microcosm, bringing the concentrations to 0.2244 mM of benzene and 0.1888 mM of toluene in the respective microcosm sets. Twelve bottles were also made for standard curves six for benzene and six for toluene. The standard curve bottles were made by adding 100 mL of DI water, autoclaving, and adding benzene stock obtain concentrations 0.01122 mM through 0.4488 mM or adding toluene stock to obtain concentrations of 0.00944 mM through 0.3776 mM. This

volumetric measurement is 0.1 µL through 4 µL for both compounds. A complete list describing both sets of microcosms are found in Table 5 (aerobic) and Table 6 (anaerobic).

Table 5: Aerobic microcosms were created using the aerobic mineral media, surface soil, benzene or toluene, and a variety of heavy metal concentrations. They were stored in a 30 ºC incubator to increase microbial population and growth. The mineral media and the controls were sterilized in an autoclave to remove any pre-existing microbial activity. The microcosms were created in triplicates and the sterile controls were created in duplicates in order to have redundancy, prevent misreading, and have a larger sample size.

Aerobic Co-Contaminated Microcosms (2 g of soil & 100 mL of Mineral Media)					
Benzene (0.2244 mmol/L)		Toluene (0.1888 mmol/L)		Heavy Metal	Heavy Metal Concentration (Cd or Pb)
Microcosms (Triplicate)	Sterile Controls (Duplicate)	Microcosms (Triplicate)	Sterile Controls (Duplicate)		
A	1	K	9	Cd	50 µg/L
B	2	L	10		500 µg/L
C	3	M	11		5,000 µg/L
D	4	N	12		50 mg/L
E	5	O	13	Pb	50 µg/L
F	6	P	14		500 µg/L
G	7	Q	15		5,000 µg/L
H	8	R	16		50 mg/L
I	J	S	T	-	0 µg/L

Table 6: Anaerobic microcosms were created using the anaerobic mineral media, saturated soil, benzene or toluene, and a variety of heavy metal concentrations. They were created and stored in an anaerobic glove box in order to prevent oxygen from entering the system. The mineral media was autoclaved to remove any pre-existing microbes. The controls were also sterilized to remove biological activity. The microcosms were created in triplicates and the sterile controls were created in duplicates in order to have redundancy, prevent misreading, and have a larger sample size.

Anaerobic Co-Contaminated Microcosms (2 g of soil & 100 mL of Mineral Media)					
Benzene (0.2244 mmol/L)		Toluene (0.1888 mmol/L)		Heavy Metal	Heavy Metal Concentration (Cd or Pb)
Microcosms (Triplicate)	Sterile Controls (Duplicate)	Microcosms (Triplicate)	Sterile Controls (Duplicate)		
AA	-	AJ	-	Cd	500 µg/L
AB	-	AK	-		5,000 µg/L
AC	-	AL	-		50 mg/L
AD	AH	AM	AQ	Pb	500 µg/L
AE	-	AN	-		5,000 µg/L
AF	AI	AO	AR		50 mg/L
AG	-	AP	-	-	0 µg/L

GC Method

After one day of incubation, the concentration of benzene or toluene left in the microcosms was determined by headspace measurements using an Agilent Technologies flame ionization detector gas chromatograph (GC-FID) (Figure 99). The specifications for the GC-FID are given in Table 6. The headspace measurements were injected manually. The FID combusts the organics using a hydrogen flame. The gas stream passes through a detector measuring the resulting ions. The amount of ions is proportional to the concentration of the organics in the headspace. Benzene and toluene are VOCs and, according to Henry's Law, there is a relationship between the concentration in the headspace and the concentration in the liquid media. When the detector read a large concentration of benzene or toluene ions a peak appears (Figure 9).

Table 7: The GC-FID settings must be set at a certain values depending on the type of compound being measured. All of the settings could be monitored from either the computer or the GC itself.

Manual GC-FID Specifications			
Splitless Inlet		Columns	
Specification	Values	Specification	Values
Heater	250 C	Constant Pressure	
Pressure	10 psi	5% Methyl Silica Column Dimensions 30 m x 250 µm x 0.25 µm	
Total Flow	18.619 mL/min	Flow	0.61938 mL/min
Septum Purge Flow	3 mL/min	Average Velocity	19.302 cm/sec
Split Vent Purge Flow	15 mL/min	Holdup Time	2.5903 min
-	-	Helium	100 C
FID Detector		Oven	
Specification	Values	Specification	Values
Heater	300 C	Temperature	100 C
Air Flow	400 mL/min	Equilibration Time	0.5 min
H_2 Fuel Flow	30 mL/min	Maximum Oven Temperature	325 C
Makeup Flow (He)	25 mL/min	FID Back Signal	
Column Flow (He)	0.61938 mL/min	Specification	Values
-	-	Data Rate	50 Hz/0.004 min

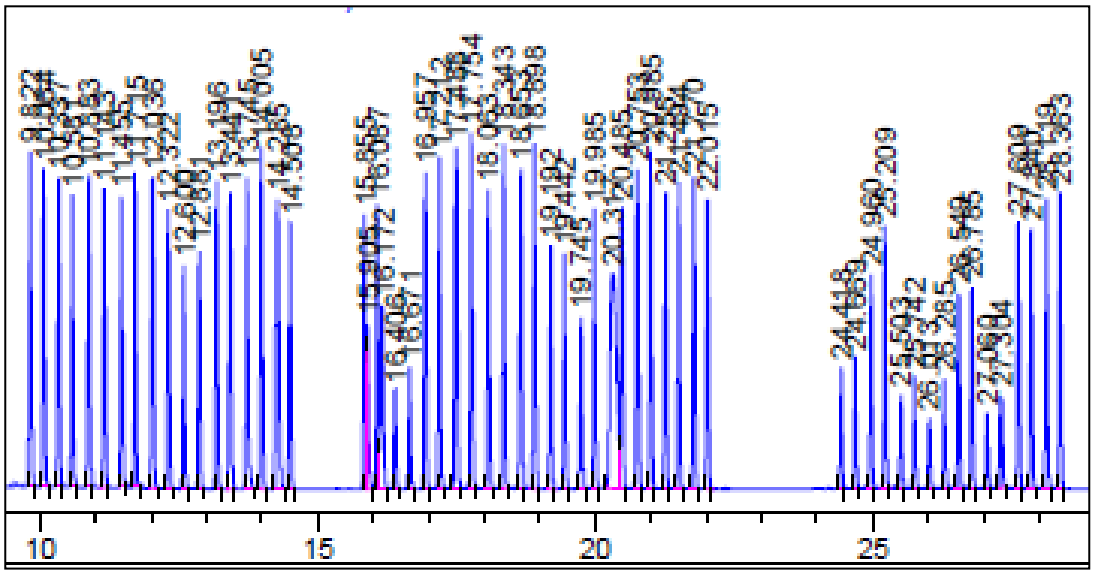

Figure 4: GC Peak area data is a representation of the concentration of an organic in the gas stream. Using this data, concentrations of the volatile benzene and toluene can be found. Proper measurement peaks are thin single peaks with space in between measurements. Proper injection technique is key to acquiring these types of readings. Injections should be made with plenty of time in between measurements with a clean syringe.

There is a correlation between peak area and concentration of the compound. By creating a standard curve based on “Known Concentration” vs. “Peak Area”, the unknown concentrations of the microcosms can be found by entering the area of the peak into the linear standard curve equation (Figure 5- Figure 21). If the 0.4488 mM standard for benzene or the 0.3776 mM standard for toluene (the highest concentrations) deviated more than 10% of the original value, a new standard was created in order to better represent the microcosms. This would reduce the error caused by using one standard curve for multiple microcosms over many days of testing. Many factors go into the area readings of compounds on the GC: such as the manual injection technique and the state of all of the equipment. These factors can vary day by day, so it is important to properly document standards individually in order to reduce false concentration changes.

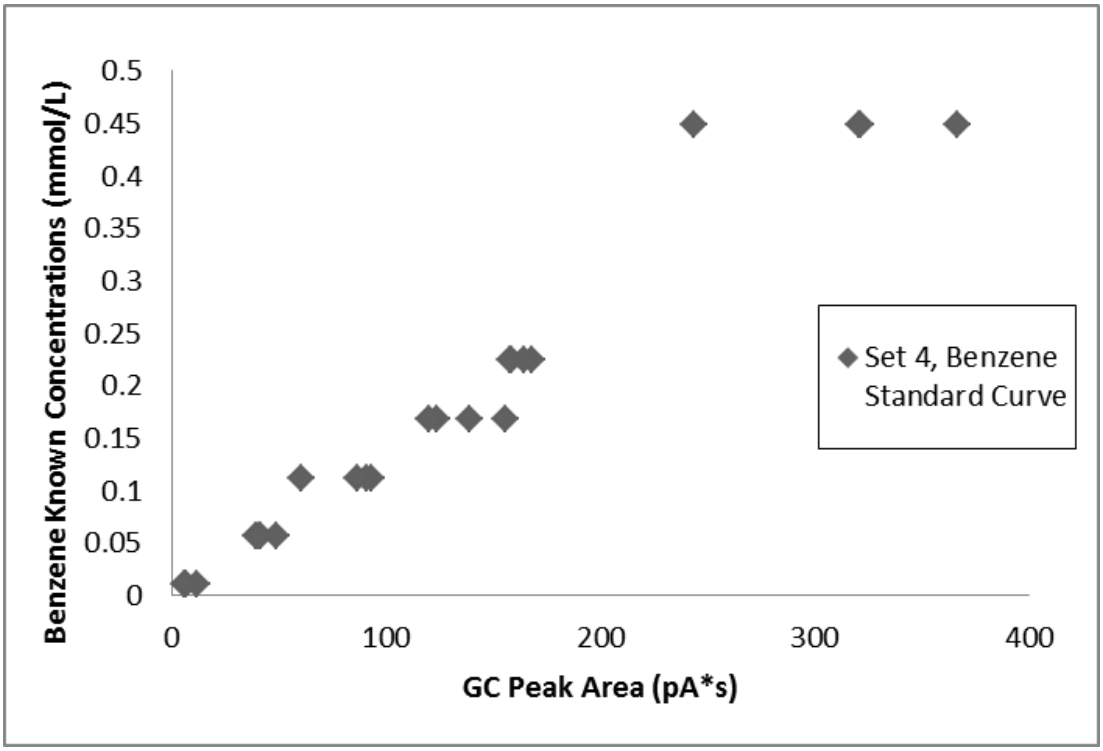

Figure 5: The figure shows the benzene standard curve for set 4 if data points from all days were used. The standard curves were created from bottles filled with 100 mL of DI water and increasing concentrations of benzene. Using Excel, the GC area was plotted against the known concentrations. The data has some variance, which can be clearly seen in the 0.4488 mM concentration points of the benzene. This would not properly represent the data taken over all of the test days. In order to avoid improper readings, if the difference between the current maximum concentration reading and the first maximum concentration reading was 10% or more, a new individual standard curve was created.

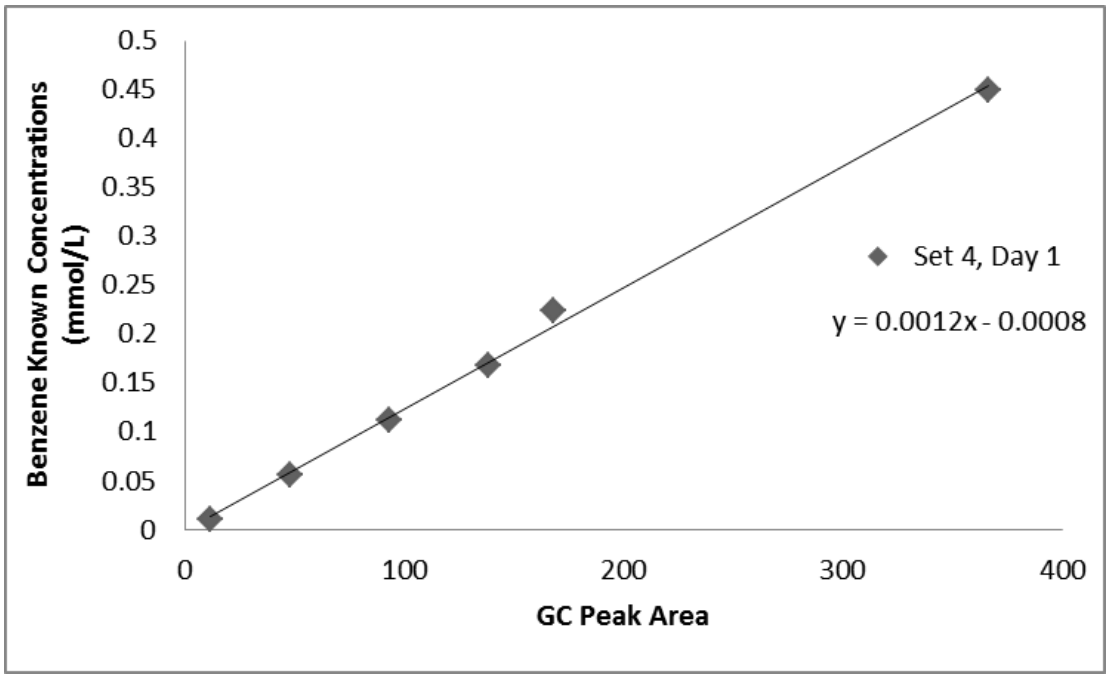

Figure 6: The figure shows the benzene standard curve for set 4, on day 1. The combined standard curves had too much variance to accurately represent the data. Individual standard curves were needed to get more accurate readings. An individual standard curve was used for all sets of readings until the 0.4488 mM data point was 10% more than the currently used maximum data point. After this occurred a new graph was created. The individual standard curves were much more accurate in representing the microcosms, as can be seen by the more linear nature of the graph.

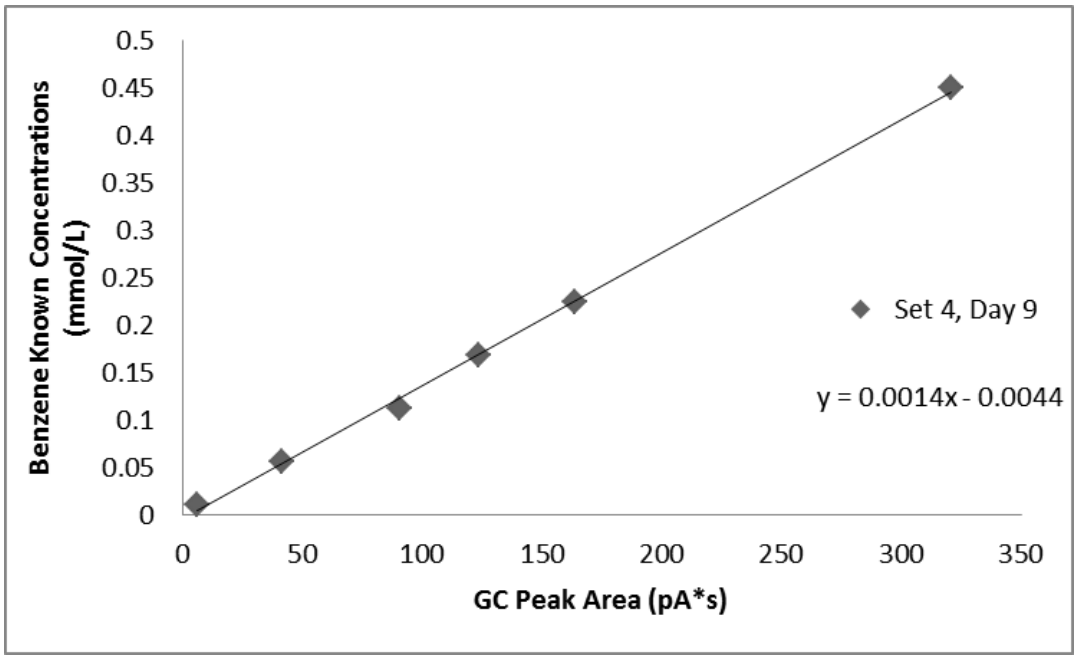

Figure 7: The figure shows the benzene standard curve for set 4, on day 9. The combined standard curves had too much variance to accurately represent the data. Individual standard curves were needed to get more accurate readings. An individual standard curve was used for all sets of readings until the 0.4488 mM data point was 10% more than the currently used maximum data point. After this occurred a new graph was created. The individual standard curves were much more accurate in representing the microcosms, as can be seen by the more linear nature of the graph.

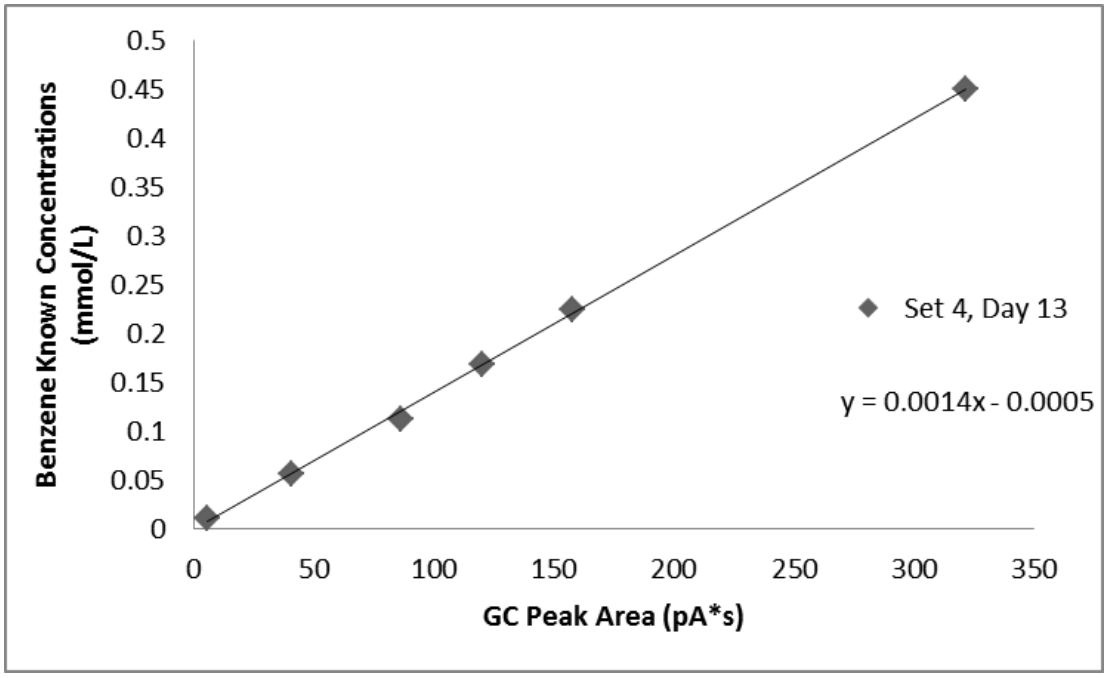

Figure 8: The figure shows the benzene standard curve for set 4, on day 13. The combined standard curves had too much variance to accurately represent the data. Individual standard curves were needed to get more accurate readings. An individual standard curve was used for all sets of readings until the 0.4488 mM data point was 10% more than the currently used maximum data point. After this occurred a new graph was created. The individual standard curves were much more accurate in representing the microcosms, as can be seen by the more linear nature of the graph.

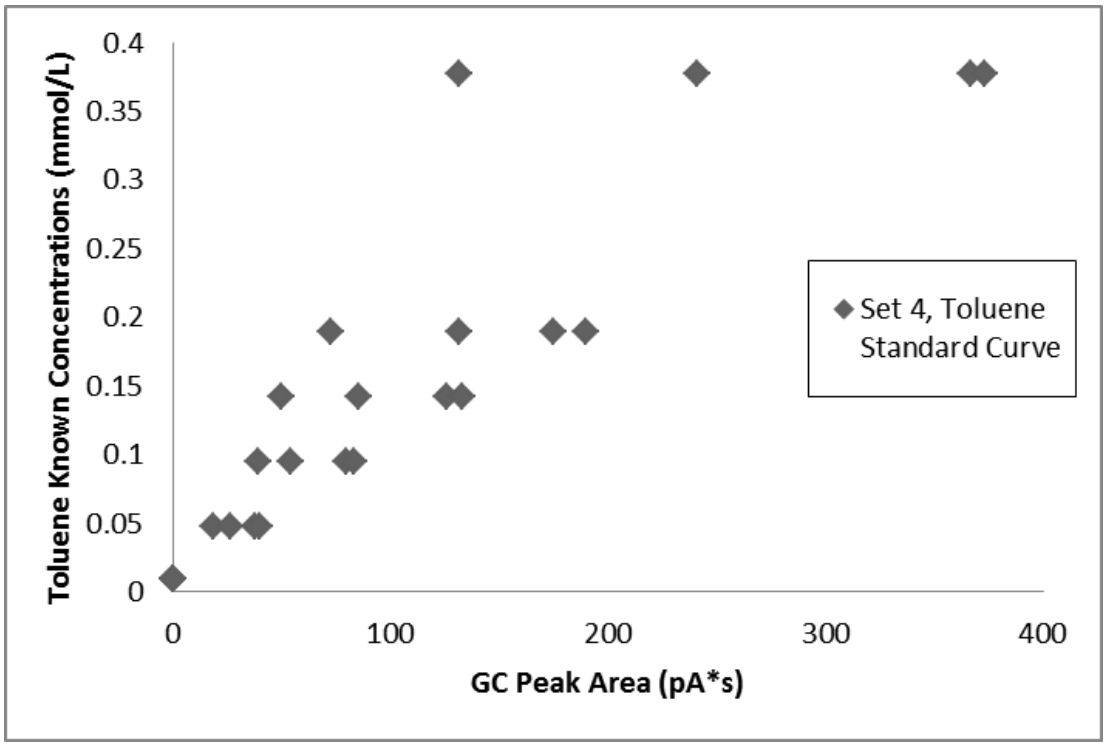

Figure 9: The figure shows the toluene standard curve for set 4 if data points from all days were used. The standard curves were created from bottles filled with 100 mL of DI water and increasing concentrations of toluene. Using Excel, the GC area was plotted against the known concentrations. The data has some variance, which can be clearly seen in the 0.3776 mM concentration points of the toluene. Toluene has much more variance in the standard curve than benzene. This would not properly represent the data taken over all of the test days. In order to avoid improper readings, if the difference between the current maximum concentration reading and the first maximum concentration reading was 10% or more, a new individual standard curve was created.

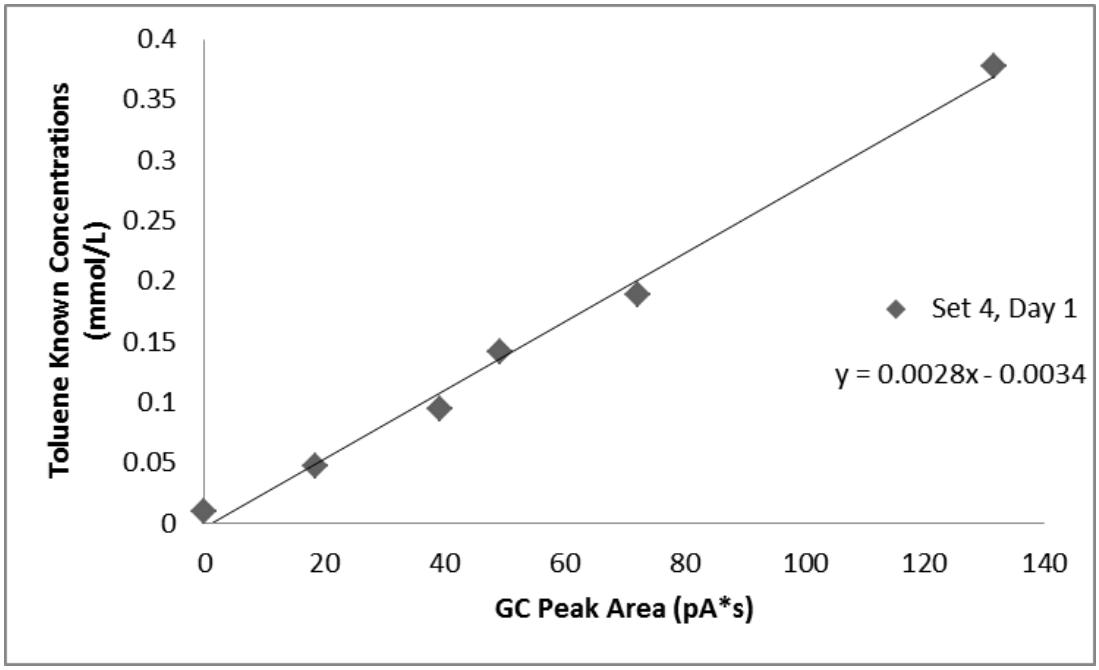

Figure 10: The figure shows the toluene standard curve for set 4, on day 1. Standard curves had high variance day to day. Standard curves that were specific for that day were needed to get more accurate readings. An individual standard curve was used for all sets of readings until the 0.4488 mM data point was 10% more or less than the currently used maximum data point. After this occurred a new graph was created. The individual standard curves were much more accurate in representing the microcosms, as can be seen by the more linear nature of the graph. This is especially noticeable in the toluene curves.

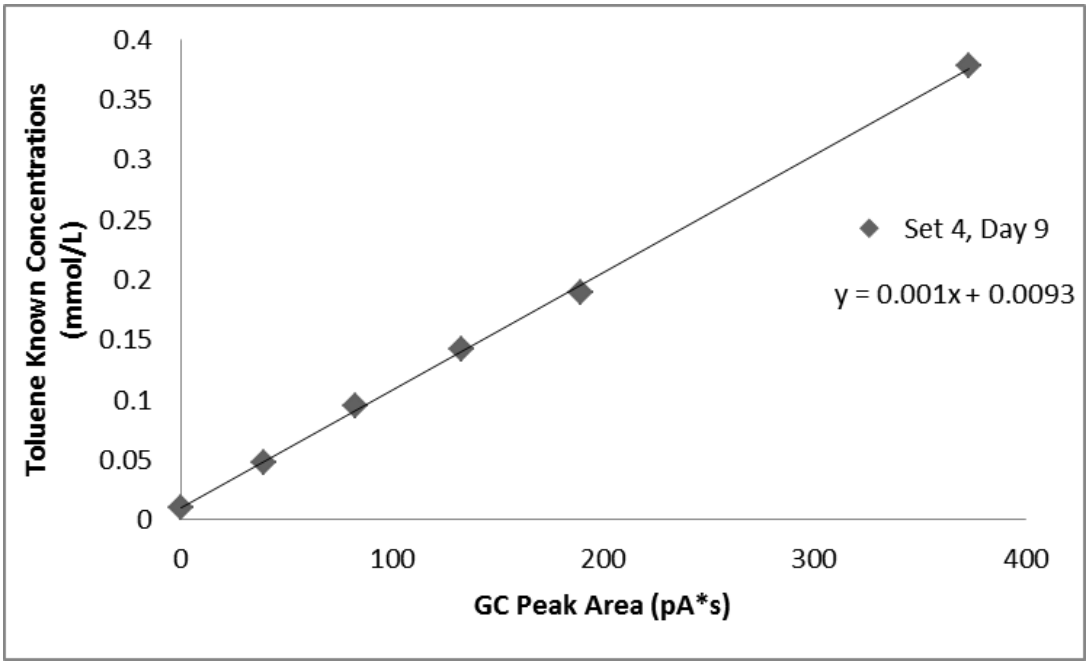

Figure 11: The figure shows the toluene standard curve for set 4, on day 9. Standard curves had high variance day to day. Standard curves that were specific for that day were needed to get more accurate readings. An individual standard curve was used for all sets of readings until the 0.4488 mM data point was 10% more or less than the currently used maximum data point. After this occurred a new graph was created. The individual standard curves were much more accurate in representing the microcosms, as can be seen by the more linear nature of the graph. This is especially noticeable in the toluene curves.

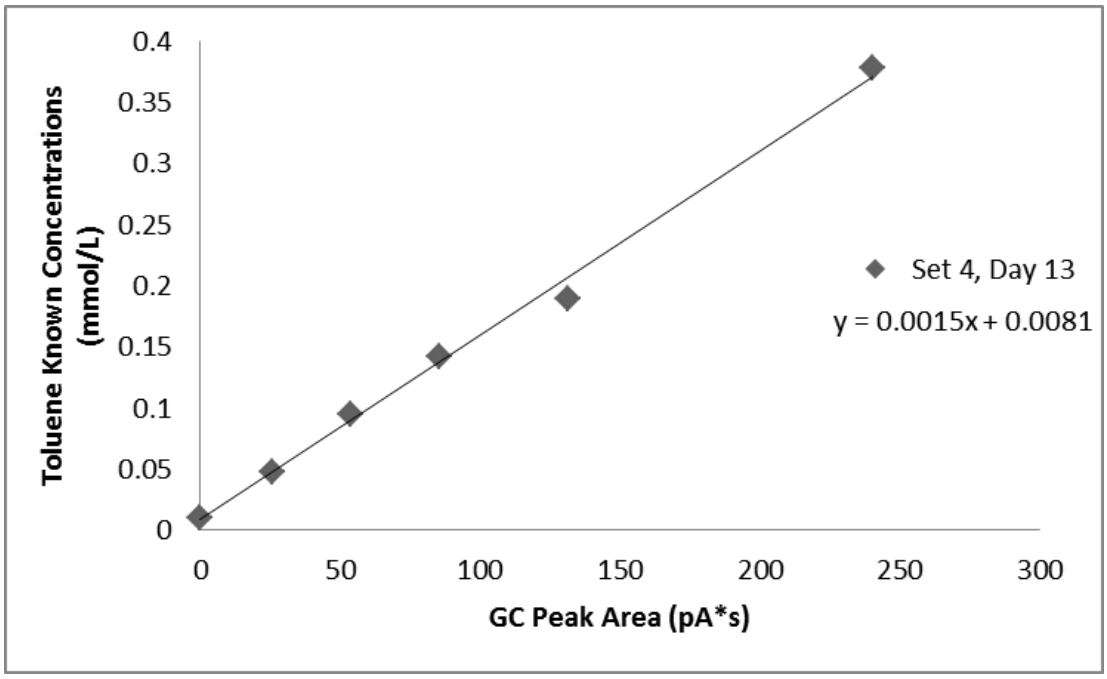

Figure 12: The figure shows the toluene standard curve for set 4, on day 13. Standard curves had high variance day to day. Standard curves that were specific for that day were needed to get more accurate readings. An individual standard curve was used for all sets of readings until the 0.4488 mM data point was 10% more or less than the currently used maximum data point. After this occurred a new graph was created. The individual standard curves were much more accurate in representing the microcosms, as can be seen by the more linear nature of the graph. This is especially noticeable in the toluene curves.

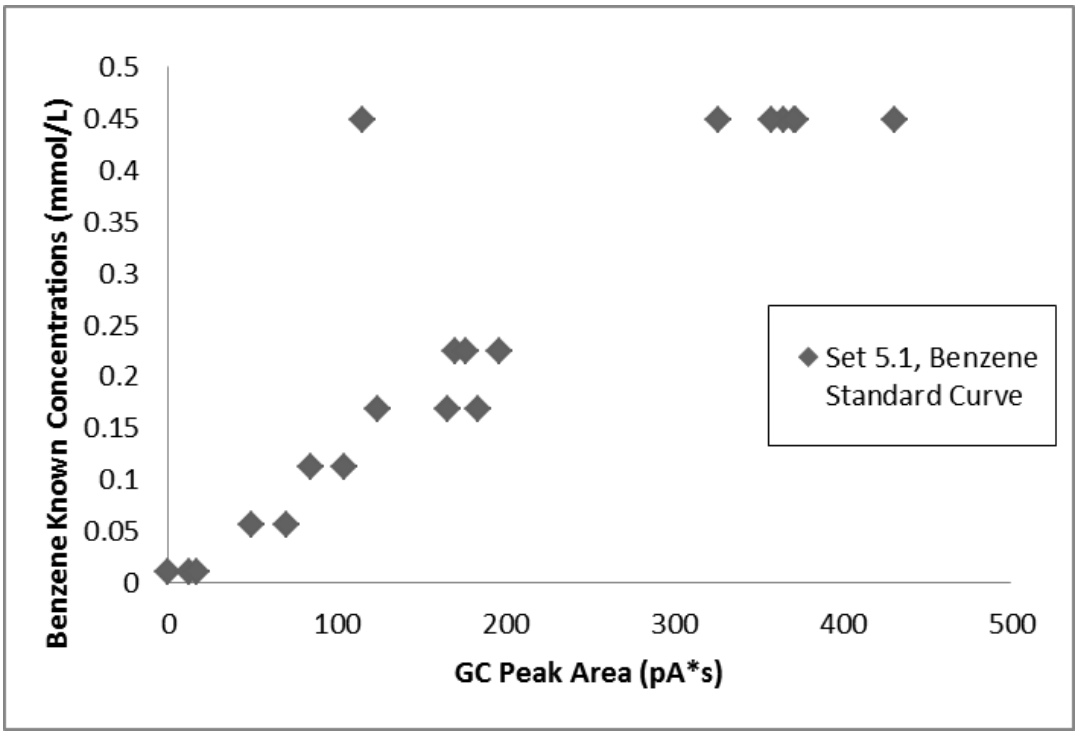

Figure 13: The figure shows the benzene standard curve for set 5.1 if data points from all days were used. Standard curves had high variance day to day. Standard curves that were specific for that day were needed to get more accurate readings. An individual standard curve was used for all sets of readings until the 0.4488 mM data point was 10% more or less than the currently used maximum data point. After this occurred a new graph was created. The individual standard curves were much more accurate in representing the microcosms, as can be seen by the more linear nature of the graph.

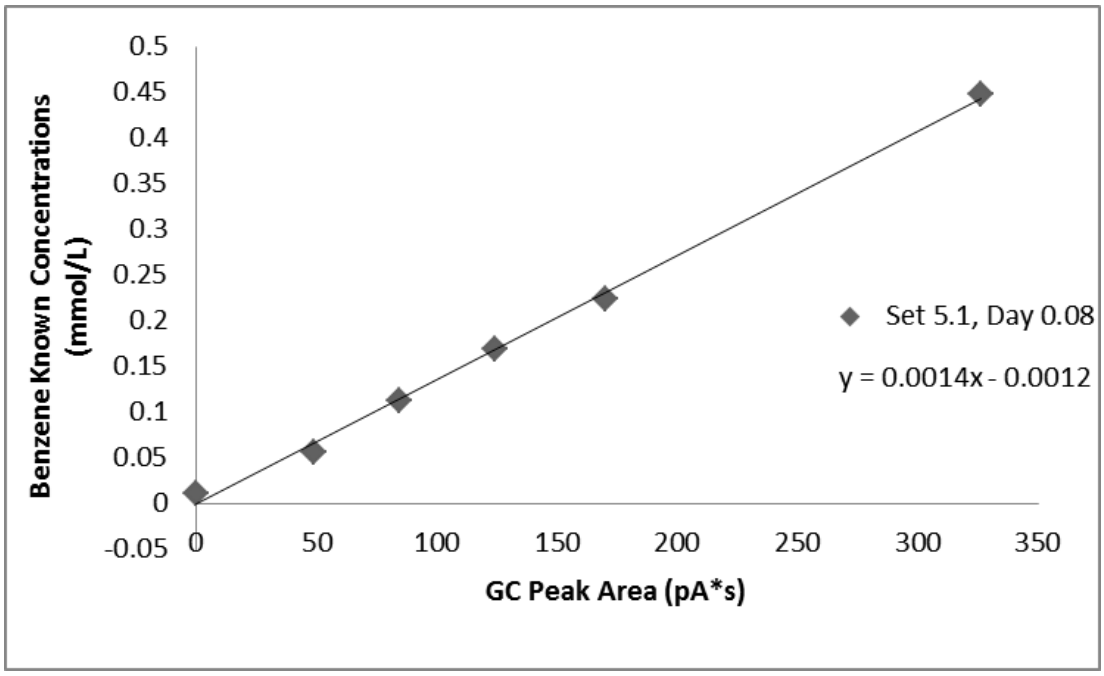

Figure 14: The figure shows the benzene standard curve for set 5.1, on day 0.08.

Standard curves had high variance day to day. Standard curves that were specific for that day were needed to get more accurate readings. An individual standard curve was used for all sets of readings until the 0.4488 mM data point was 10% more or less than the currently used maximum data point. After this occurred a new graph was created. The individual standard curves were much more accurate in representing the microcosms, as can be seen by the more linear nature of the graph.

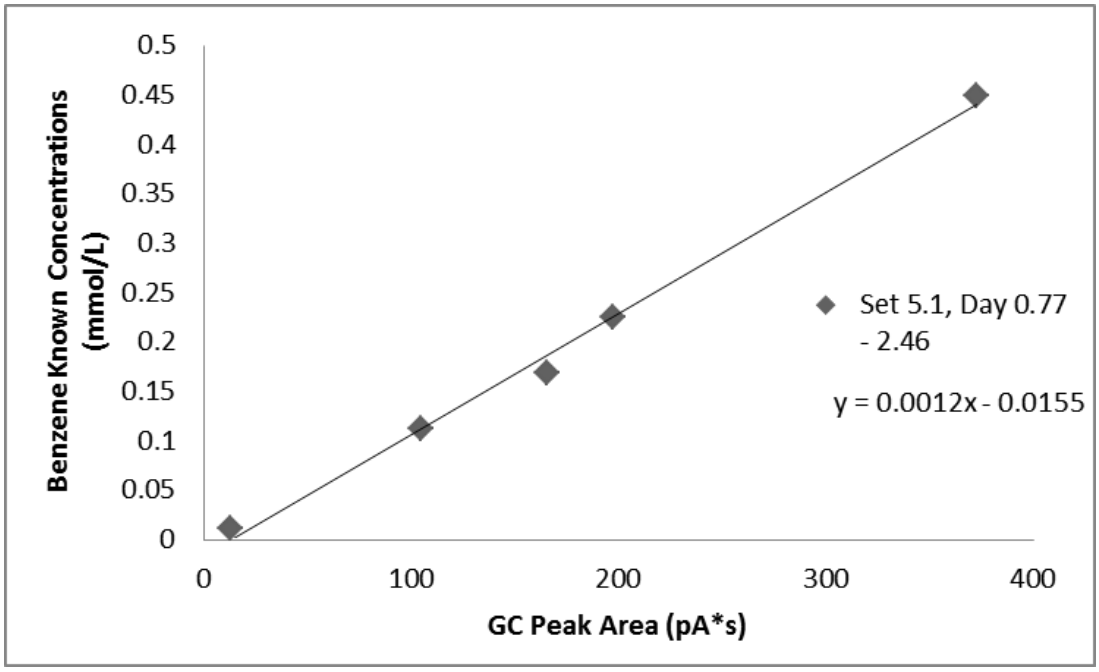

Figure 15: The figure shows the benzene standard curve for set 5.1, on days 0.77 through 2.46. Standard curves had high variance day to day. Standard curves that were specific for that day were needed to get more accurate readings. An individual standard curve was used for all sets of readings until the 0.4488 mM data point was 10% more or less than the currently used maximum data point. After this occurred a new graph was created. The individual standard curves were much more accurate in representing the microcosms, as can be seen by the more linear nature of the graph.

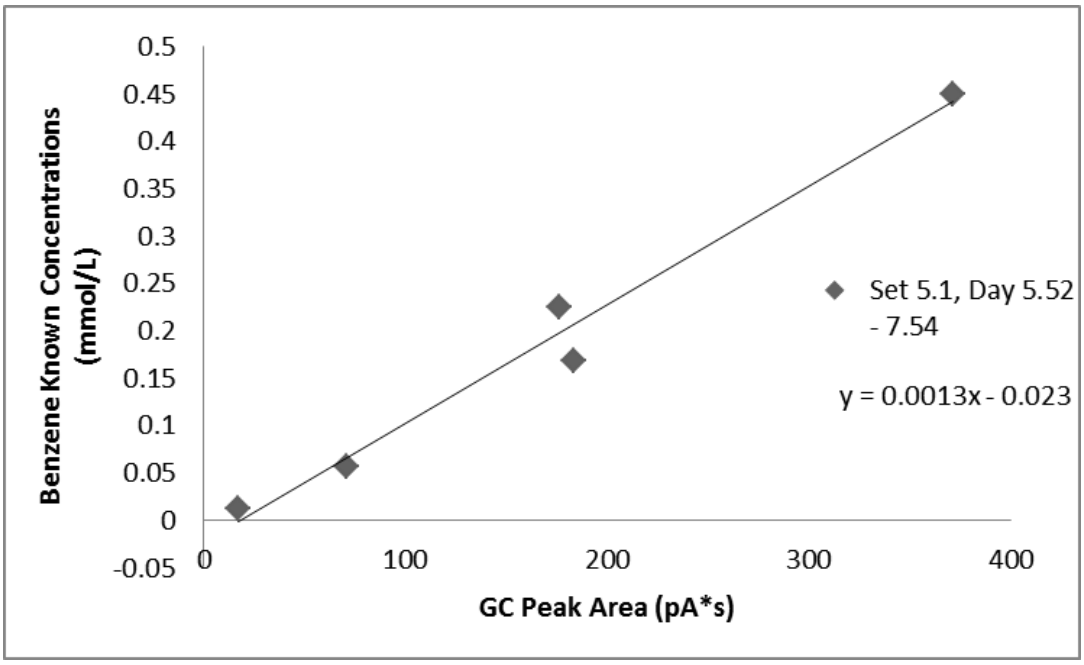

Figure 16: The figure shows the benzene standard curve for set 5.1, on days 5.52 through 7.54. Standard curves had high variance day to day. Standard curves that were specific for that day were needed to get more accurate readings. An individual standard curve was used for all sets of readings until the 0.4488 mM data point was 10% more or less than the currently used maximum data point. After this occurred a new graph was created. The individual standard curves were much more accurate in representing the microcosms, as can be seen by the more linear nature of the graph.

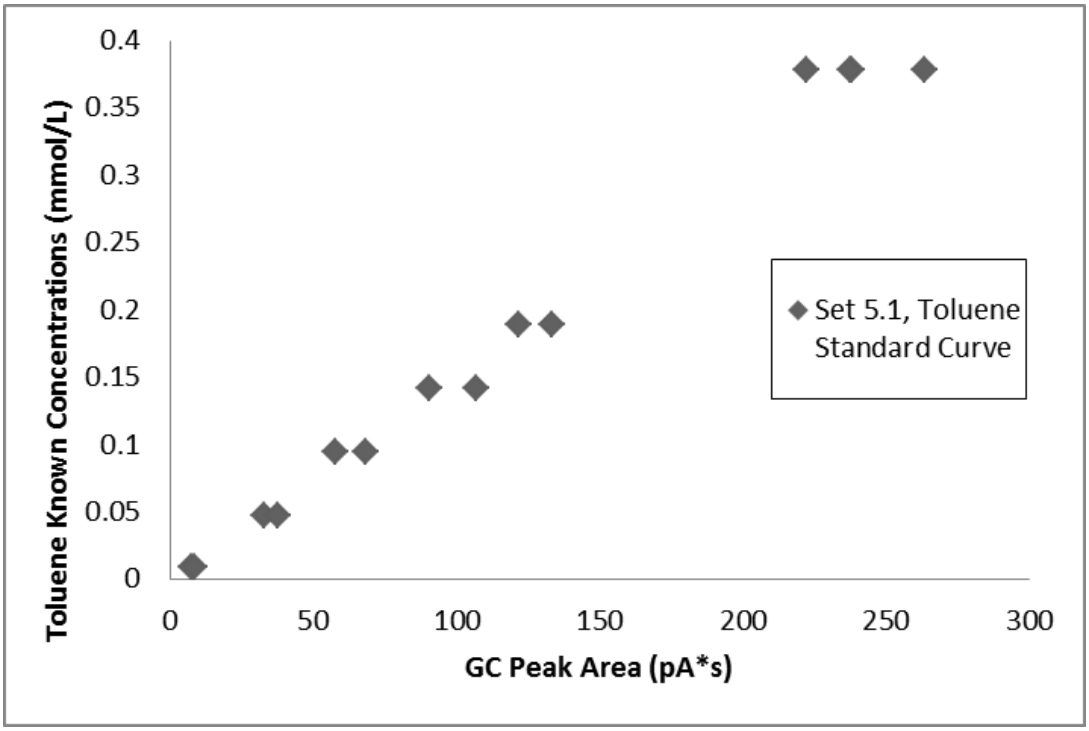

Figure 17: The figure shows the toluene standard curve for set 5.1 if data points from all days were used. Standard curves had high variance day to day. Standard curves that were specific for that day were needed to get more accurate readings. An individual standard curve was used for all sets of readings until the 0.3776 mM data point was 10% more or less than the currently used maximum data point. After this occurred a new graph was created. The individual standard curves were much more accurate in representing the microcosms, as can be seen by the more linear nature of the graph.

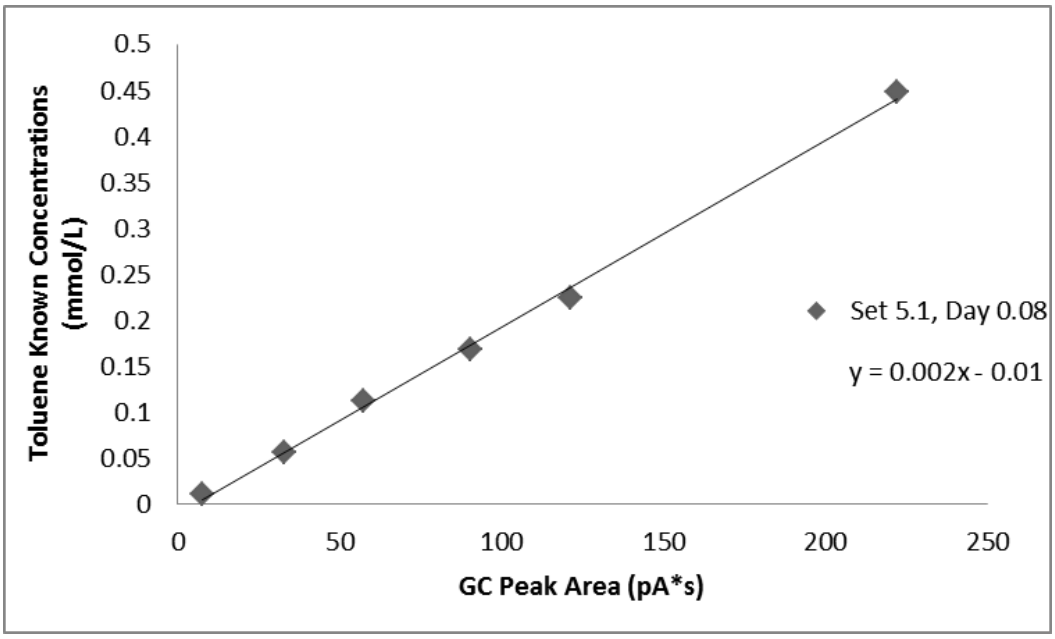

Figure 18: The figure shows the toluene standard curve for set 5.1, day 0.08. Standard curves had high variance day to day. Standard curves that were specific for that day were needed to get more accurate readings. An individual standard curve was used for all sets of readings until the 0.3776 mM data point was 10% more or less than the currently used maximum data point. After this occurred a new graph was created. The individual standard curves were much more accurate in representing the microcosms, as can be seen by the more linear nature of the graph.

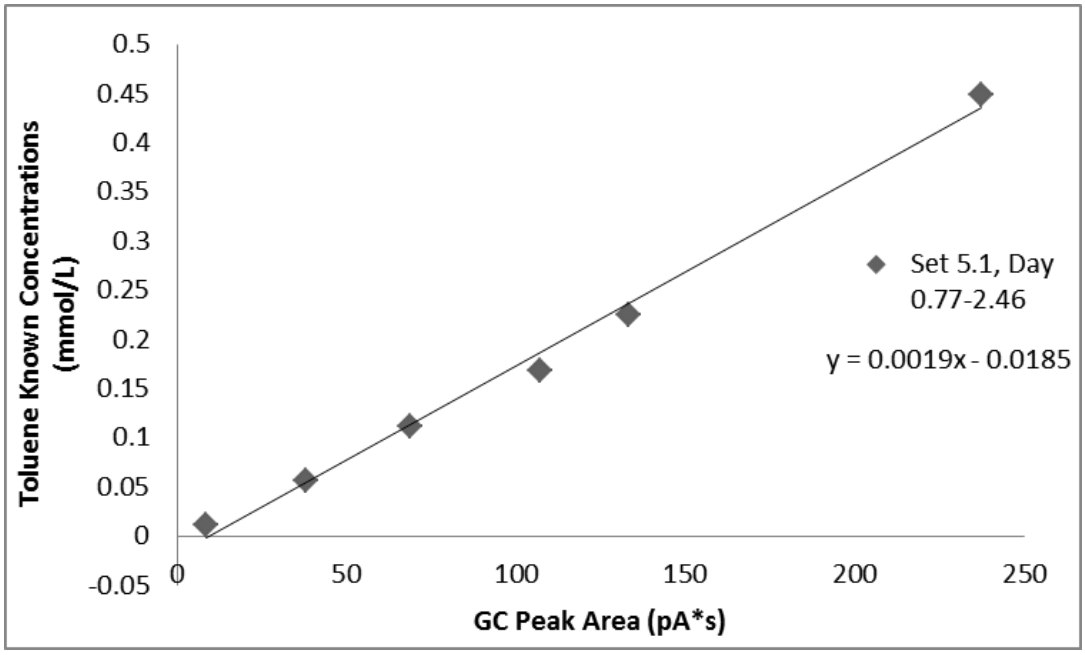

Figure 19: The figure shows the toluene standard curve for set 5.1, days 0.77 through 2.46. The figure shows the toluene standard curve for set 5.2. Standard curves had high variance represent day to day. Standard curves that were specific for that day were needed to get more accurate readings. An individual standard curve was used for all sets of readings until the 0.3776 mM data point was 10% more or less than the currently used maximum data point. After this occurred a new graph was created. The individual standard curves were much more accurate in representing the microcosms, as can be seen by the more linear nature of the graph.

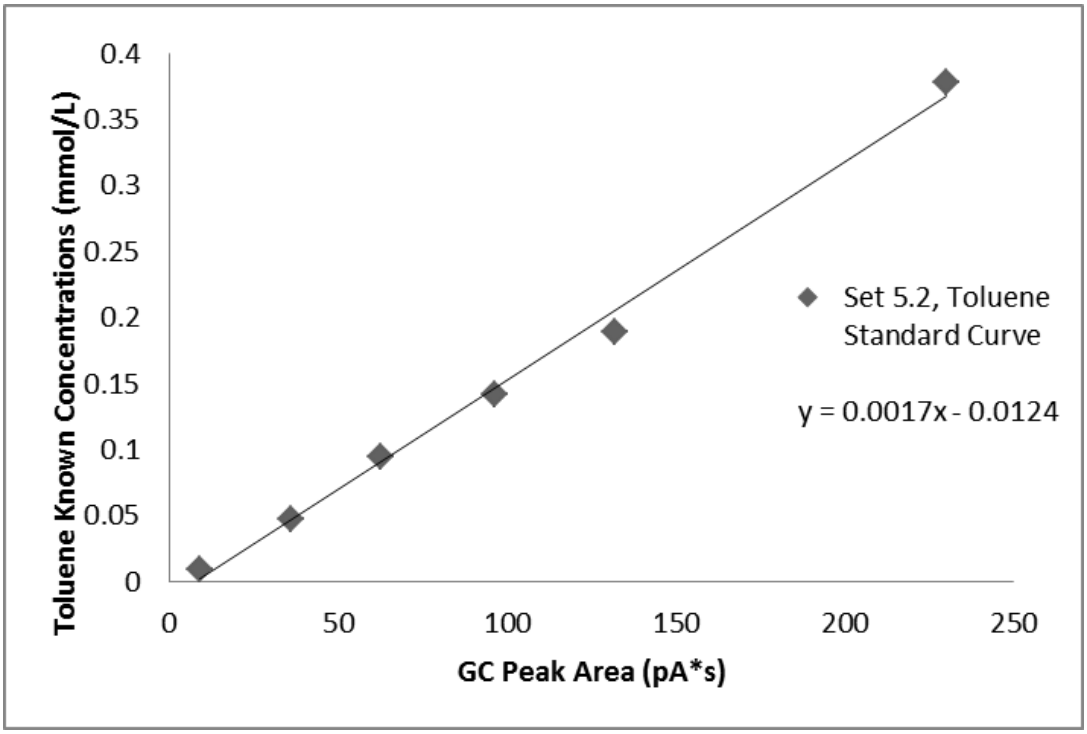

Figure 20: The figure shows the toluene standard curve for set 5.2. The standard curves were created from bottles filled with 100 mL of DI water and increasing concentrations of toluene. Using Excel, the GC area was plotted against the known concentrations.

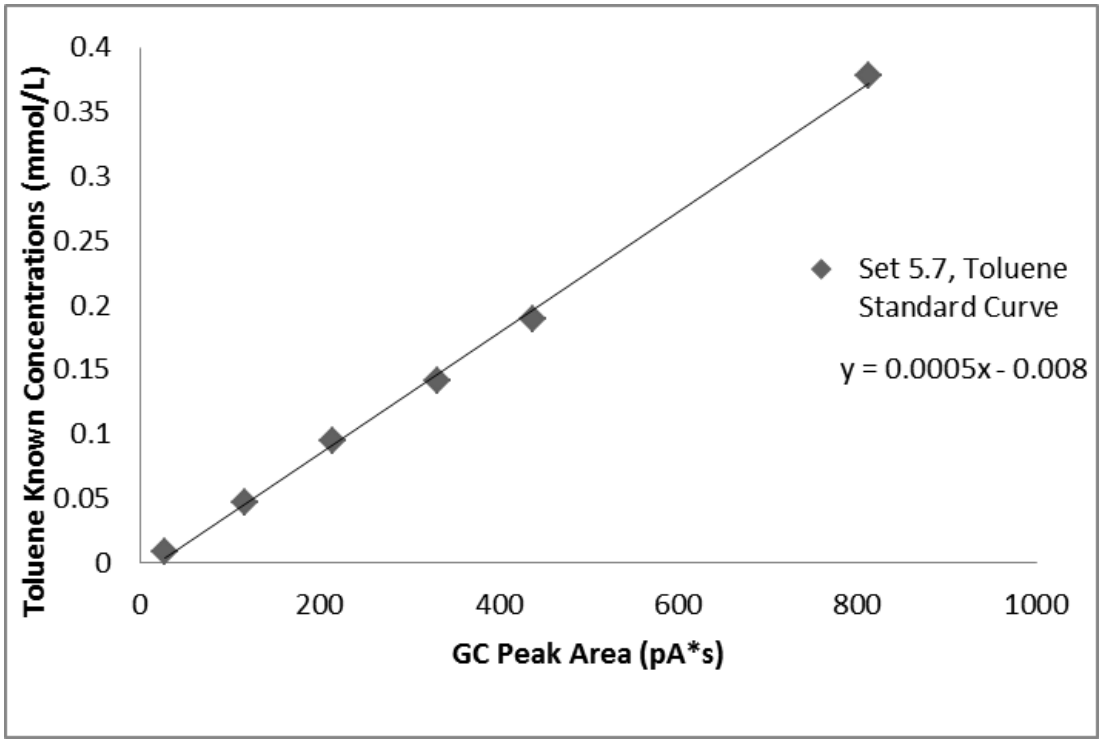

Figure 21: The figure shows the toluene standard curve for set 5.7. The standard curves were created from bottles filled with 100 mL of DI water and increasing concentrations of toluene. Using Excel, the GC area was plotted against the known concentrations.

The syringe used was a 10 µL gas tight glass syringe with a rounded tip needle. The gas tight syringe had a valve that could be closed in order to prevent air from escaping. The rounded tip needle was used in order to prevent tearing of the rubber stopper on the microcosms and the GC septa. In order to prevent cross contamination between bottles, after every measurement, the air tight syringe was rinsed with hexane and then placed in a Hamilton Company syringe cleaner. The cleaner used heat to sterilize the needle and vacuumed out any remaining hexane. There was residual hexane in the syringe; tests were run in order to pinpoint the hexane readings on the GC. Five different bottles containing 100 mL of DI water and pure hexane, pure benzene, pure toluene, a hexane/benzene mixture, and a hexane toluene mixture were created and headspace measurements were taken. The order and time between injections of benzene, toluene, and hexane were found. This allowed for proper interpretations of peak sequences (Figure 9).

The injection syringe is rinsed with hexane after every injection. The syringe is vacuumed for 5 seconds to remove excess hexane; however, some residual does remain. This residual was picked up by the GC-FID. Each microcosm is injected twice for redundancy, so each microcosm will have six readings: two for benzene or toluene, and four for hexane (the ACS grade hexanes used produces 2 peaks). Spike and elution time tests showed that hexane would be the first two readings on the GC-FID followed by one benzene and then toluene.

Compound	Time		GC #	GC Area
Hexane	33.17	3.17	20	251.28850
Hexane	33.26	3.26	21	60.70722
Benzene	33.36	3.36	22	79.74960
Hexane	33.61	3.61	23	135.99226
Hexane	33.70	3.70	24	30.98448
Benzene	33.80	3.80	25	78.24203
Hexane	43.20	3.20	15	1592.53809
Hexane	43.28	3.28	16	399.31705
Hexane	43.38	3.38	17	26.11973
Hexane	43.67	3.67	18	1034.24658
Hexane	43.75	3.75	19	257.37595
Toluene	43.81	3.81	20	17.07615
Toluene	44.28	4.28	21	25.99991
			22	28.04090

Figure 22: This test of 2 injections about 30 seconds apart using the isothermal GC-FID method was performed to properly identify benzene or toluene readings on the GC-FID. After the hexane rinse of the syringe (even after vacuuming) residual hexane remained in the syringe. This residual is picked up by the GC-FID, making reading the data difficult. This quality check contained five different mixtures: pure benzene, pure toluene, pure hexane, two different mixture of benzene and hexane, and toluene and hexane. Measurements were taken separately and time of detection was recorded and compared to the GC data. The test data was compared to the GC-FID data, the data and times for hexane and benzene or toluene matched up. The GC-FID data then could be read and analyzed much easier by knowing the order and times at which the individual compound would show up.

Enrichment

Degradation was observed and analyzed. Once there was complete degradation of benzene or toluene in the microcosms, a 1 mL sample of mixed media was taken and stored in a Frigidaire Commercial freezer at -20 ºC for later research concerning the microbiological communities. Then the microcosms were re-spiked with benzene or toluene in order to build a strong microbial population. This cycle was repeated seven times. After the seventh re-spike, one toluene microcosms (from each heavy metal concentration set) with the greatest rate of degradation were diluted into eight new microcosms, each new microcosm was inoculated by the community as a dilution by factors of 10. The diluted microcosms were then re-spiked to determine the most dilute microcosm that would still degrade toluene. This would contain the media with the least diverse microbial population still able to degrade toluene, making it easier to identify the specific microbes responsible for the biodegradation of toluene while still being resistant to the heavy metal toxicity. Once the most dilute microcosms, that were still able to degrade toluene, were identified, those microcosms were re-spiked.

CHAPTER IV

FINDINGS

Results

Results from the GC-FID found that across the concentrations of both lead and cadmium, benzene and toluene can be biodegraded naturally by indigenous aerobic bacteria. All concentrations of cadmium, ranging from 50 µg/L to 50 mg/L, had little to no effect on the aerobic biodegradation of benzene or toluene in the normal microcosm conditions (Table 8 and Table 9) (Figure 23 – Figure 40).

For the first round of tests, sterile standard curves were created to find the concentrations of the unknown microcosms. It was determined from the standard curve data that the detection of benzene and toluene in the GC-FID varied from day to day. This was especially true at higher concentrations. This prompted individual standard curves based on the difference of the maximum standard curve sample. If the difference between the first maximum standard and the most recent is greater than 10%, a new standard curve was created. Using the standard curve equation concentrations of the unknown microcosms could be found.

Degradation was found in all microcosms across all heavy metal concentrations. The degradation was linear and resulted in near complete and complete degradation. Benzene samples had a longer degradation time than the toluene samples. Data showed that the sterile controls containing soil did not degrade over a ten day period, the time period that the longest

microcosm degraded (Table 10 and Table 11) (Figure 41 – Figure 58). This proves that the degradation in the microcosms was due to biological activity. This shows that there are bacteria commonly found in soils that are resistant to heavy metal toxicity that are able to degrade both benzene and toluene.

Table 8: The data displayed in the table are all of the individual data points for degradation in the set 4 benzene microcosms. The data is representing degradation percentage. Complete degradation is represented by 100%. The table shows that the majority of microcosms fully degraded.

Set 4: Benzene Percent Degradation Data					
Concentration Metal	Sample	Day 1 Degradation (%)	Day 7 Degradation (%)	Day 9 Degradation (%)	Day 13 Degradation (%)
50 µg/L Cd	A-1	61.2	100.0	100.0	100.0
	A-2	54.0	26.2	84.6	100.0
	A-3	66.9	86.0	89.2	100.0
500 µg/L Cd	B-1	56.5	91.0	99.5	100.0
	B-2	59.1	83.9	100.0	100.0
	B-3	85.7	95.2	96.7	87.6
5,000 µg/L Cd	C-1	59.8	96.2	98.2	100.0
	C-2	66.1	88.8	94.9	100.0
	C-3	60.7	94.6	100.0	100.0
50 mg/L Cd	D-1	60.5	91.0	94.2	100.0
	D-2	63.9	90.5	98.7	100.0
	D-3	72.2	95.3	93.7	100.0
50 µg/L Pb	E-1	47.1	92.9	93.6	100.0
	E-2	74.0	84.6	91.0	100.0
	E-3	67.3	88.6	93.5	91.5
500 µg/L Pb	F-1	56.9	96.8	96.4	100.0
	F-2	62.8	90.4	91.6	73.7
	F-3	42.6	87.3	94.2	100.0
5,000 µg/L Pb	G-1	71.0	93.3	95.5	84.9
	G-2	62.6	84.2	93.6	94.5
	G-3	65.4	89.4	96.4	100.0
50 mg/L Pb	H-1	82.0	100.0	97.7	100.0
	H-2	71.5	96.9	100.0	88.3
	H-3	96.8	97.5	98.1	100.0
0 µg/L Cd & Pb	I-1	58.0	96.1	97.7	100.0
	I-2	58.0	93.2	98.2	100.0
	I-3	73.6	95.2	98.5	100.0

Table 9: The data displayed in the table are all of the individual data points for degradation in the set 4 toluene microcosms. The data is representing degradation percentage. Complete degradation is represented by 100%. The table shows that the majority of microcosms fully degrade.

Set 4: Toluene Percent Degradation Data					
Concentration Metal	Sample	Day 1 Degradation (%)	Day 7 Degradation (%)	Day 9 Degradation (%)	Day 13 Degradation (%)
50 µg/L Cd	K-1	16.3	93.5	95.1	95.7
	K-2	49.5	100.0	100.0	93.2
	K-3	-	100.0	97.7	100.0
500 µg/L Cd	L-1	24.1	100.0	97.6	100.0
	L-2	71.4	84.8	74.3	89.6
	L-3	28.7	100.0	73.8	100.0
5,000 µg/L Cd	M-1	44.6	100.0	100.0	100.0
	M-2	15.1	97.2	100.0	100.0
	M-3	53.1	100.0	97.0	100.0
50 mg/L Cd	N-1	-	100.0	100.0	100.0
	N-2	-	91.7	99.0	100.0
	N-3	-	100.0	97.0	100.0
50 µg/L Pb	O-1	30.0	75.3	82.6	100.0
	O-2	-	94.2	71.7	91.5
	O-3	-	87.1	97.8	100.0
500 µg/L Pb	P-1	-	96.7	74.1	96.3
	P-2	-	93.6	96.7	80.8
	P-3	42.2	100.0	100.0	100.0
5,000 µg/L Pb	Q-1	12.0	97.0	73.2	93.4
	Q-2	-	91.5	97.2	89.1
	Q-3	12.3	87.0	97.2	100.0
50 mg/L Pb	R-1	-	96.7	96.6	93.5
	R-2	-	93.9	96.5	88.8
	R-3	-	96.0	96.6	100.0
0 µg/L Cd & Pb	S-1	0.4	97.5	96.3	90.6
	S-2	10.2	100.0	96.8	100.0
	S-3	56.6	100.0	67.9	100.0

Table 10: The data displayed in the table are all of the individual data points for degradation in the set 4 sterile benzene microcosms. The data is representing degradation percentage. Complete degradation is represented by 100%. The sterile controls had little to no degradation, proving that the degradation in the active microcosms was due to biological activity.

Set 4: Sterile Benzene Percent Degradation Data					
Concentration Metal	Sample	Day 1 Degradation (%)	Day 7 Degradation (%)	Day 9 Degradation (%)	Day 13 Degradation (%)
0 µg/L Cd & Pb	J-1	7.1	9.7	0.0	6.5
	J-2	10.6	15.3	5.0	5.3
	J-3	22.1	18.6	5.3	10.3
50 µg/L Cd	1-A	8.4	10.2	0.0	0.0
	1-B	5.9	16.7	0.0	0.0
500 µg/L Cd	2-A	1.2	15.3	0.0	0.0
	2-B	4.8	9.5	0.0	0.0
5,000 µg/L Cd	3-A	14.8	0.0	2.0	0.0
	3-B	21.1	0.0	0.0	1.1
50 mg/L Cd	4-A	70.7	0.0	7.6	0.0
	4-B	50.6	0.0	0.6	0.0
50 µg/L Pb	5-A	32.8	0.0	20.9	0.0
	5-B	34.5	0.0	12.8	0.0
500 µg/L Pb	6-A	40.3	0.0	7.9	0.3
	6-B	36.1	0.0	5.1	2.1
5,000 µg/L Pb	7-A	35.2	0.0	0.0	7.4
	7-B	35.7	0.0	0.0	9.1
50 mg/L Pb	8-A	33.6	0.0	13.0	8.3
	8-B	31.5	0.0	14.4	10.4

Table 11: The data displayed in the table are all of the individual data points for degradation in the set 4 sterile toluene microcosms. The data is representing degradation percentage. Complete degradation is represented by 100%. The sterile controls had little to no degradation, proving that the degradation in the active microcosms was due to biological activity.

Set 4: Sterile Toluene Percent Degradation Data					
Concentration Metal	Sample	Day 1 Degradation (%)	Day 7 Degradation (%)	Day 9 Degradation (%)	Day 13 Degradation (%)
0 µg/L Cd & Pb	T-1	0.0	9.1	5.6	2.2
	T-2	13.2	15.2	9.2	7.8
	T-3	22.2	17.7	18.5	8.6
50 µg/L Cd	9-A	8.6	9.7	5.2	0.0
	9-B	0.0	16.6	7.1	0.8
500 µg/L Cd	10-A	5.9	13.5	12.2	1.5
	10-B	0.0	13.7	12.5	0.0
5,000 µg/L Cd	11-A	11.5	17.0	16.2	0.3
	11-B	0.0	13.2	16.4	5.2
50 mg/L Cd	12-A	0.0	17.2	15.4	3.9
	12-B	0.0	16.7	15.1	3.6
50 µg/L Pb	13-A	0.0	21.3	19.4	15.6
	13-B	0.0	19.2	25.2	11.5
500 µg/L Pb	14-A	0.0	28.6	21.0	14.1
	14-B	0.0	30.6	23.4	18.3
5,000 µg/L Pb	15-A	0.0	30.1	27.6	22.8
	15-B	0.0	31.0	28.7	24.0
50 mg/L Pb	16-A	0.0	36.5	28.6	20.2
	16-B	0.0	34.7	29.7	26.8

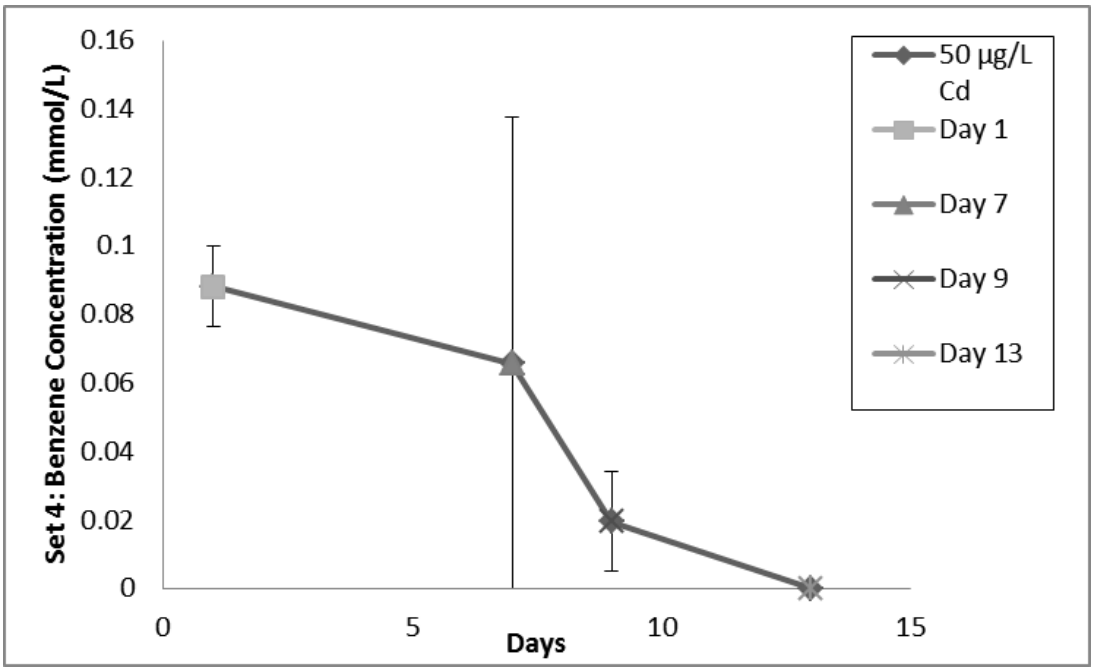

Figure 23: The figure shows the set 4 benzene degradation curve in the 50 µg/L Cd microcosms. The degradation of benzene mostly is linear. Starting benzene concentration was 0.2244 mM. Due to the immediate drop in concentration there was no real lag time observed. As shown in the previous tables the degradation is a result of biological activity, due to a lack of degradation in the sterile controls. Complete degradation occurred on day 13.

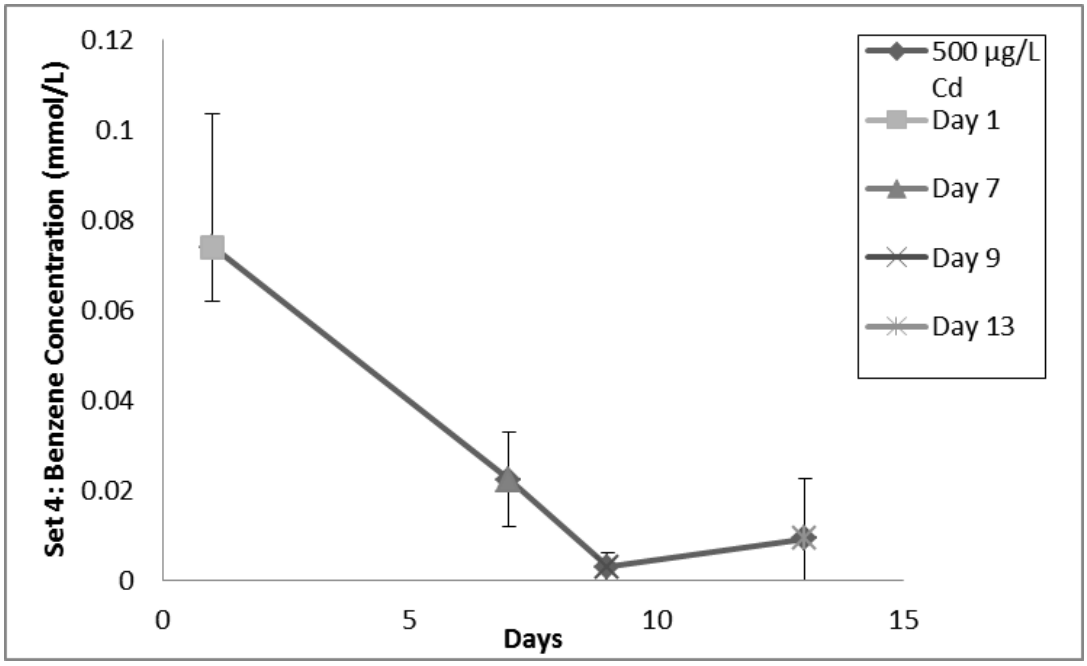

Figure 24: The figure shows the set 4 benzene degradation curve in the 500 µg/L Cd microcosms. The degradation of benzene is linear. Starting benzene concentration was 0.2244 mM. Due to the immediate drop in concentration there was no real lag time observed. As shown in the previous tables the degradation is a result of biological activity, due to a lack of degradation in the sterile controls.

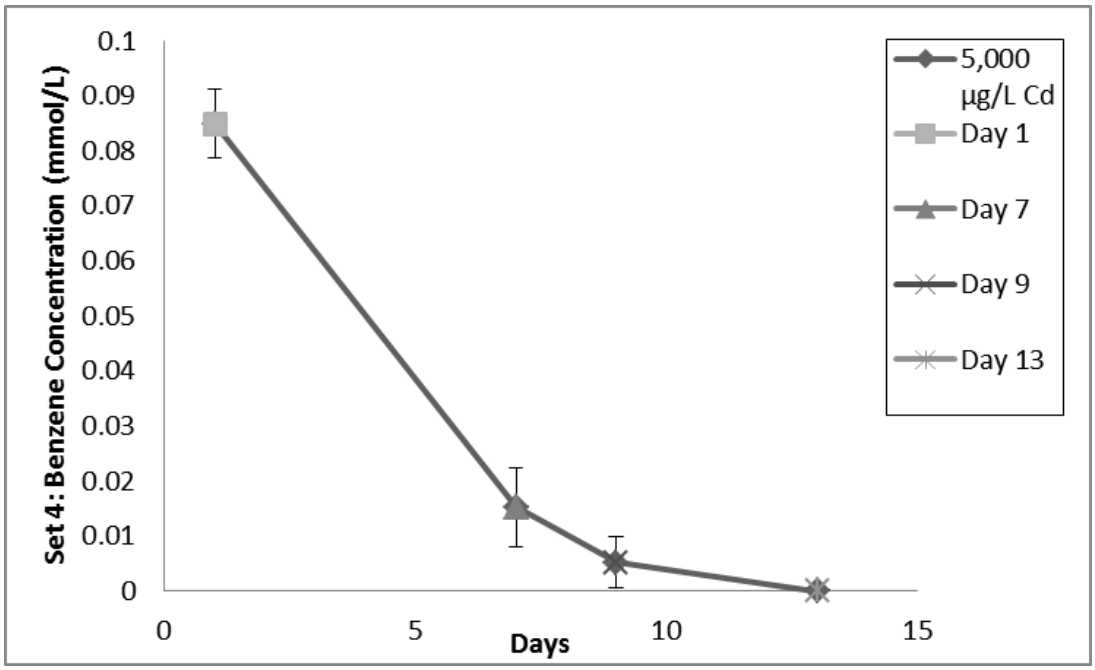

Figure 25: The figure shows the set 4 benzene degradation curve in the 5,000 µg/L Cd microcosms. The degradation of benzene occurs over an exponential slope. Starting benzene concentration was 0.2244 mM. Due to the immediate drop in concentration there was no real lag time observed. As shown in the previous tables the degradation is a result of biological activity, due to a lack of degradation in the sterile controls. Standard deviation between all microcosms is really low. Complete degradation occurred on day 13.

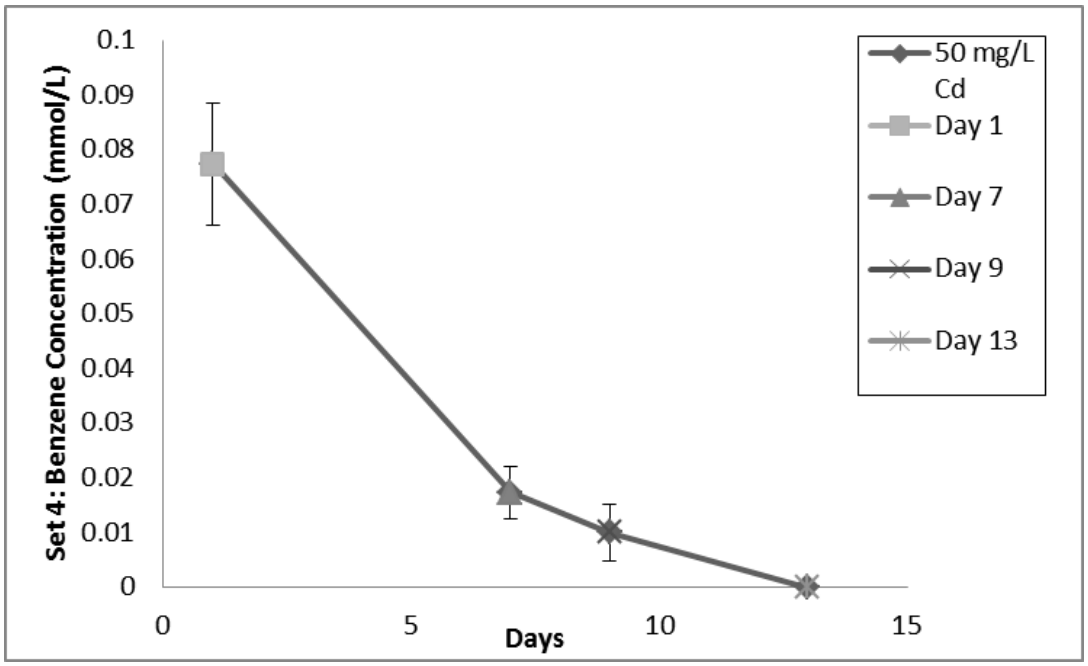

Figure 26: The figure shows the set 4 benzene degradation curve in the 50 mg/L Cd microcosms. The degradation of benzene is linear. Starting benzene concentration was 0.2244 mM. Due to the immediate drop in concentration there was no real lag time observed. As shown in the previous tables the degradation is a result of biological activity, due to a lack of degradation in the sterile controls. Standard deviation between all microcosms is really low. Complete degradation occurred on day 13.

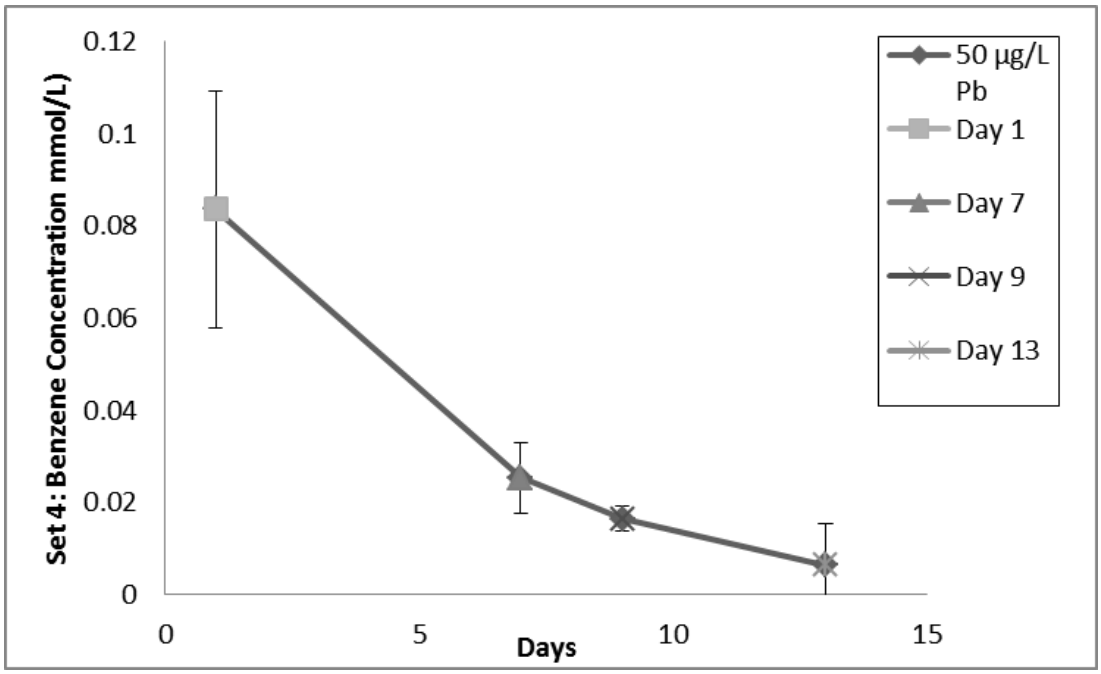

Figure 25: The figure shows the set 4 benzene degradation curve in the 50 µg/L Pb microcosms. The degradation of benzene is linear. Starting benzene concentration was 0.2244 mM. Due to the immediate drop in concentration there was no real lag time observed. As shown in the previous tables the degradation is a result of biological activity, due to a lack of degradation in the sterile controls.

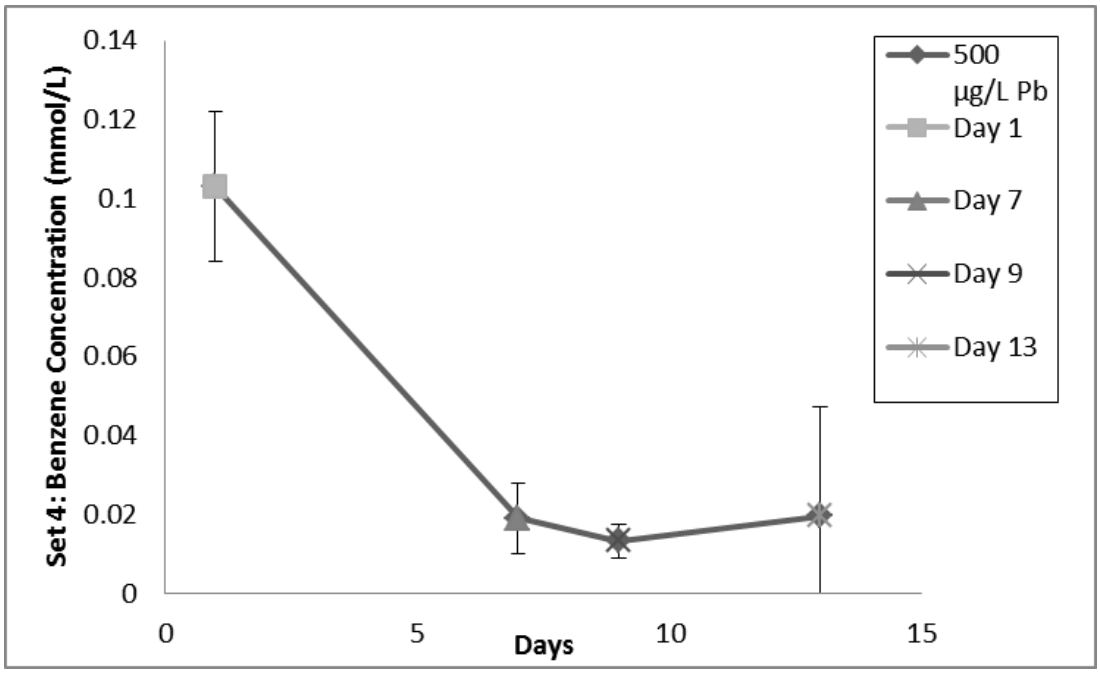

Figure 28: The figure shows the set 4 benzene degradation curve in the 500 µg/L Pb microcosms. The degradation of benzene is linear. Starting benzene concentration was 0.2244 mM. Due to the immediate drop in concentration there was no real lag time observed. As shown in the previous tables the degradation is a result of biological activity, due to a lack of degradation in the sterile controls.

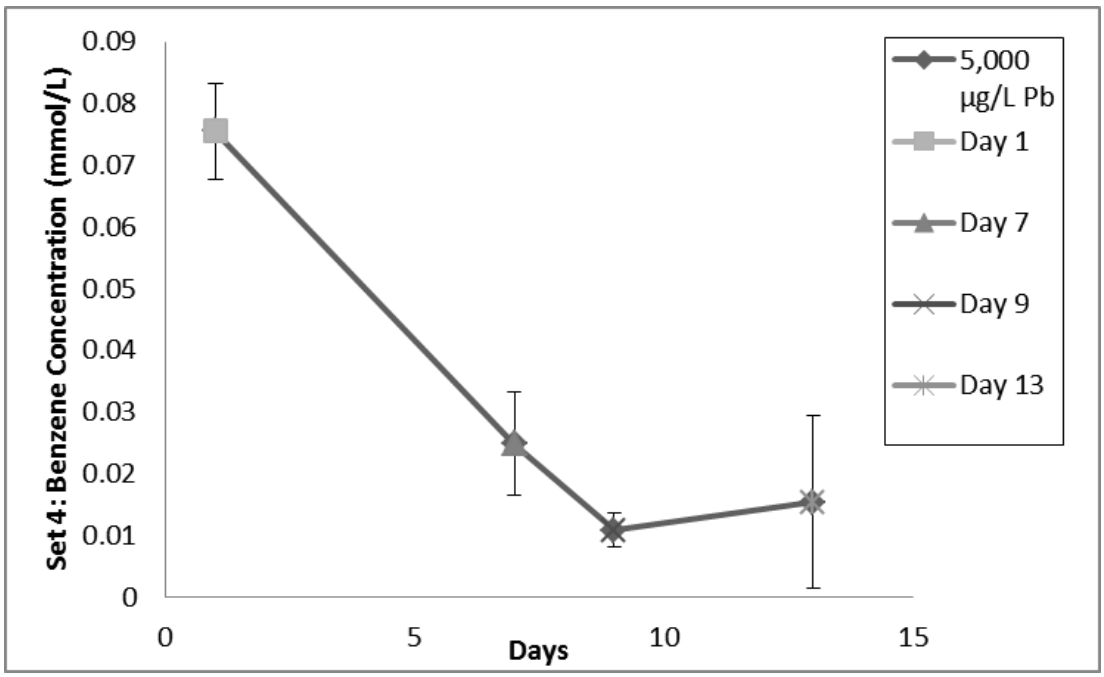

Figure 25: The figure shows the set 4 benzene degradation curve in the 5,000 µg/L Pb microcosms. The degradation of benzene is linear. Starting benzene concentration was 0.2244 mM. Due to the immediate drop in concentration there was no real lag time observed. As shown in the previous tables the degradation is a result of biological activity, due to a lack of degradation in the sterile controls. Standard deviation between all microcosms is really low.

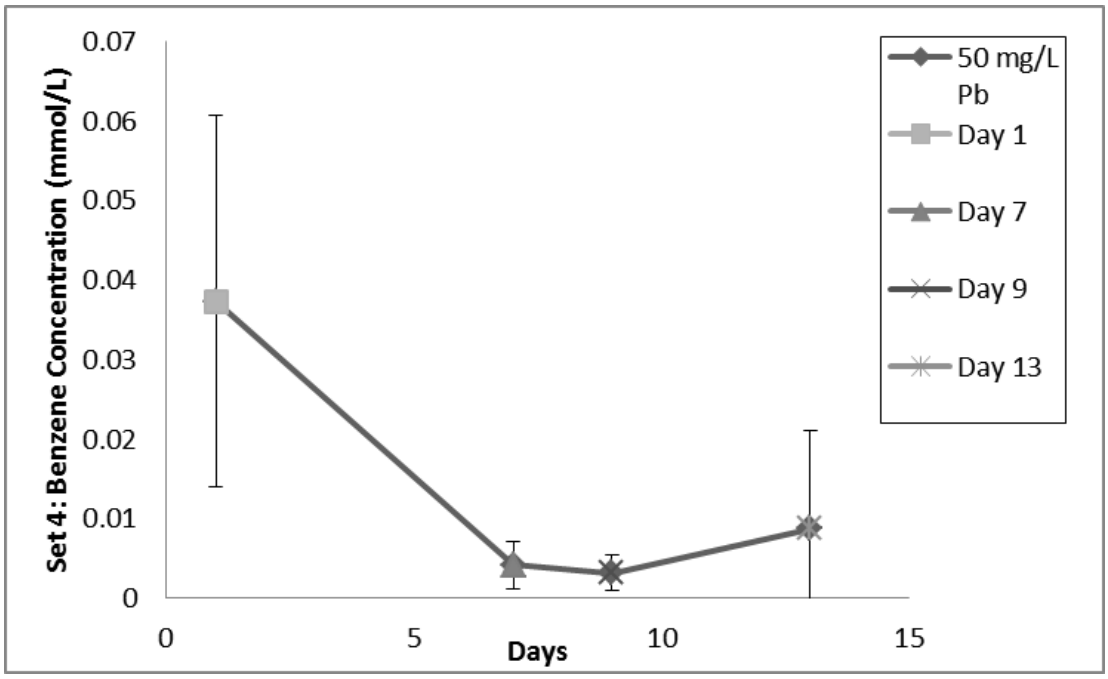

Figure 30: The figure shows the set 4 benzene degradation curve in the 50 mg/L Pb microcosms. The degradation of benzene occurs is linear. Starting benzene concentration was 0.2244 mM. Due to the immediate drop in concentration there was no real lag time observed. As shown in the previous tables the degradation is a result of biological activity, due to a lack of degradation in the sterile controls.

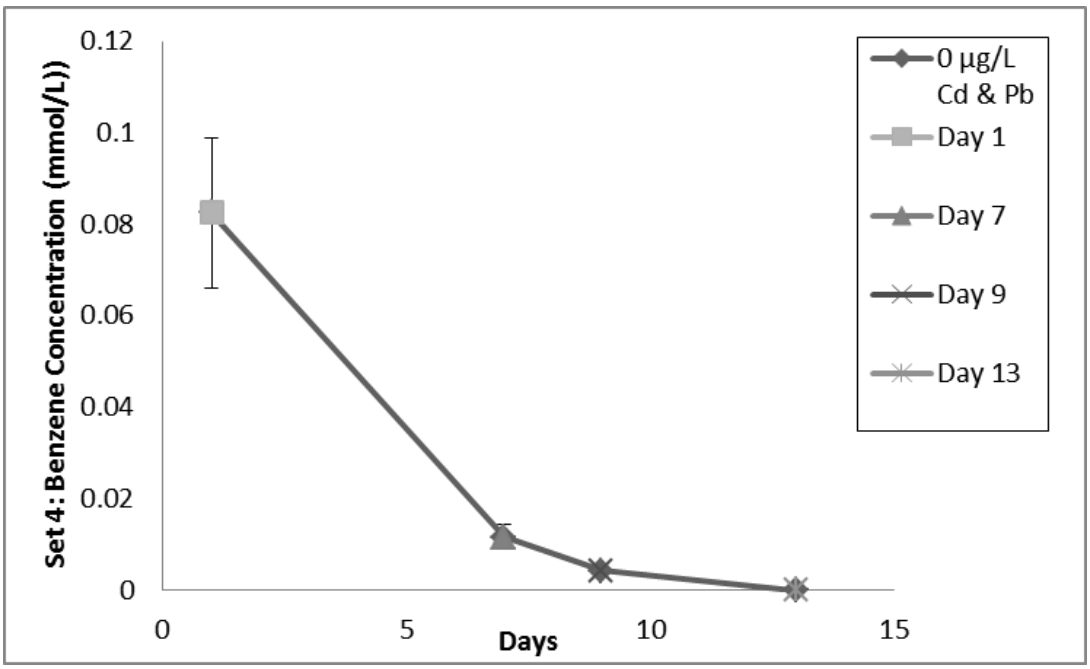

Figure 31: The figure shows the set 4 benzene degradation curve in the 0 µg/L Cd and Pb microcosms. The degradation of benzene occurs over an exponential slope. Starting benzene concentration was 0.2244 mM. Due to the immediate drop in concentration there was no real lag time observed. As shown in the previous tables the degradation is a result of biological activity, due to a lack of degradation in the sterile controls. Complete degradation occurred on day 13.

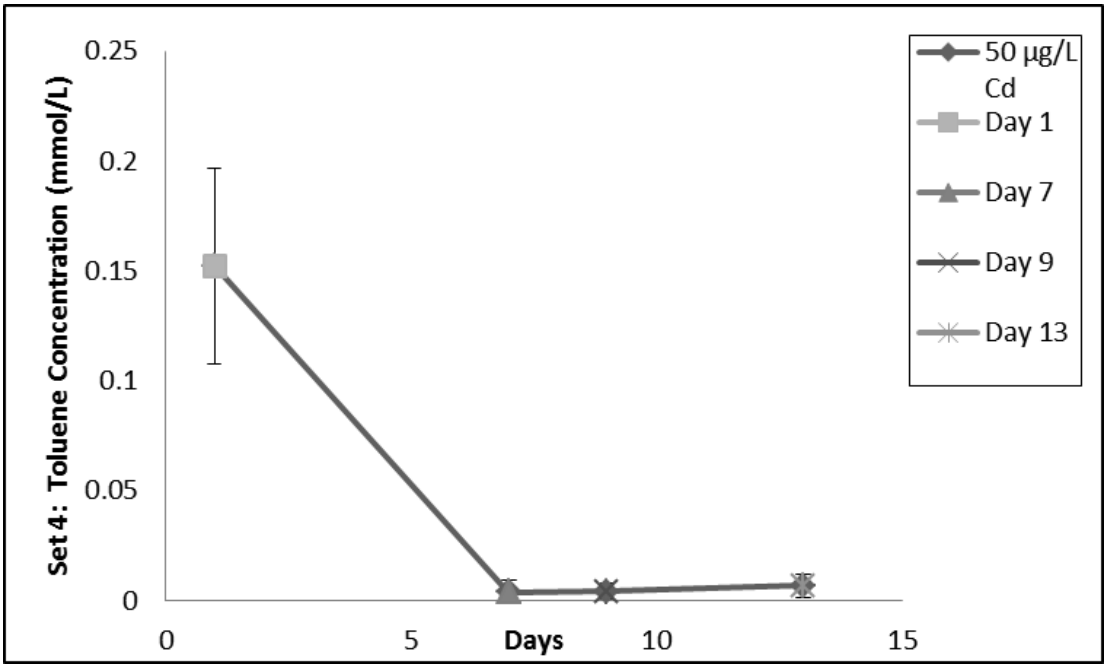

Figure 32: The figure shows the set 4 toluene degradation curve in the 50 µg/L Cd microcosms. The degradation of toluene occurs is linear. Starting toluene concentration was 0.1888 mM. Due to the immediate drop in concentration there was no real lag time observed. As shown in the previous tables the degradation is a result of biological activity, due to a lack of degradation in the sterile controls. Complete degradation occurred on day 7.

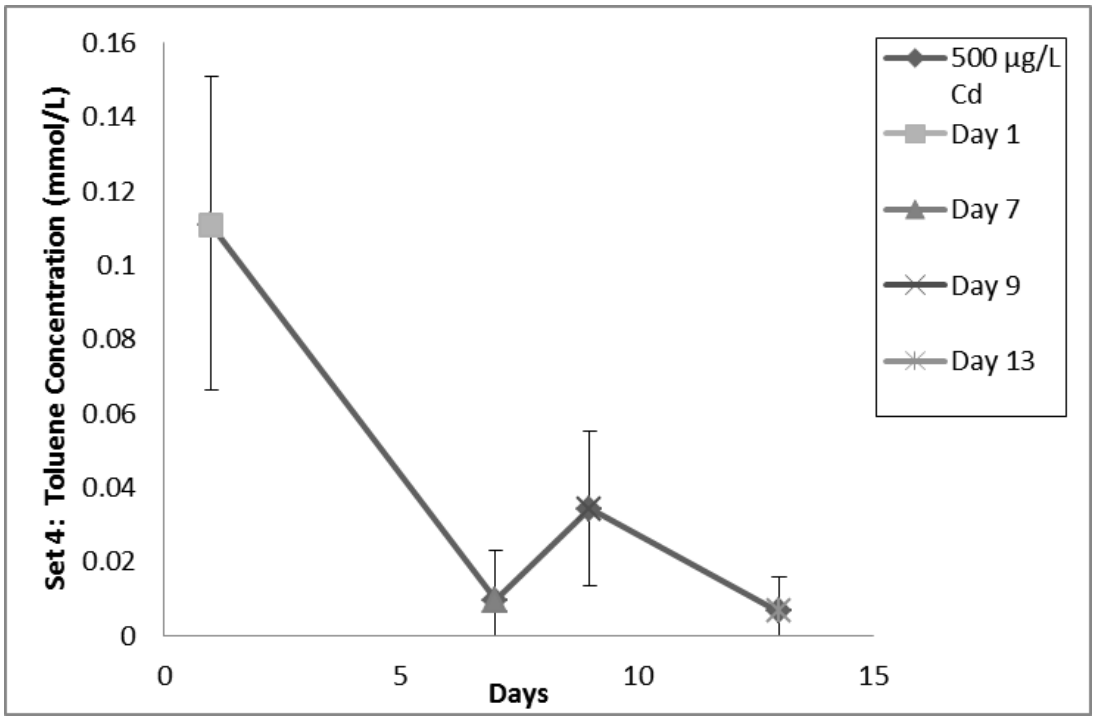

Figure 33: The figure shows the set 4 toluene degradation curve in the 500 µg/L Cd microcosms. The degradation of toluene occurs is linear. Starting toluene concentration was 0.1888 mM. Due to the immediate drop in concentration there was no real lag time observed. As shown in the previous tables the degradation is a result of biological activity, due to a lack of degradation in the sterile controls.

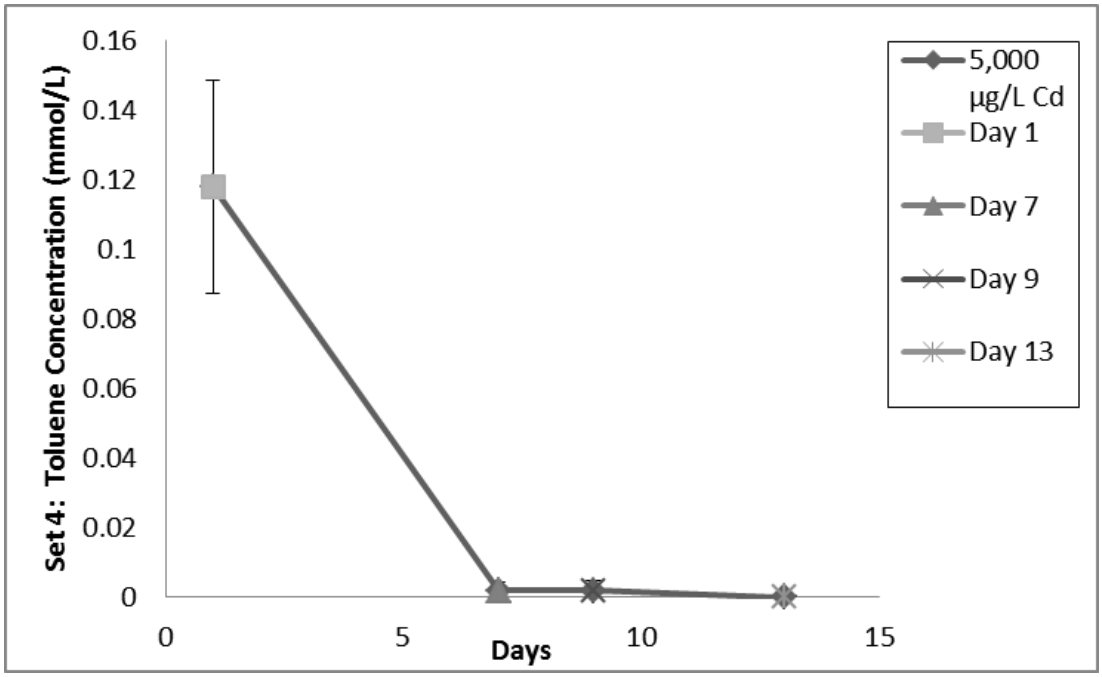

Figure 34: The figure shows the set 4 toluene degradation curve in the 5,000 µg/L Cd microcosms. The degradation of toluene occurs is linear. Starting toluene concentration was 0.1888 mM. Due to the immediate drop in concentration there was no real lag time observed. As shown in the previous tables the degradation is a result of biological activity, due to a lack of degradation in the sterile controls. Complete degradation occurred on day 7.

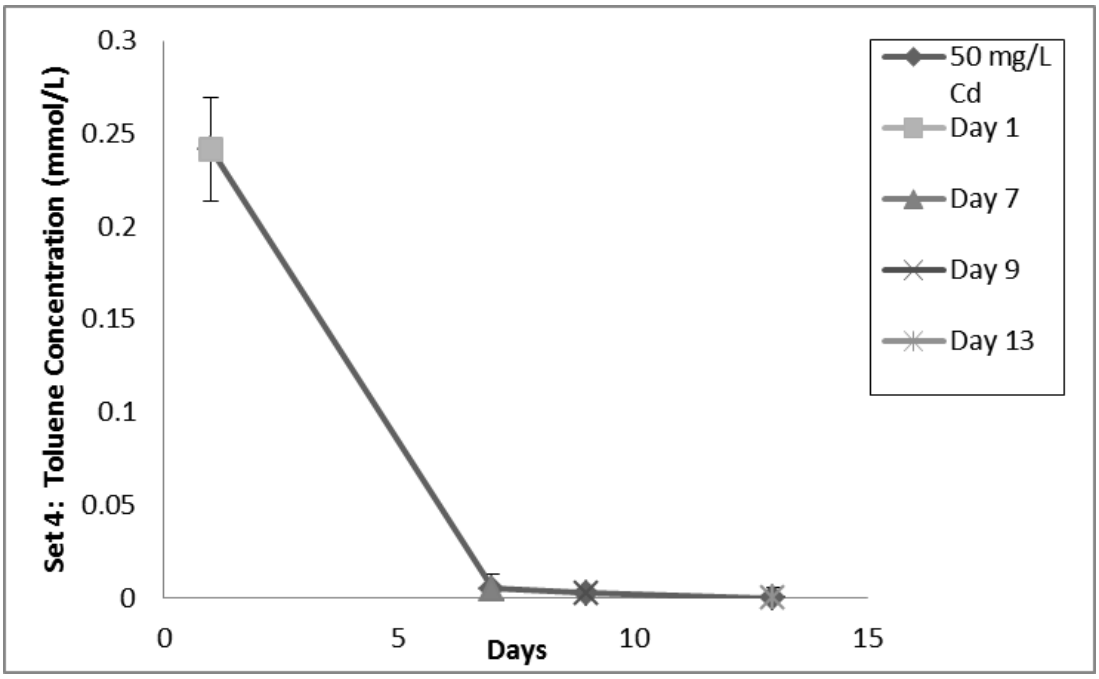

Figure 35: The figure shows the set 4 toluene degradation curve in the 50 mg/L Cd microcosms. The degradation of toluene occurs is linear. Starting toluene concentration was 0.1888 mM. As shown in the previous tables the degradation is a result of biological activity, due to a lack of degradation in the sterile controls. Complete degradation occurred on day 9.

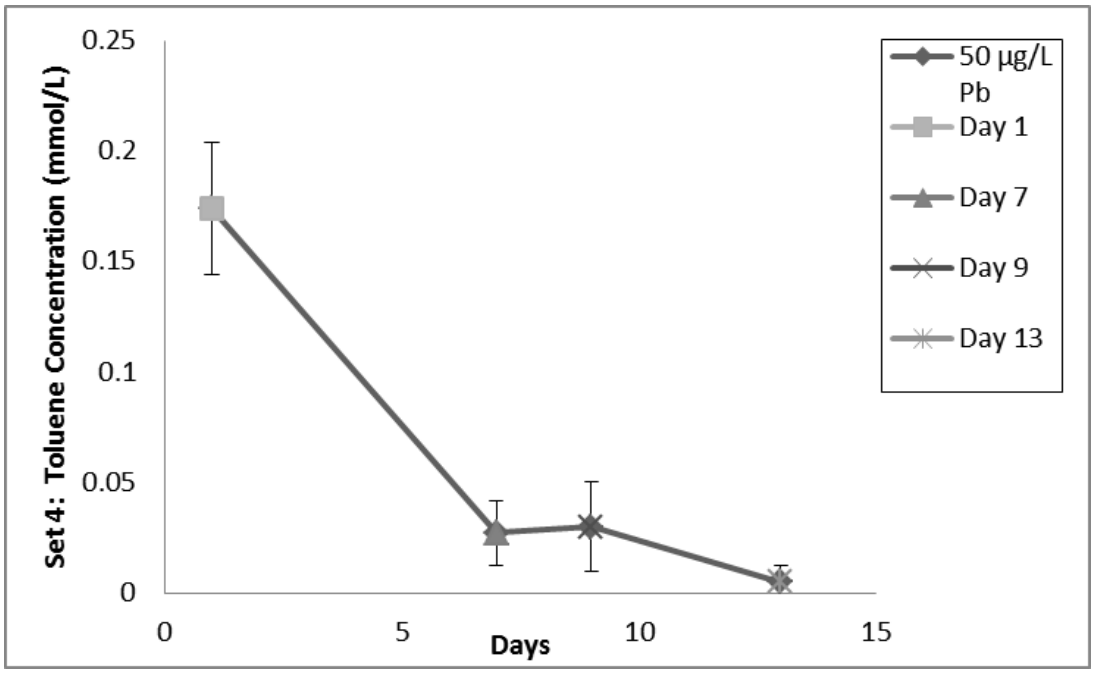

Figure 36: The figure shows the set 4 toluene degradation curve in the 50 µg/L Pb microcosms. The degradation of toluene occurs is linear. Starting toluene concentration was 0.1888 mM. As shown in the previous tables the degradation is a result of biological activity, due to a lack of degradation in the sterile controls.

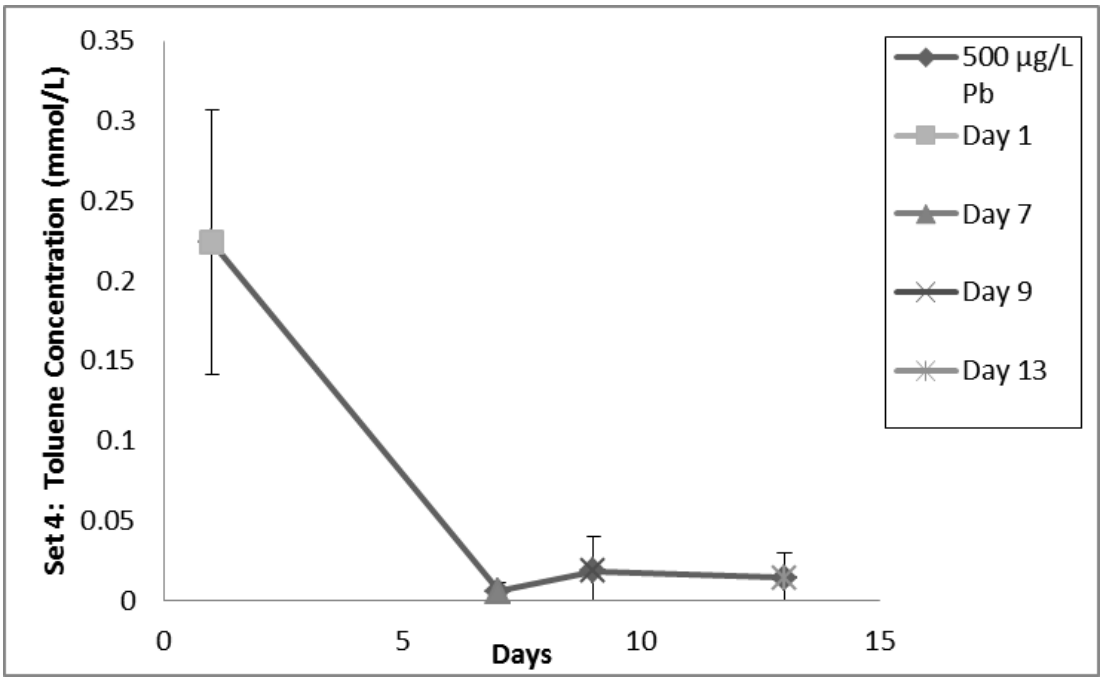

Figure 37: The figure shows the set 4 toluene degradation curve in the 500 µg/L Pb microcosms. The degradation of toluene occurs is linear. Starting toluene concentration was 0.1888 mM. As shown in the previous tables the degradation is a result of biological activity, due to a lack of degradation in the sterile controls.

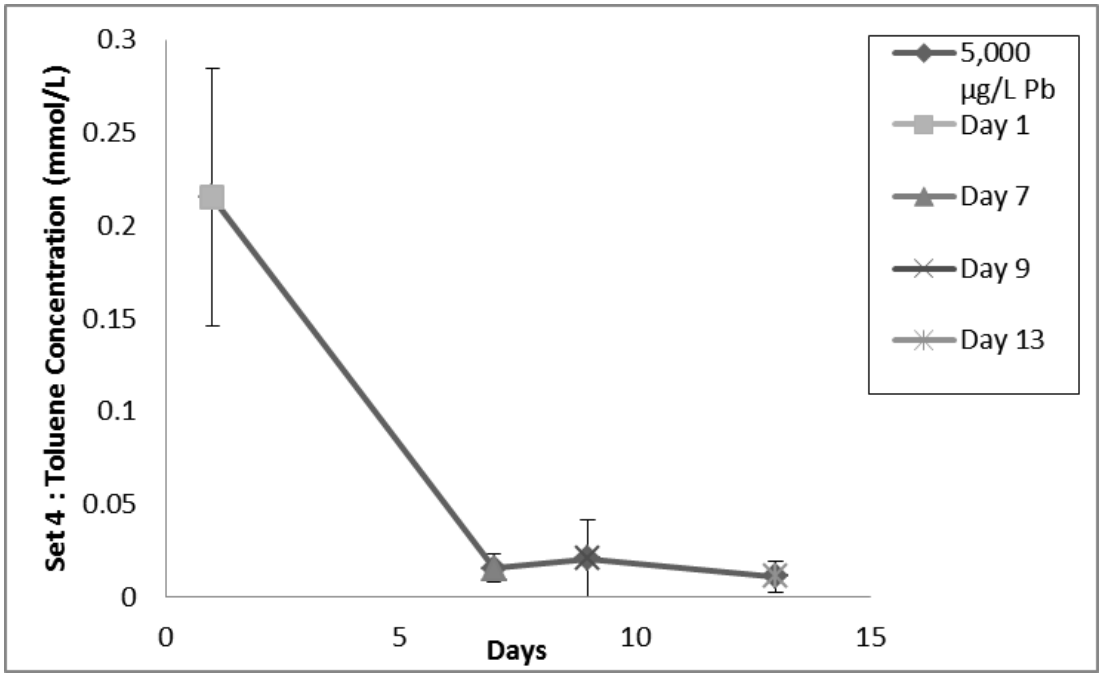

Figure 38: The figure shows the set 4 toluene degradation curve in the 5,000 µg/L Pb microcosms. The degradation of toluene occurs is linear. Starting toluene concentration was 0.1888 mM. As shown in the previous tables the degradation is a result of biological activity, due to a lack of degradation in the sterile controls.

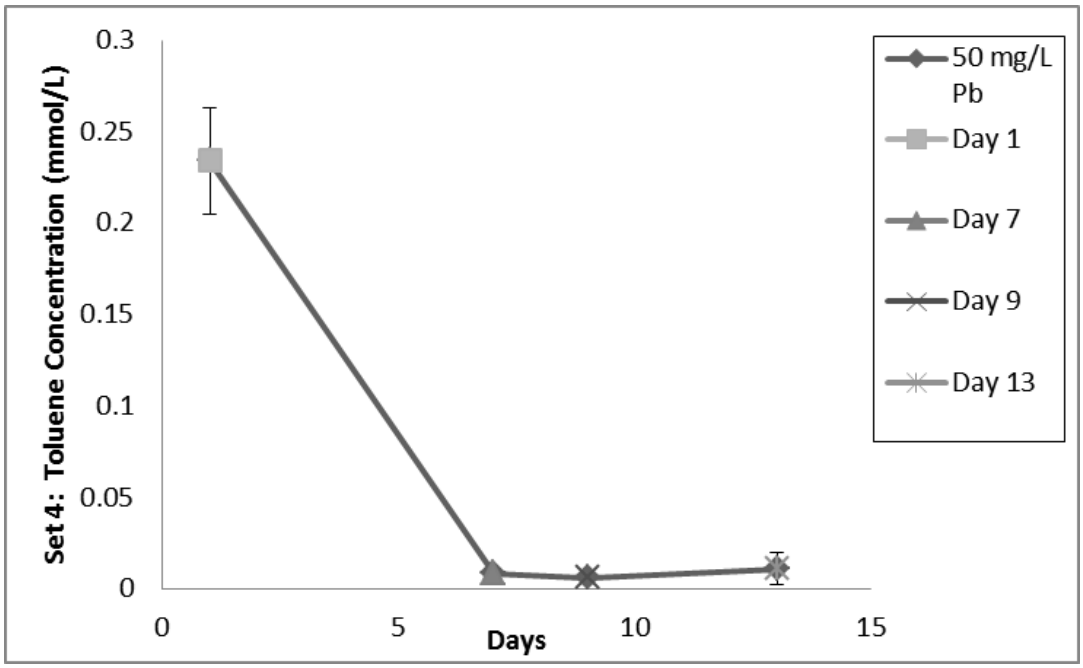

Figure 39: The figure shows the set 4 toluene degradation curve in the 50 mg/L Pb microcosms. The degradation of toluene occurs is linear. Starting toluene concentration was 0.1888 mM. As shown in the previous tables the degradation is a result of biological activity, due to a lack of degradation in the sterile controls. Complete degradation occurred on day 7.

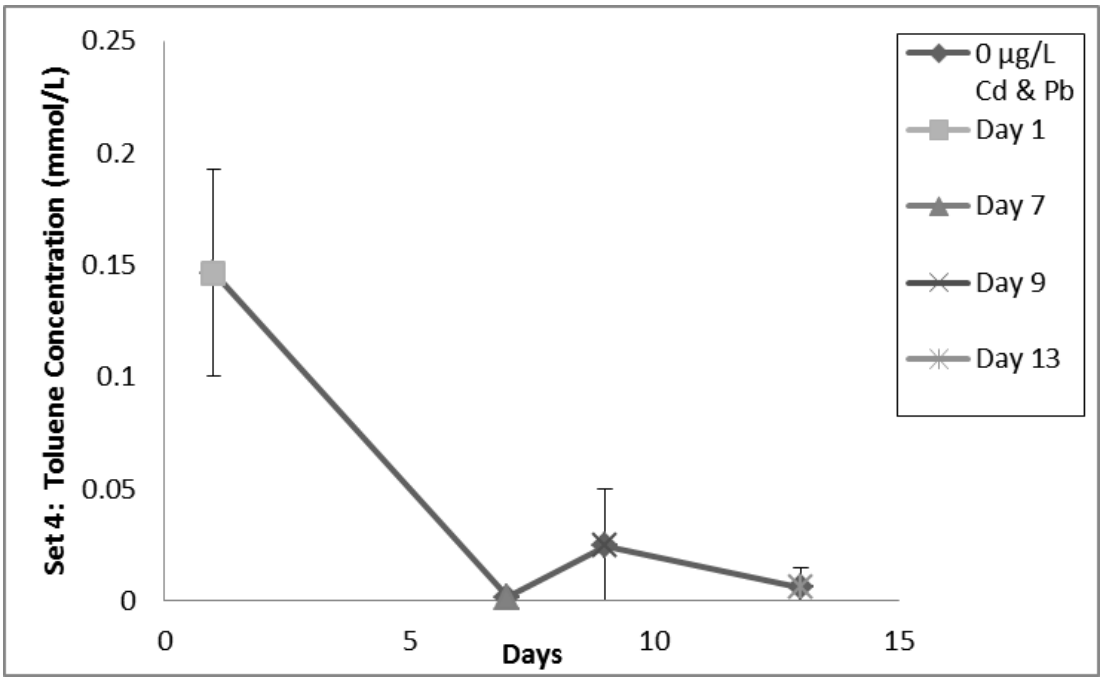

Figure 40: The figure shows the set 4 toluene degradation curve in the 0 µg/L Cd and Pb microcosms. The degradation of toluene occurs is linear. Starting toluene concentration was 0.1888 mM. Due to the immediate drop in concentration there was no real lag time observed. As shown in the previous tables the degradation is a result of biological activity, due to a lack of degradation in the sterile controls.

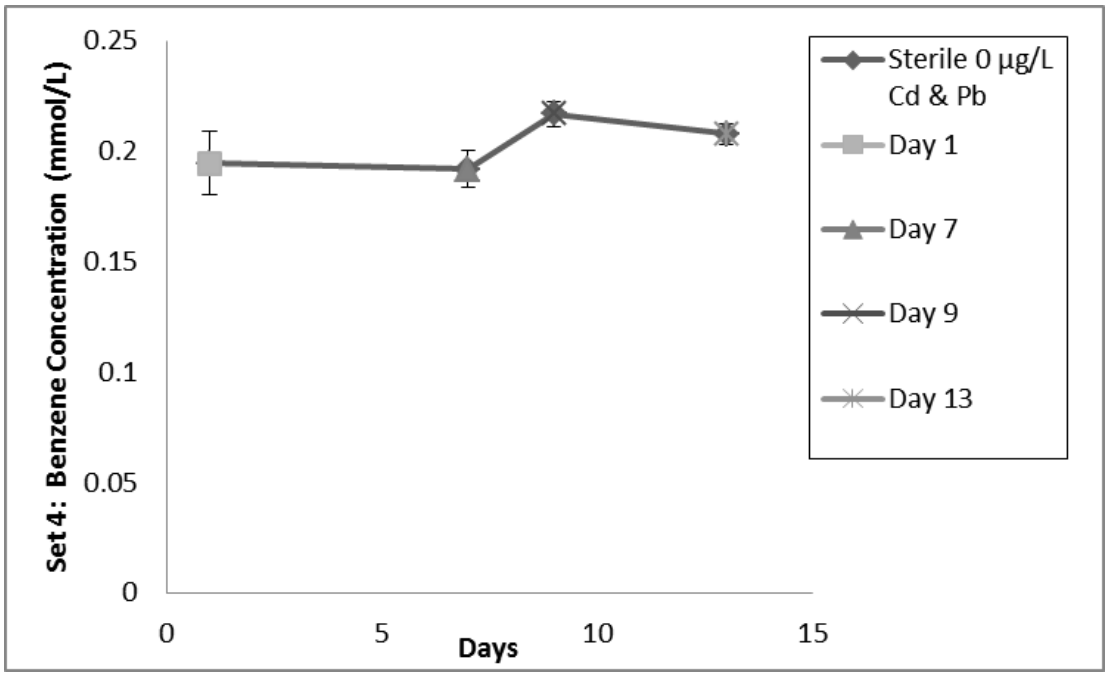

Figure 41: The figure shows the set 4 benzene sterile control for the 0 µg/L Cd and Pb microcosms. The sterile controls were autoclaved for three days straight to remove all microbiological activity. The standard deviation of the concentration of the microcosms was very low. There was no degradation detected in the microcosms, proving the degradation found in the normal microcosms was due to biological activity.

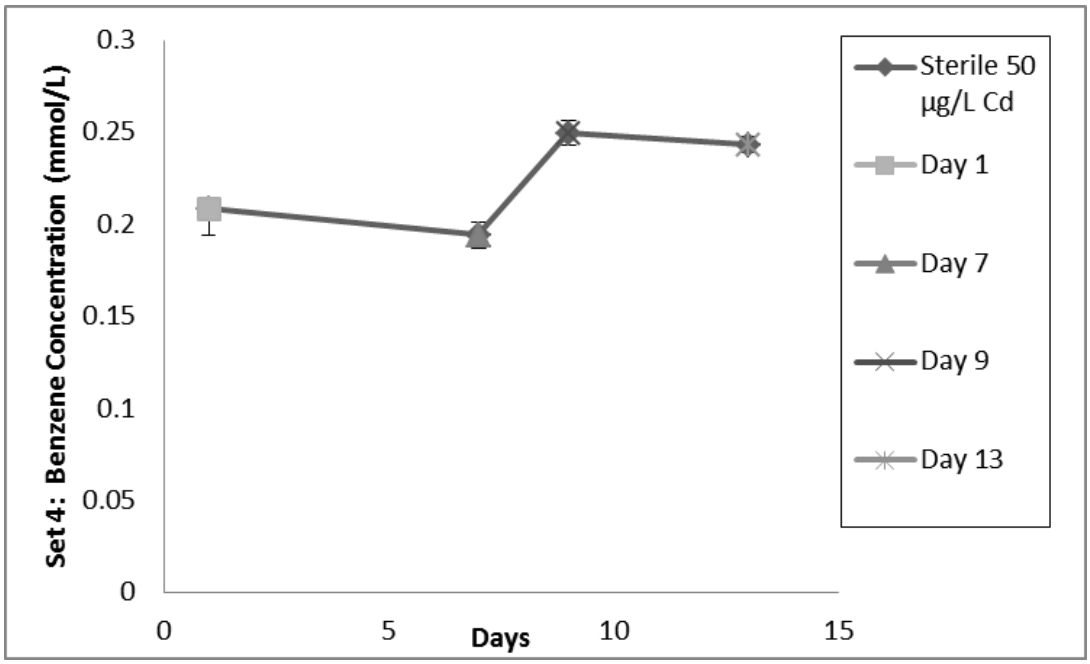

Figure 42: The figure shows the set 4 benzene sterile control for the 50 µg/L Cd microcosms. The sterile controls were autoclaved for three days straight to remove all microbiological activity. The standard deviation of the concentration of the microcosms was very low. There is also a small amount of variance in the linear concentration data. There was no degradation detected in the microcosms, proving the degradation found in the normal microcosms was due to biological activity.

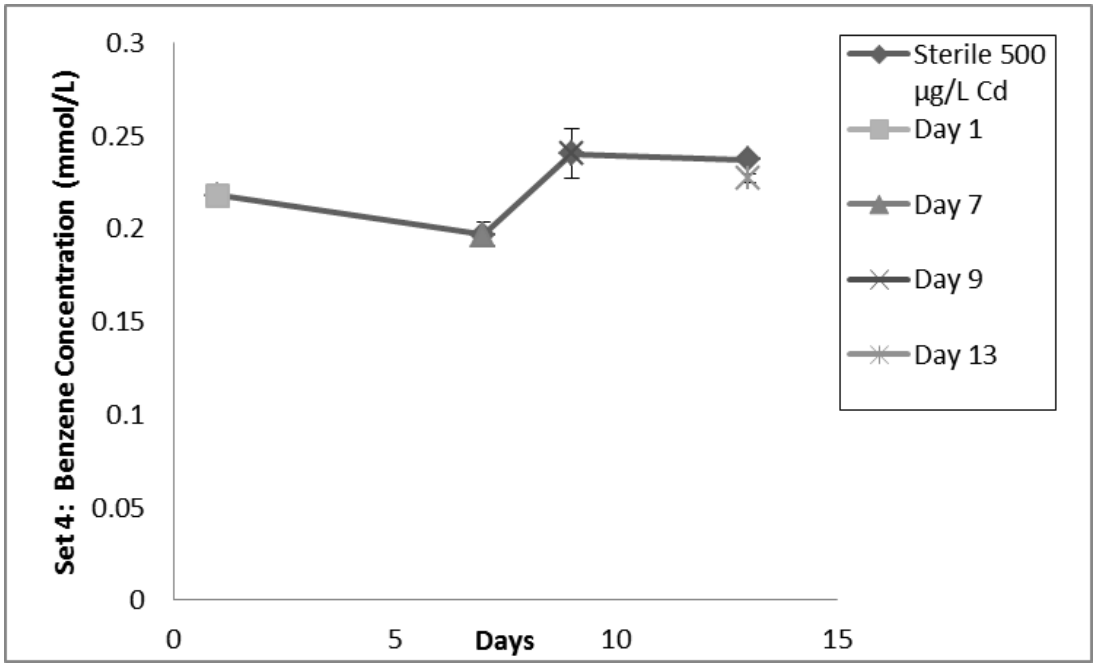

Figure 43: The figure shows the set 4 benzene sterile control for the 500 µg/L Cd microcosms. The sterile controls were autoclaved for three days straight to remove all microbiological activity. The standard deviation of the concentration of the microcosms was very low. There is also a small amount of variance in the linear concentration data. There was no degradation detected in the microcosms, proving the degradation found in the normal microcosms was due to biological activity.

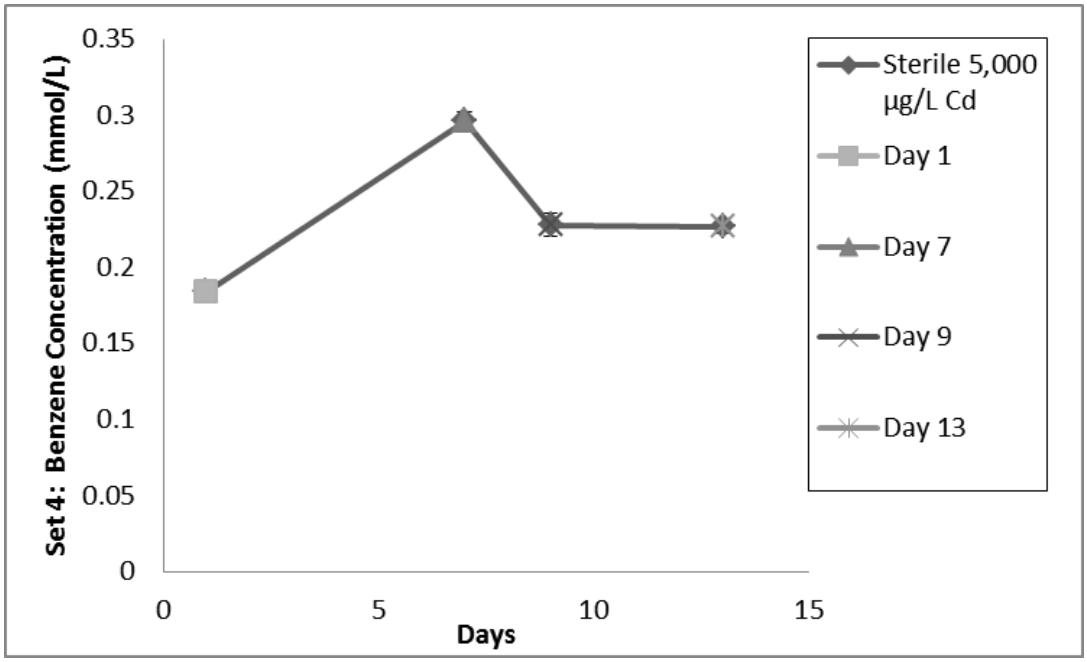

Figure 44: The figure shows the set 4 benzene sterile control for the 5,000 µg/L Cd microcosms. The sterile controls were autoclaved for three days straight to remove all microbiological activity. The standard deviation of the concentration of the microcosms was very low. There is also a greater amount of variance in the data points. Though the data is not very precise, the overall tread is no degradation. There was no degradation detected in the microcosms, proving the degradation found in the normal microcosms was due to biological activity.

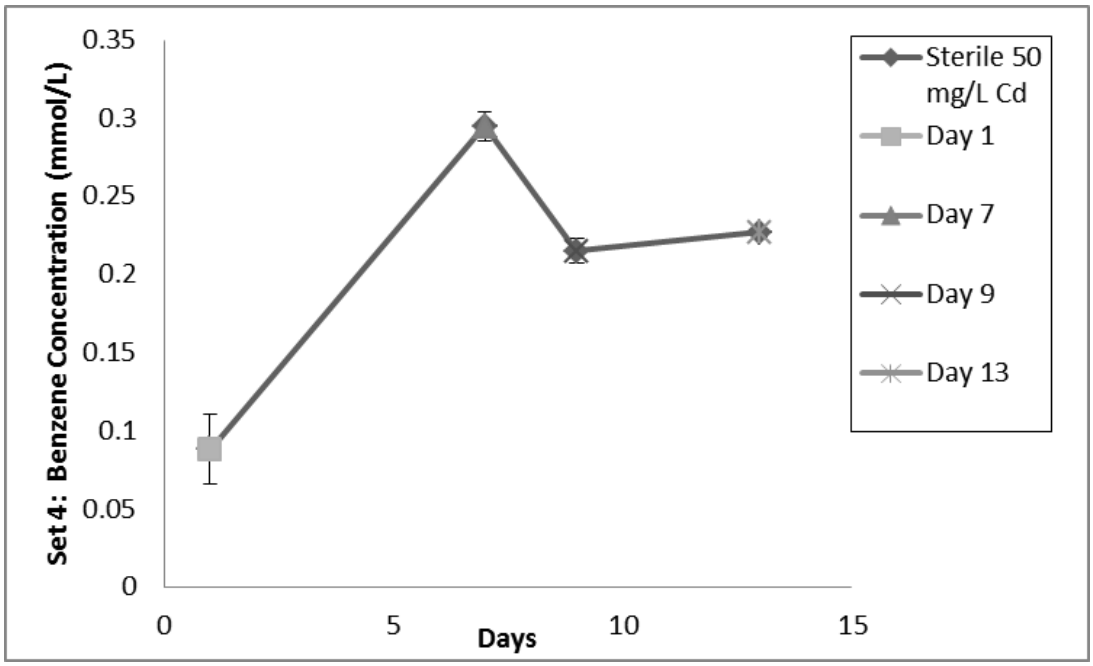

Figure 45: The figure shows the set 4 benzene sterile control for the 50 mg/L Cd microcosms. The sterile controls were autoclaved for three days straight to remove all microbiological activity. The standard deviation of the concentration of the microcosms was very low. There is also a greater amount of variance in the data points. Though the data is not very precise, the overall tread is no degradation. There was no degradation detected in the microcosms, proving the degradation found in the normal microcosms was due to biological activity.

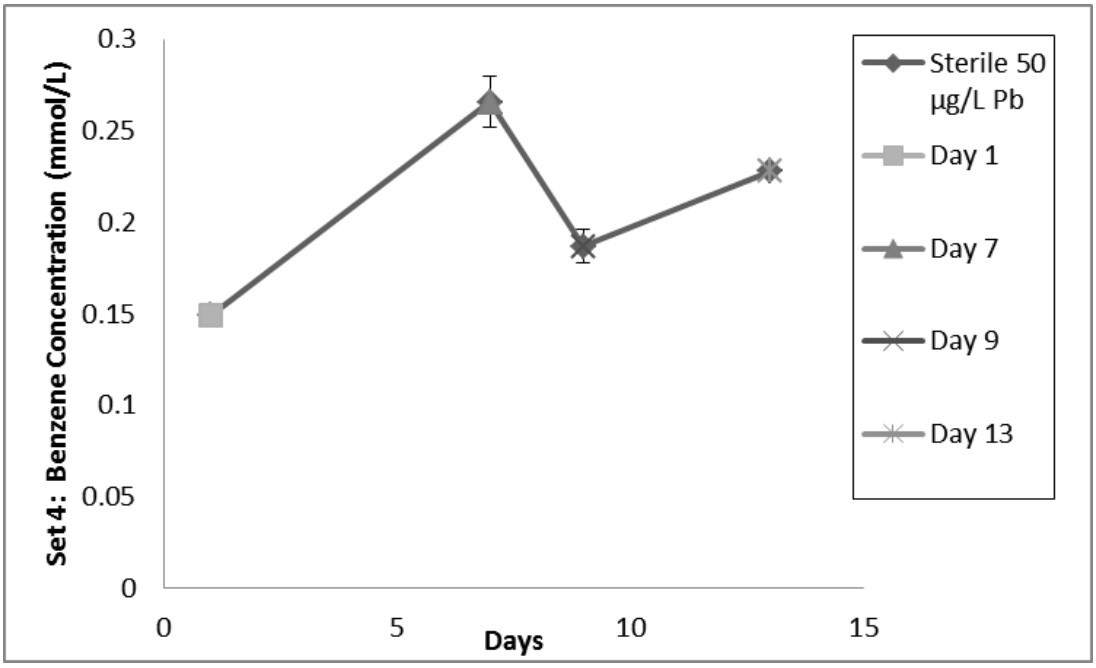

Figure 46: The figure shows the set 4 benzene sterile control for the 50 µg/L Pb microcosms. The sterile controls were autoclaved for three days straight to remove all microbiological activity. The standard deviation of the concentration of the microcosms was very low. There is also a greater amount of variance in the linear concentration data. Though the data is not very precise, the overall tread is no degradation. There was no degradation detected in the microcosms, proving the degradation found in the normal microcosms was due to biological activity.

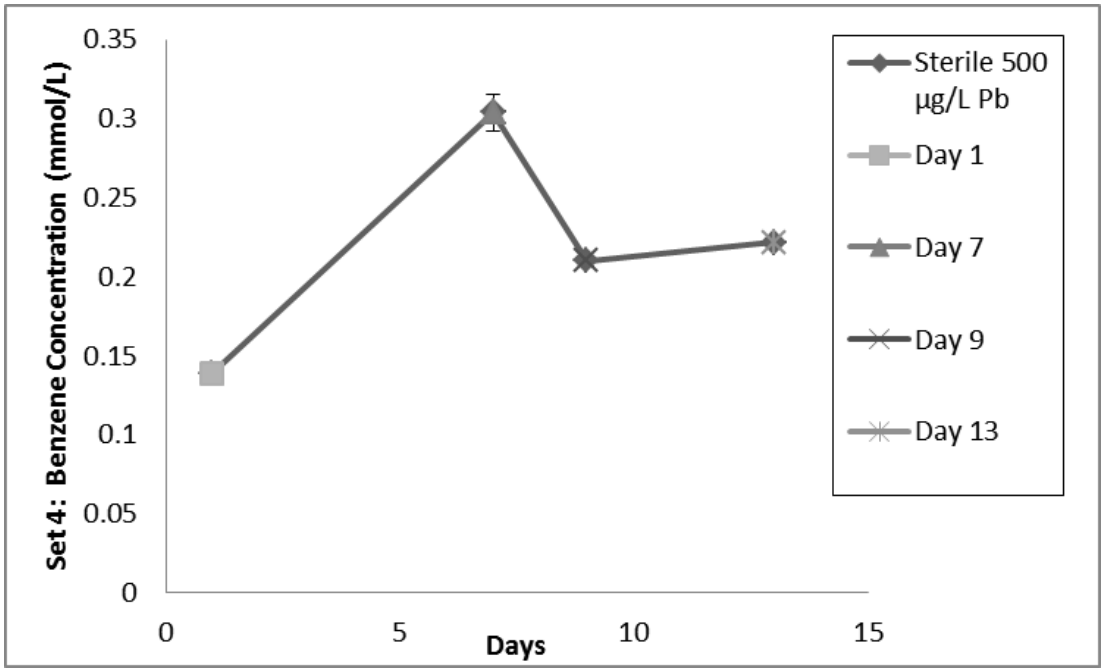

Figure 47: The figure shows the set 4 benzene sterile control for the 500 µg/L Pb microcosms. The sterile controls were autoclaved for three days straight to remove all microbiological activity. The standard deviation of the concentration of the microcosms was very low. There is also a greater amount of variance in the data points. Though the data is not very precise, the overall tread is no degradation. There was no degradation detected in the microcosms, proving the degradation found in the normal microcosms was due to biological activity.

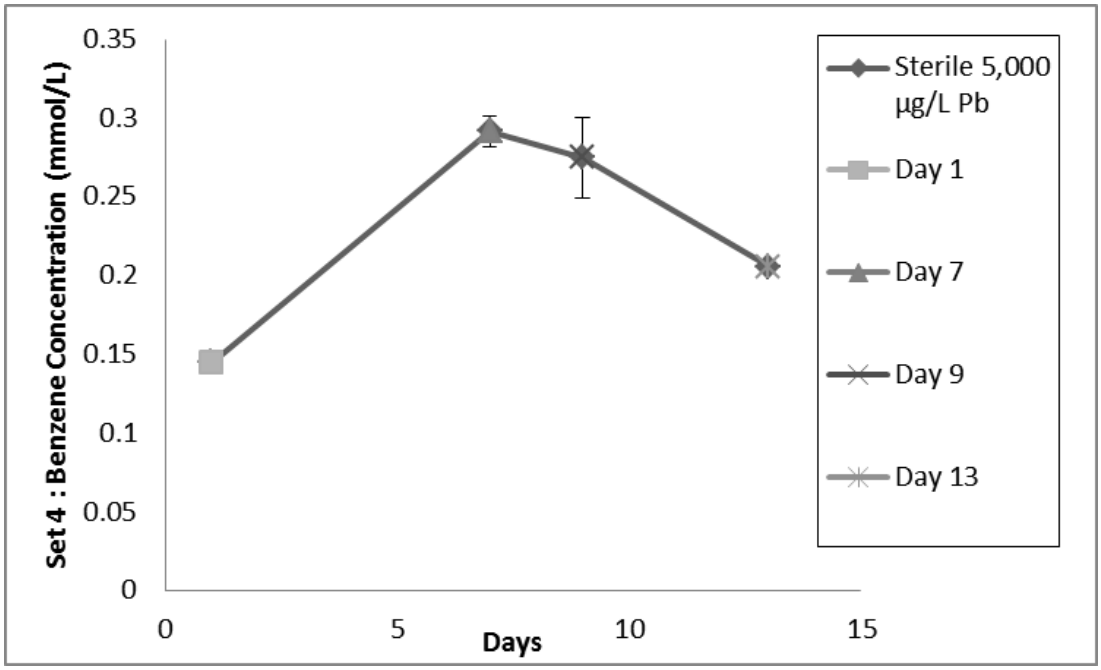

Figure 48: The figure shows the set 4 benzene sterile control for the 5,000 µg/L Pb microcosms. The sterile controls were autoclaved for three days straight to remove all microbiological activity. The standard deviation of the concentration of the microcosms was very low. There is also a greater amount of variance in the data points. There was no degradation detected in the microcosms, proving the degradation found in the normal microcosms was due to biological activity.

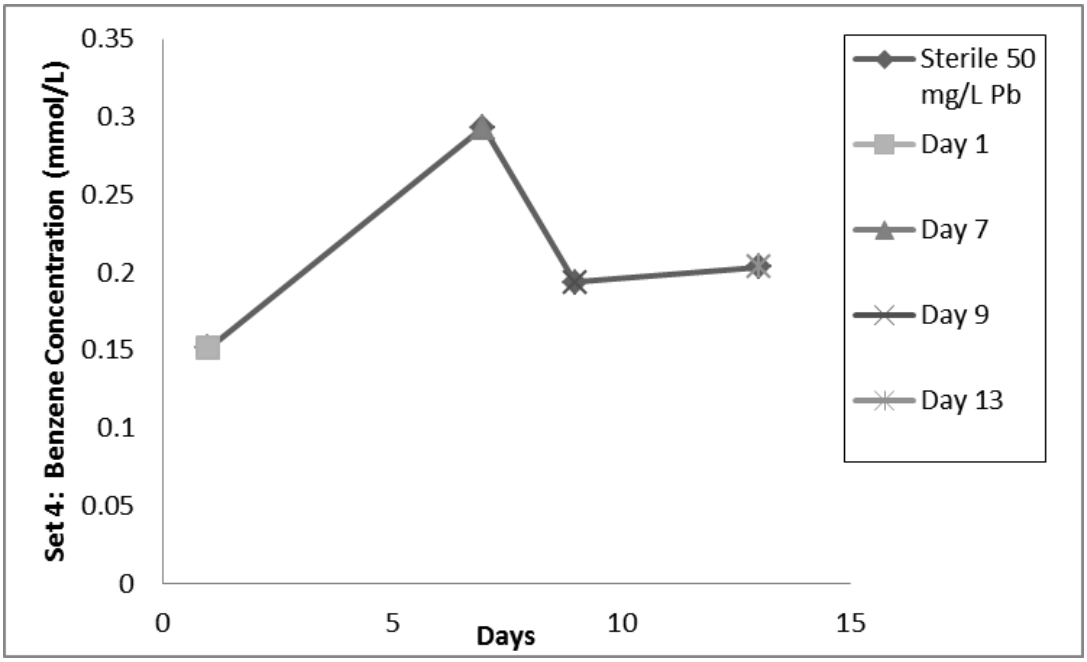

Figure 49: The figure shows the set 4 benzene sterile control for the 50 mg/L Pb microcosms. The sterile controls were autoclaved for three days straight to remove all microbiological activity. The standard deviation of the concentration of the microcosms was very low. There is also a greater amount of variance in the data points. Though the data is not very precise, the overall tread is no degradation. There was no degradation detected in the microcosms, proving the degradation found in the normal microcosms was due to biological activity.

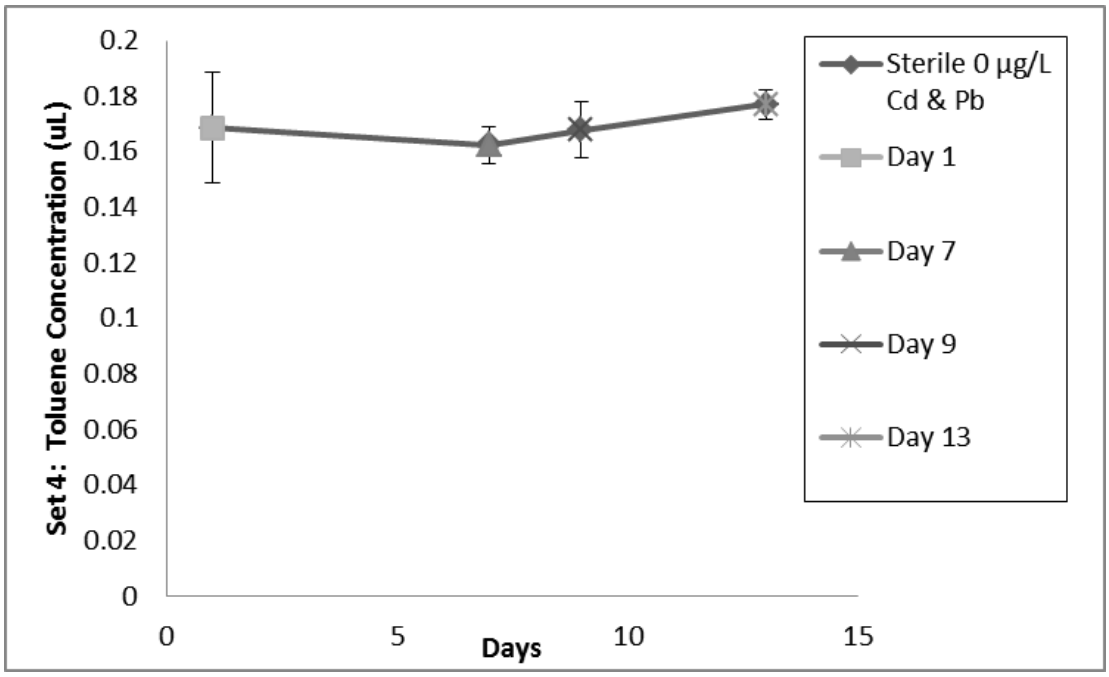

Figure 50: The figure shows the set 4 toluene sterile control for the 0 µg/L Cd and Pb microcosms. The sterile controls were autoclaved for three days straight to remove all microbiological activity. The standard deviation of the concentration of the microcosms was very low. There is also a little to no variance in the linear concentration data. There was no degradation detected in the microcosms, proving the degradation found in the normal microcosms was due to biological activity.

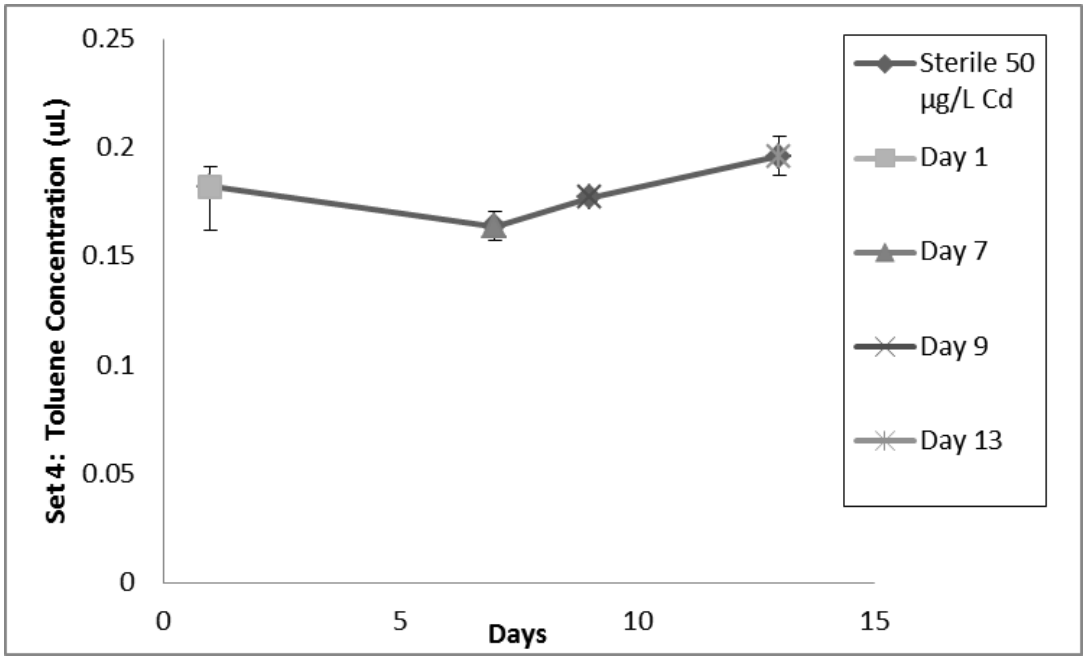

Figure 51: The figure shows the set 4 toluene sterile control for the 50 µg/L Cd microcosms. The sterile controls were autoclaved for three days straight to remove all microbiological activity. The standard deviation of the concentration of the microcosms was very low. There is also a small amount of variance in the linear concentration data. There was no degradation detected in the microcosms, proving the degradation found in the normal microcosms was due to biological activity.

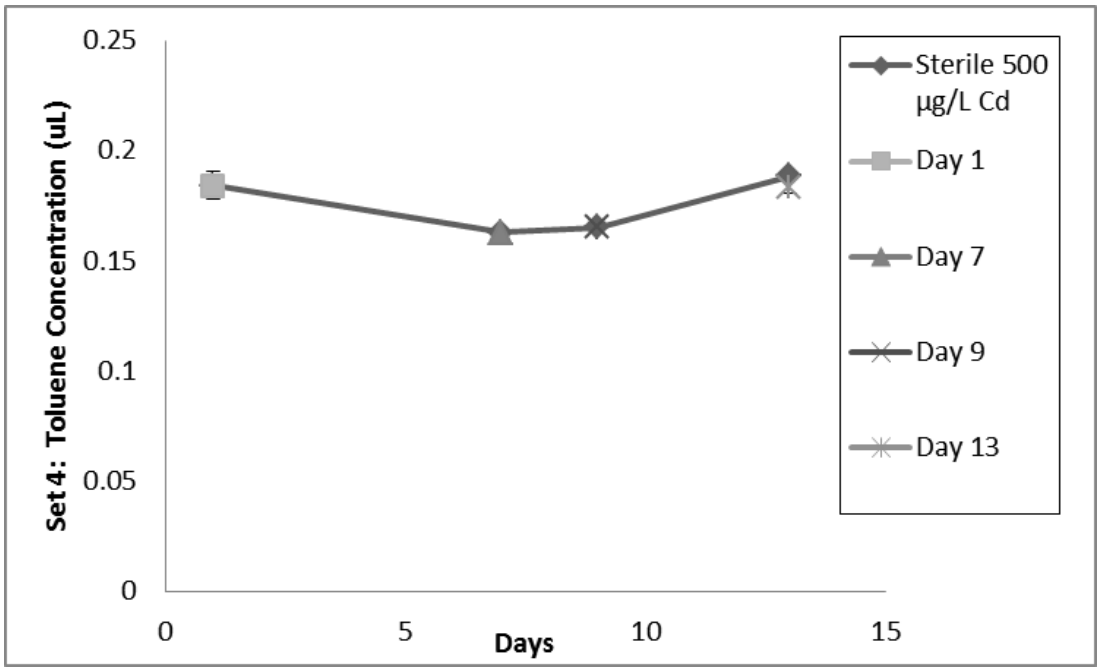

Figure 52: The figure shows the set 4 toluene sterile control for the 500 µg/L Cd microcosms. The sterile controls were autoclaved for three days straight to remove all microbiological activity. The standard deviation of the concentration of the microcosms was very low. There is also a small amount of variance in the linear concentration data. There was no degradation detected in the microcosms, proving the degradation found in the normal microcosms was due to biological activity.

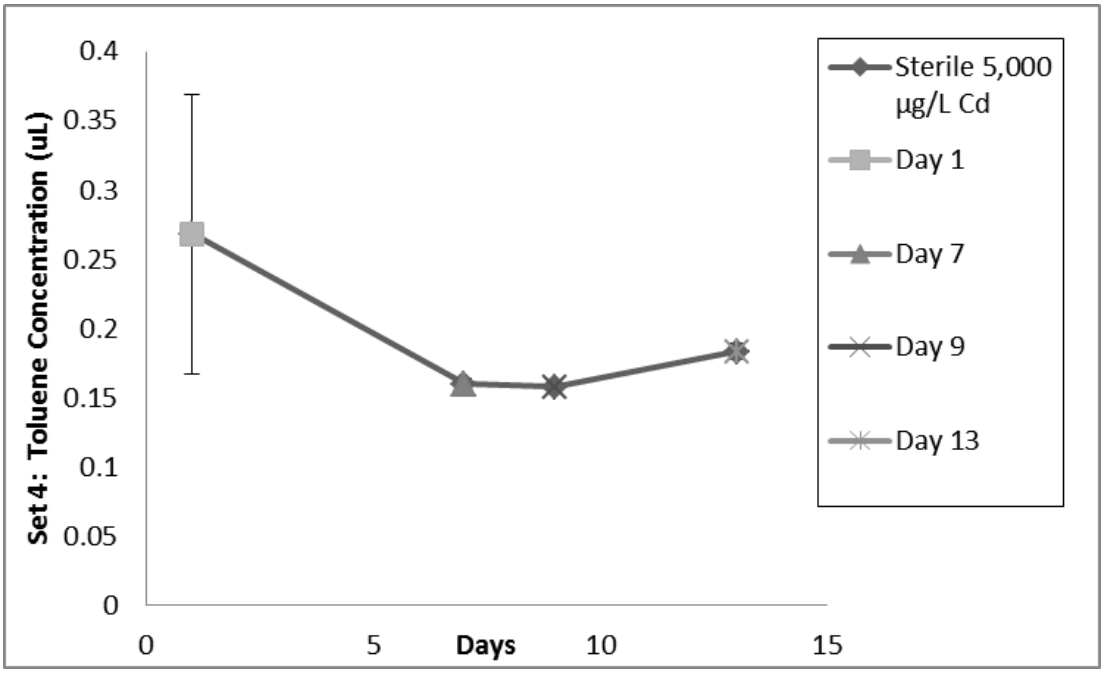

Figure 53: The figure shows the set 4 toluene sterile control for the 5,000 µg/L Cd microcosms. The sterile controls were autoclaved for three days straight to remove all microbiological activity. There is also a greater amount of variance in the linear concentration data. Though the data is not very precise, the overall tread is no degradation. Even though the slope of the function is negative, it ends around 0.1888 mM of toluene, showing there is still no degradation. There was no degradation detected in the microcosms, proving the degradation found in the normal microcosms was due to biological activity.

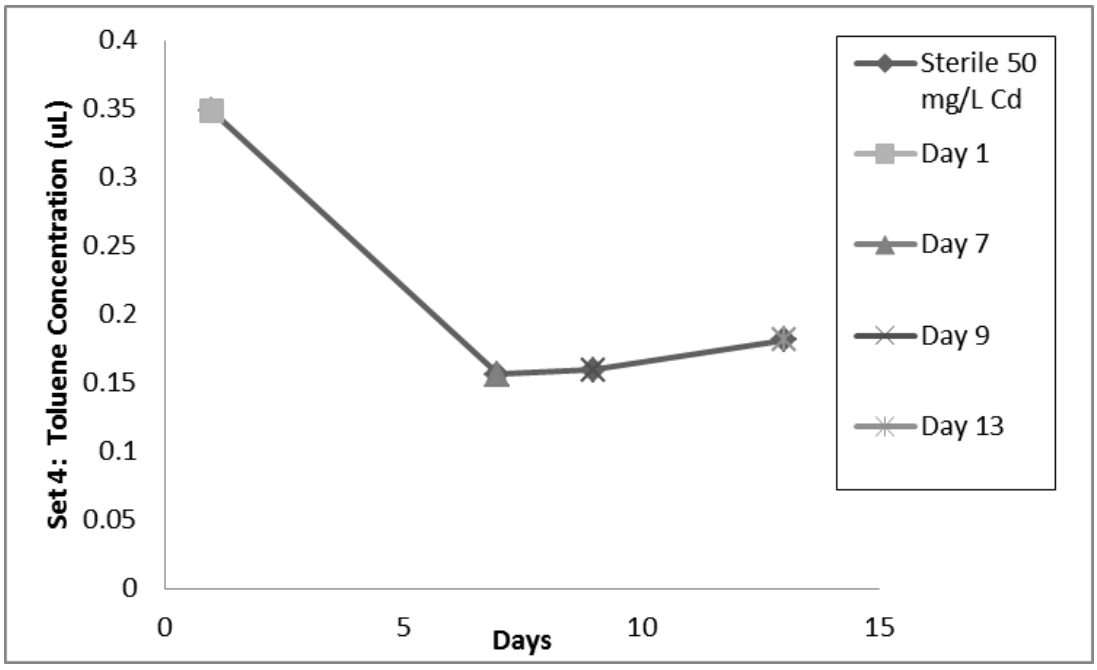

Figure 54: The figure shows the set 4 toluene sterile control for the 50 mg/L Cd microcosms. The sterile controls were autoclaved for three days straight to remove all microbiological activity. The standard deviation of the concentration of the microcosms was very low. There is also a greater amount of variance in the linear data points. Though the data is not very precise, the overall tread is no degradation. Even though the slope of the function is negative, it ends around 0.1888 mM of toluene, showing there is still no degradation. There was no degradation detected in the microcosms, proving the degradation found in the normal microcosms was due to biological activity.

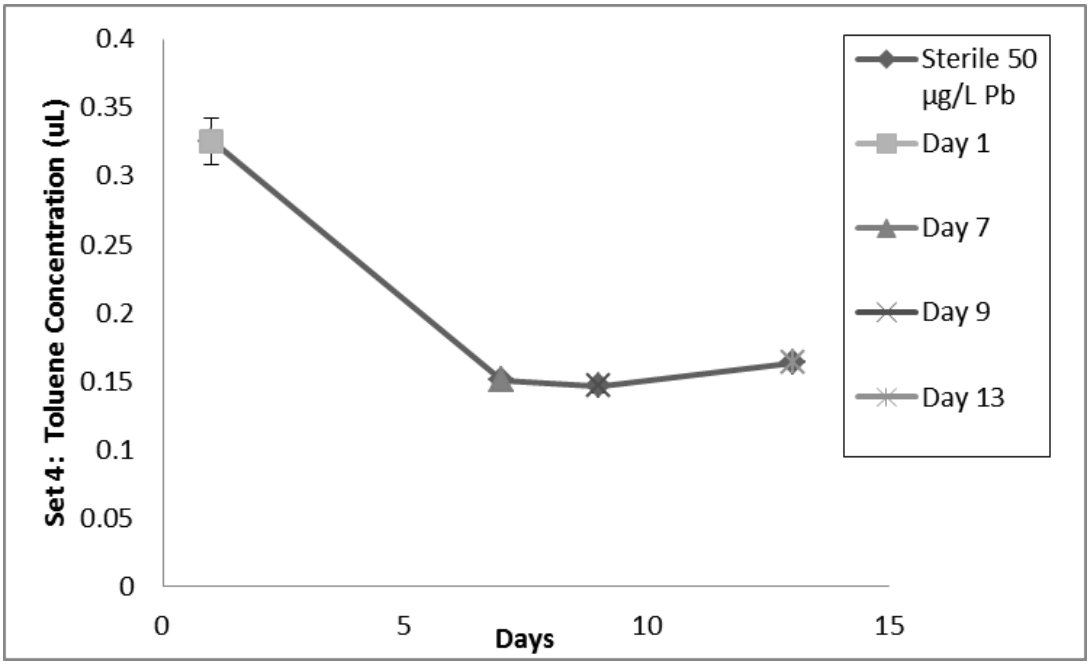

Figure 55: The figure shows the set 4 toluene sterile control for the 50 µg/L Pb microcosms. The sterile controls were autoclaved for three days straight to remove all microbiological activity. The standard deviation of the concentration of the microcosms was very low. There is also a greater amount of variance in the linear data points. Though the data is not very precise, the overall tread is no degradation. Even though the slope of the function is negative, it ends around 0.1888 mM of toluene, showing there is still no degradation. There was no degradation detected in the microcosms, proving the degradation found in the normal microcosms was due to biological activity.

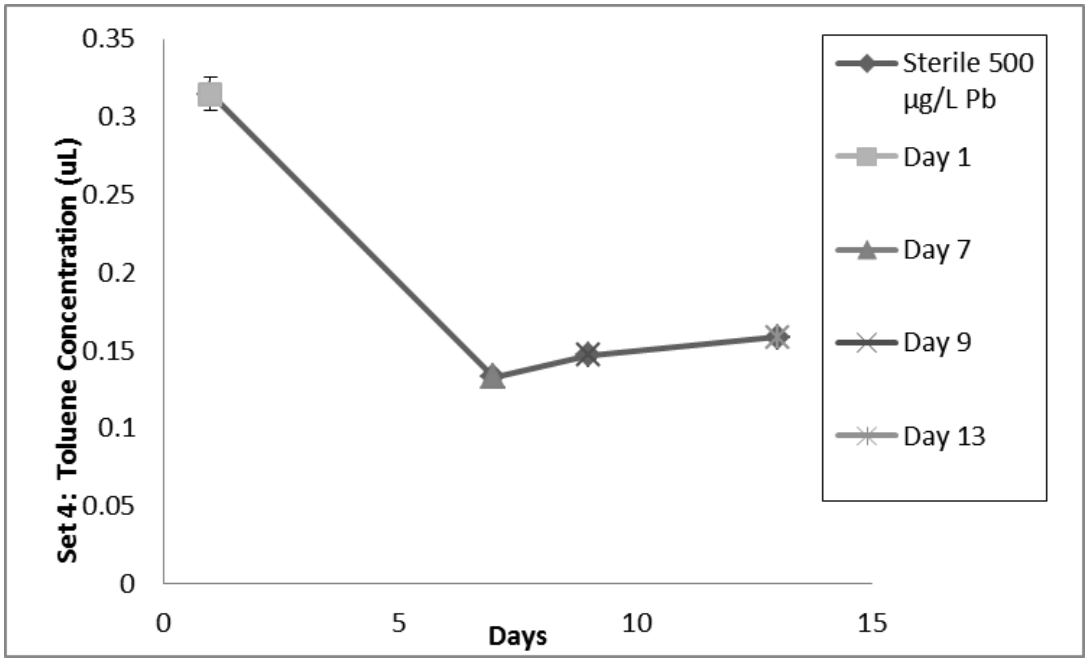

Figure 56: The figure shows the set 4 toluene sterile control for the 500 µg/L Pb microcosms. The sterile controls were autoclaved for three days straight to remove all microbiological activity. The standard deviation of the concentration of the microcosms was very low. There is also a greater amount of variance in the linear data points. Though the data is not very precise, the overall tread is no degradation. Even though the slope of the function is negative, it ends around 0.1888 mM of toluene, showing there is still no degradation. There was no degradation detected in the microcosms, proving the degradation found in the normal microcosms was due to biological activity.

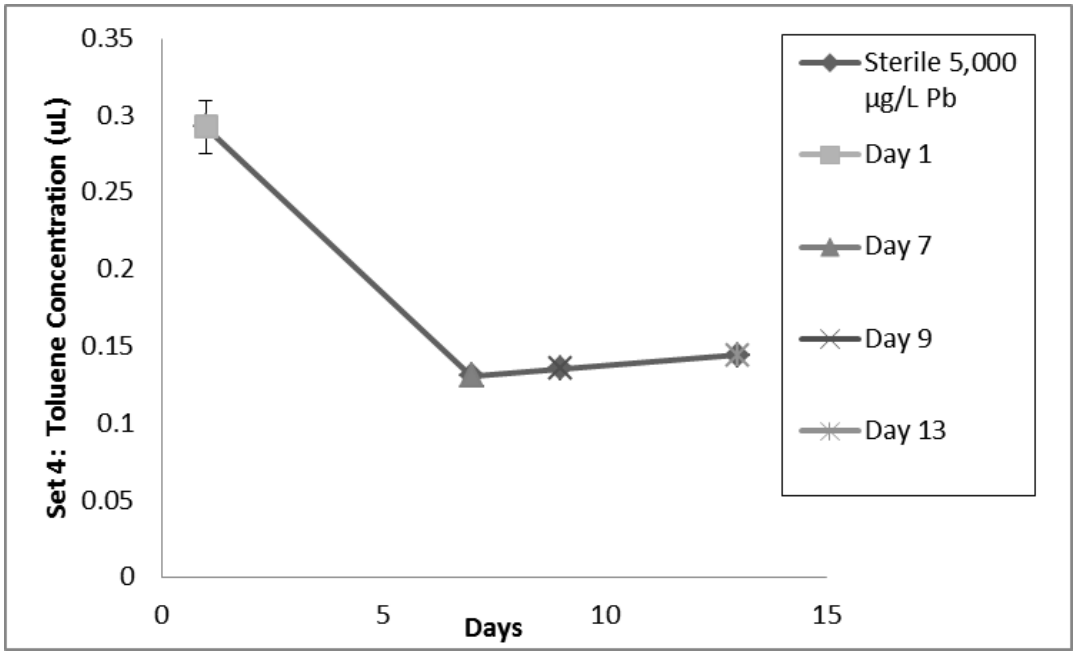

Figure 57: The figure shows the set 4 toluene sterile control for the 5,000 µg/L Pb microcosms. The sterile controls were autoclaved for three days straight to remove all microbiological activity. The standard deviation of the concentration of the microcosms was very low. There is also a greater amount of variance in the linear data points. Though the data is not very precise, the overall tread is no degradation. Even though the slope of the function is negative, it ends around 0.1888 mM of toluene, showing there is still no degradation. There was no degradation detected in the microcosms, proving the degradation found in the normal microcosms was due to biological activity.

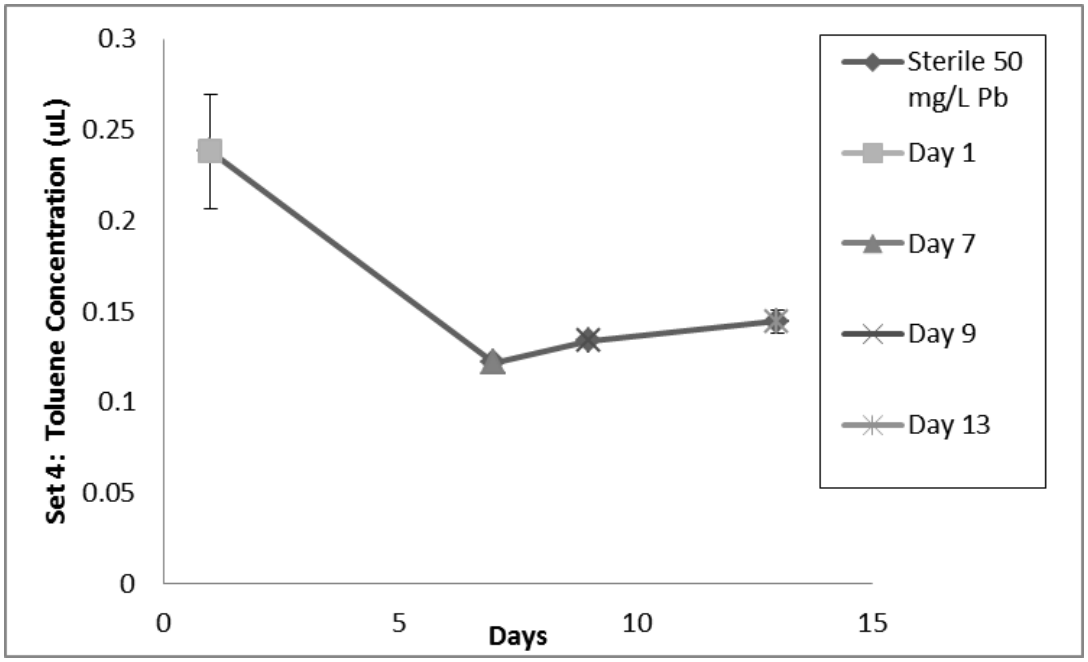

Figure 58: The figure shows the set 4 toluene sterile control for the 50 mg/L Pb microcosms. The sterile controls were autoclaved for three days straight to remove all microbiological activity. Though the data is not very precise, the overall tread is no degradation. There is also a greater amount of variance in the linear data points. Even though the slope of the function is negative, it ends around 0.1888 mM of toluene, showing there is still no degradation. There was no degradation detected in the microcosms, proving the degradation found in the normal microcosms was due to biological activity.

After the aerobic microcosms were found to biologically degrade benzene and toluene, the microcosms were re-spiked for 7 cycles. The re-spike was performed in order to build up the microbial community. This process allowed for easier identification of specific microbes during the dilution process by creating a larger stronger microbial community. The microcosms continued to degrade benzene or toluene, as shown in Tables 12 - 16 and Figures 59 - 85. Since it was determined that the degradation of benzene and toluene was due to biological activity, the sterile controls were removed from further aerobic experiments.

Toluene biodegradation was much faster than the degradation of benzene after the microbial population grew. The average degradation time for toluene was three days, while for benzene it was ten days. This shows that toluene is an easier to degrade than benzene. As the microbial population grows, benzene and toluene degradation increases.

Table 12: The data displayed in the table are all of the individual data points for degradation in the set 5.1 benzene microcosms. The data is representing degradation percentage. Complete degradation is represented by 100%. The table shows that the majority of microcosms fully degraded.

Set 5.1: Benzene Percent Degradation Data							
Concentration Metal	Sample	Day 0.08 Degradation (%)	Day 0.77 Degradation (%)	Day 1.56 Degradation (%)	Day 2.46 Degradation (%)	Day 5.52 Degradation (%)	Day 7.54 Degradation (%)
50 µg/L Cd	A-1	14.5	43.9	68.2	81.4	76.0	92.6
	A-2	28.3	52.6	70.5	71.0	89.8	93.2
	A-3	40.1	82.2	85.4	96.1	93.4	96.6
500 µg/L Cd	B-1	31.8	53.9	64.5	86.5	79.9	97.1
	B-2	23.8	58.5	70.4	77.5	71.4	96.0
	B-3	0.3	1.4	2.4	26.7	1.8	30.8
5,000 µg/L Cd	C-1	38.8	73.3	86.3	86.6	96.2	100.0
	C-2	9.0	9.2	30.4	69.4	83.6	98.3
	C-3	30.5	0.0	36.0	50.1	45.1	47.1
50 mg/L Cd	D-1	3.0	0.0	0.0	39.2	63.2	96.5
	D-2	9.1	22.1	41.9	70.6	85.1	99.7
	D-3	18.7	28.2	51.7	70.7	94.7	95.7
50 µg/L Pb	E-1	45.0	66.6	83.9	83.5	15.3	99.2
	E-2	13.6	30.8	22.4	58.6	76.9	93.0
	E-3	12.9	6.6	-4.2	10.7	4.3	14.0
500 µg/L Pb	F-1	38.1	59.1	74.3	79.7	92.2	100.0
	F-2	17.5	37.1	41.6	67.5	70.8	76.3
	F-3	40.1	62.1	75.4	79.4	77.9	88.4
5,000 µg/L Pb	G-1	45.1	70.5	84.8	88.1	90.8	99.3
	G-2	0.0	10.2	37.7	64.6	66.6	75.9
	G-3	18.7	7.5	29.0	42.3	42.8	47.3
50 mg/L Pb	H-1	46.1	65.6	79.0	77.4	91.3	96.4
	H-2	45.9	67.1	80.6	86.2	0.7	97.7
	H-3	32.0	24.2	9.5	17.6	-44.0	27.5
0 µg/L Cd & Pb	I-1	48.8	65.1	73.2	80.5	7.6	96.0
	I-2	53.1	28.9	85.0	79.5	92.6	100.0
	I-3	27.9	32.7	50.9	43.6	43.8	59.4

Table 13: The data displayed in the table are all of the individual data points for degradation in the set 5.1 toluene microcosms. The data is representing degradation percentage. Complete degradation is represented by 100%. The table shows that the majority of microcosms fully degraded.

Set 5.1: Toluene Percent Degradation Data					
Concentration Metal	Sample	Day 0.08 Degradation (%)	Day 0.77 Degradation (%)	Day 1.56 Degradation (%)	Day 2.46 Degradation (%)
50 µg/L Cd	K-1	17.2	78.4	100.0	100.0
	K-2	5.4	56.0	99.1	100.0
	K-3	52.0	100.0	100.0	100.0
500 µg/L Cd	L-1	44.0	99.4	100.0	100.0
	L-2	10.5	56.8	100.0	100.0
	L-3	46.0	97.5	100.0	100.0
5,000 µg/L Cd	M-1	34.9	95.2	100.0	100.0
	M-2	14.3	82.9	100.0	100.0
	M-3	55.7	100.0	100.0	100.0
50 mg/L Cd	N-1	33.5	96.3	100.0	100.0
	N-2	37.3	96.7	100.0	100.0
	N-3	62.0	97.2	100.0	100.0
50 µg/L Pb	O-1	31.2	91.0	100.0	100.0
	O-2	23.7	52.1	100.0	100.0
	O-3	37.1	86.6	100.0	100.0
500 µg/L Pb	P-1	25.1	80.3	100.0	100.0
	P-2	52.5	88.6	100.0	100.0
	P-3	63.3	100.0	98.9	100.0
5,000 µg/L Pb	Q-1	25.4	98.4	100.0	100.0
	Q-2	17.9	65.8	100.0	100.0
	Q-3	57.6	92.8	100.0	100.0
50 mg/L Pb	R-1	29.7	81.8	100.0	100.0
	R-2	56.1	98.1	100.0	100.0
	R-3	63.0	94.7	100.0	100.0
0 µg/L Cd & Pb	S-1	20.4	58.6	100.0	100.0
	S-2	47.8	70.0	100.0	100.0
	S-3	29.0	76.5	100.0	100.0

Table 14: The data displayed in the table are all of the individual data points for degradation in the set 5.2 toluene microcosms. The data is representing degradation percentage. Complete degradation is represented by 100%. The table shows that the majority of microcosms fully degraded.

Set 5.2: Toluene Percent Degradation Data			
Concentration Metal	Sample	Day 0.00 Degradation (%)	Day 0.98 Degradation (%)
50 µg/L Cd	K-1	82.3	100.0
	K-2	77.9	100.0
	K-3	96.5	100.0
500 µg/L Cd	L-1	84.1	100.0
	L-2	88.0	100.0
	L-3	100.0	100.0
5,000 µg/L Cd	M-1	86.8	100.0
	M-2	99.2	100.0
	M-3	99.5	100.0
50 mg/L Cd	N-1	98.8	100.0
	N-2	89.7	100.0
	N-3	100.0	100.0
50 µg/L Pb	O-1	91.3	100.0
	O-2	66.6	100.0
	O-3	100.0	100.0
500 µg/L Pb	P-1	69.5	100.0
	P-2	63.5	100.0
	P-3	85.1	100.0
5,000 µg/L Pb	Q-1	60.1	100.0
	Q-2	64.6	100.0
	Q-3	52.7	100.0
50 mg/L Pb	R-1	71.3	100.0
	R-2	100.0	100.0
	R-3	76.7	100.0
0 µg/L Cd & Pb	S-1	73.9	100.0
	S-2	78.1	100.0
	S-3	99.7	100.0

Table 15: The data displayed in the table are all of the individual data points for degradation in the set 5.7 toluene microcosms. The data is representing degradation percentage. Complete degradation is represented by 100%. The table shows that the majority of microcosms fully degraded.

Set 5.7: Toluene Percent Degradation Data		
Concentration Metal	Sample	Day 1.00 Degradation (%)
50 µg/L Cd	K-1	100.0
	K-2	100.0
	K-3	100.0
500 µg/L Cd	L-1	100.0
	L-2	100.0
	L-3	100.0
5,000 µg/L Cd	M-1	100.0
	M-2	95.5
	M-3	100.0
50 mg/L Cd	N-1	100.0
	N-2	100.0
	N-3	90.5
50 µg/L Pb	O-1	100.0
	O-2	100.0
	O-3	100.0
500 µg/L Pb	P-1	100.0
	P-2	100.0
	P-3	100.0
5,000 µg/L Pb	Q-1	100.0
	Q-2	100.0
	Q-3	90.5
50 mg/L Pb	R-1	100.0
	R-2	100.0
	R-3	100.0
0 µg/L Cd & Pb	S-1	100.0
	S-2	100.0
	S-3	94.6

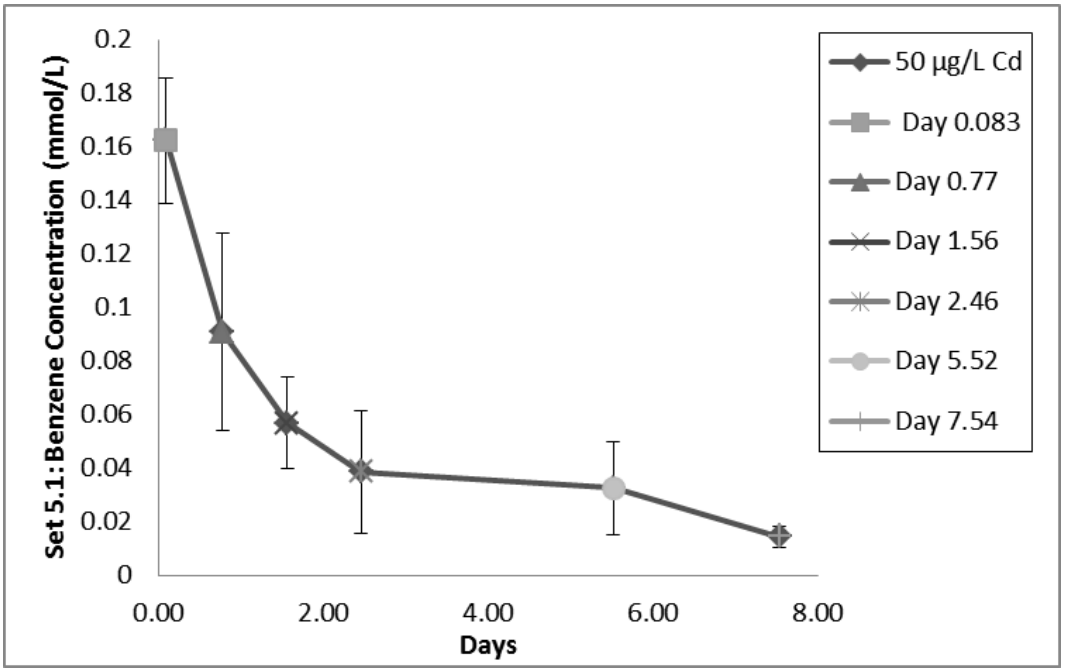

Figure 59: The figure shows the set 5.1 benzene degradation curve for the 50 µg/L Cd microcosms. The degradation of benzene is linear. Starting benzene concentration was 0.2244 mM. Due to the immediate drop in concentration there was no real lag time observed. As shown in the previous tables the degradation is a result of biological activity due to a lack of degradation in the sterile controls. The degradation of benzene has a slower rate than toluene.

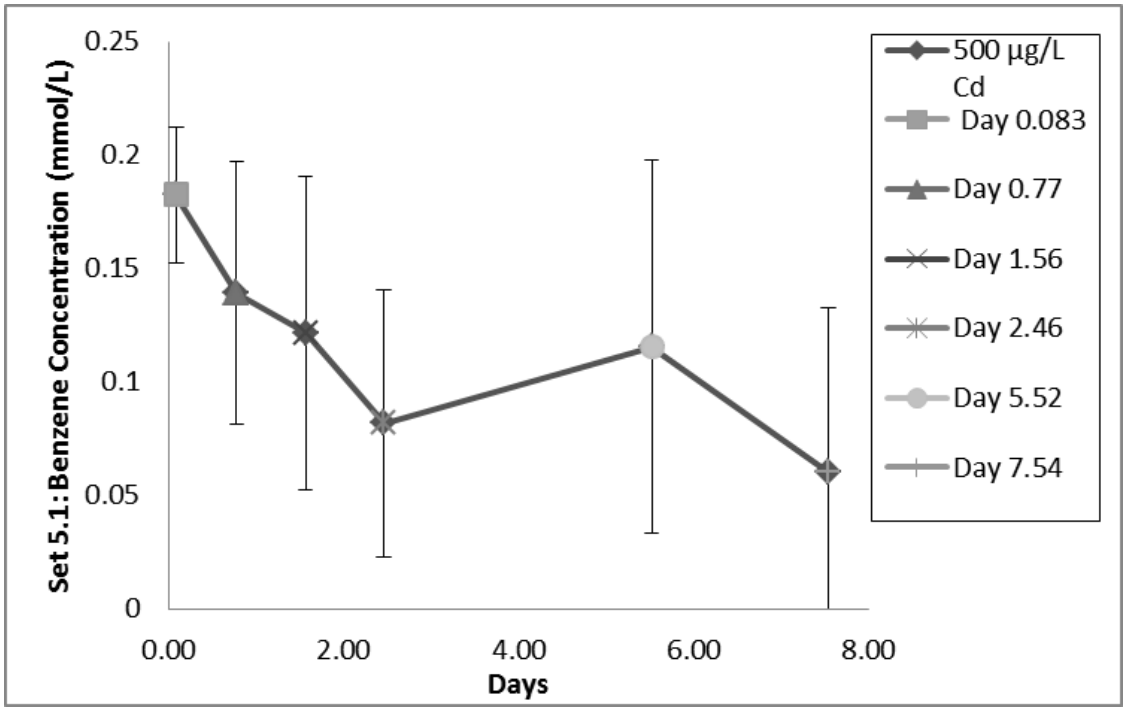

Figure 60: The figure shows the set 5.1 benzene degradation curve for the 500 µg/L Cd microcosms. The degradation of benzene is linear. Starting benzene concentration was 0.2244 mM. Due to the immediate drop in concentration there was no real lag time observed. As shown in the previous tables the degradation is a result of biological activity due to a lack of degradation in the sterile controls. Though there was a high variance in the data, the overall slope of the line shows degradation. The degradation of benzene has a slower rate than toluene. Complete degradation was not observed.

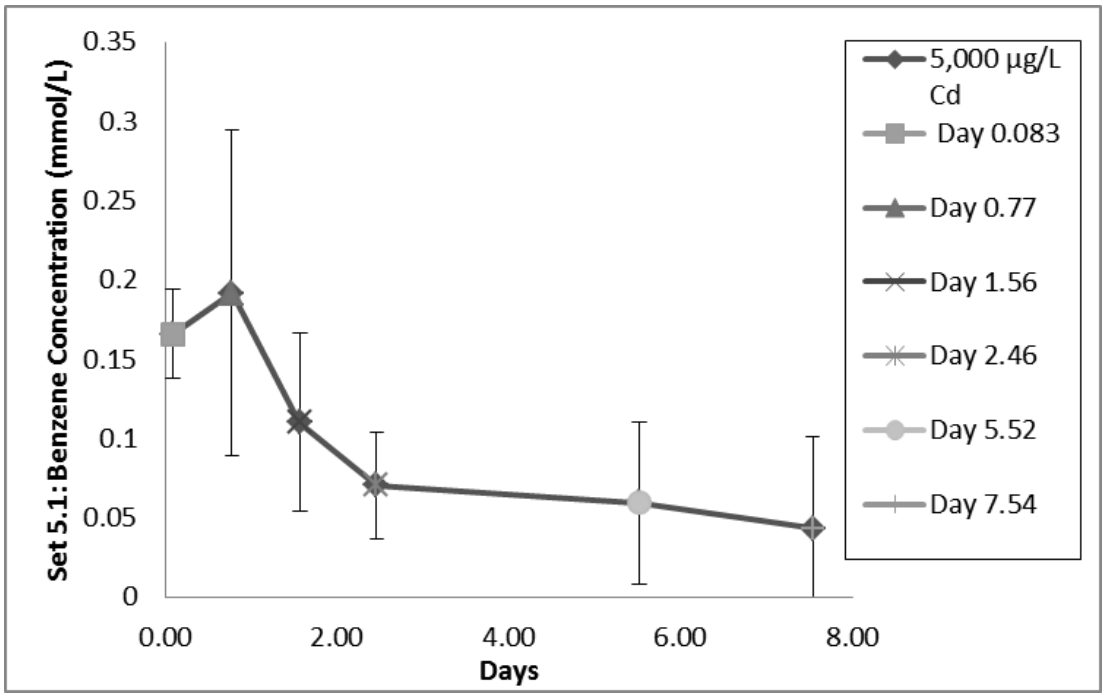

Figure 61: The figure shows the set 5.1 benzene degradation curve for the 5,000 µg/L Cd microcosms. The degradation of benzene is linear. Starting benzene concentration was 0.2244 mM. As shown in the previous tables the degradation is a result of biological activity due to a lack of degradation in the sterile controls. The degradation of benzene has a slower rate than toluene. Complete degradation was not observed.

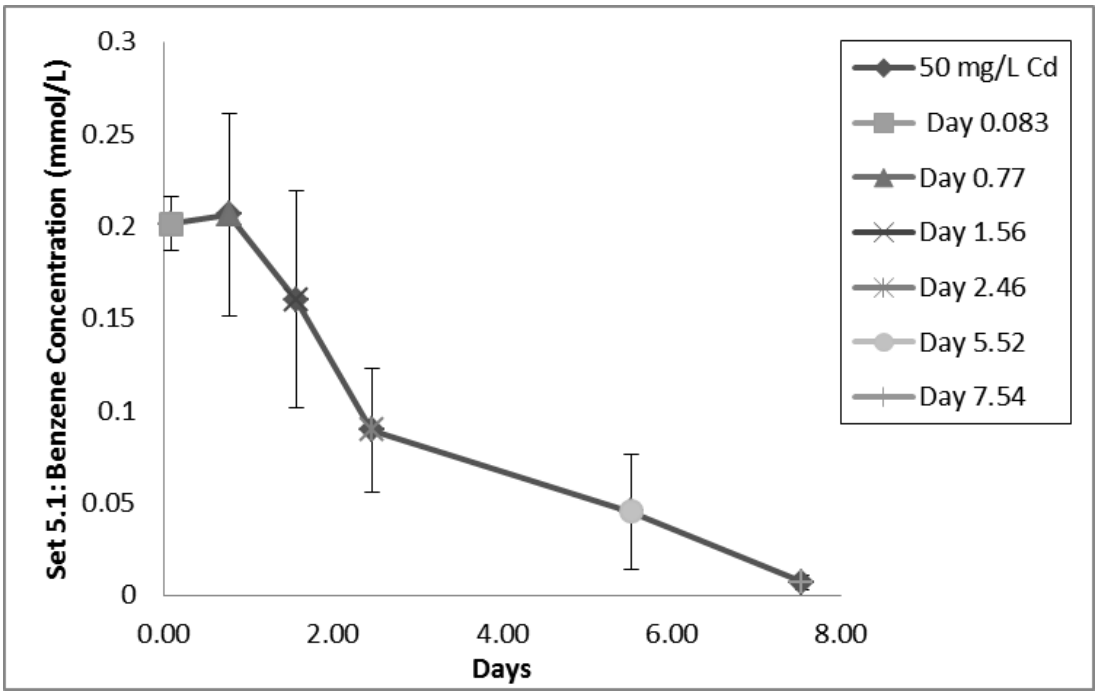

Figure 62: The figure shows the set 5.1 benzene degradation curve for the 50 mg/L Cd microcosms. The degradation of benzene is linear. Starting benzene concentration was 0.2244 mM. As shown in the previous tables the degradation is a result of biological activity due to a lack of degradation in the sterile controls. The degradation of benzene has a slower rate than toluene. Complete degradation was observed on day 8.

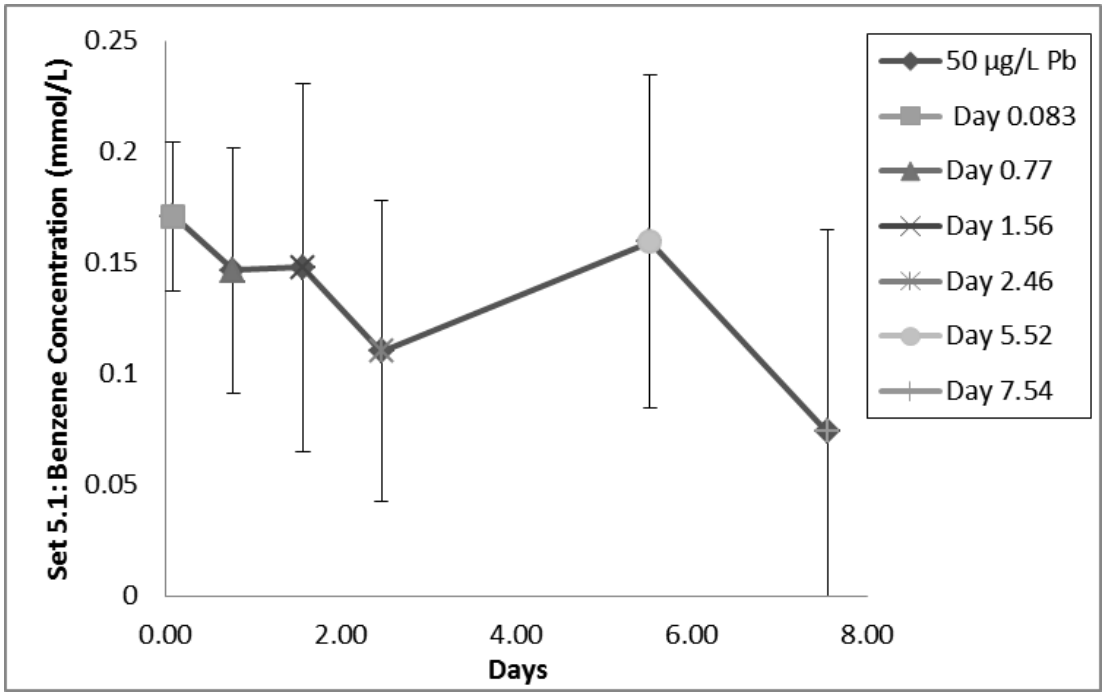

Figure 63: The figure shows the set 5.1 benzene degradation curve for the 50 µg/L Pb microcosms. The degradation of benzene is linear. Starting benzene concentration was 0.2244 mM. As shown in the previous tables the degradation is a result of biological activity due to a lack of degradation in the sterile controls. Though there was a high variance in the data, the overall slope of the line shows degradation. The degradation of benzene has a slower rate than toluene. Complete degradation was not observed.

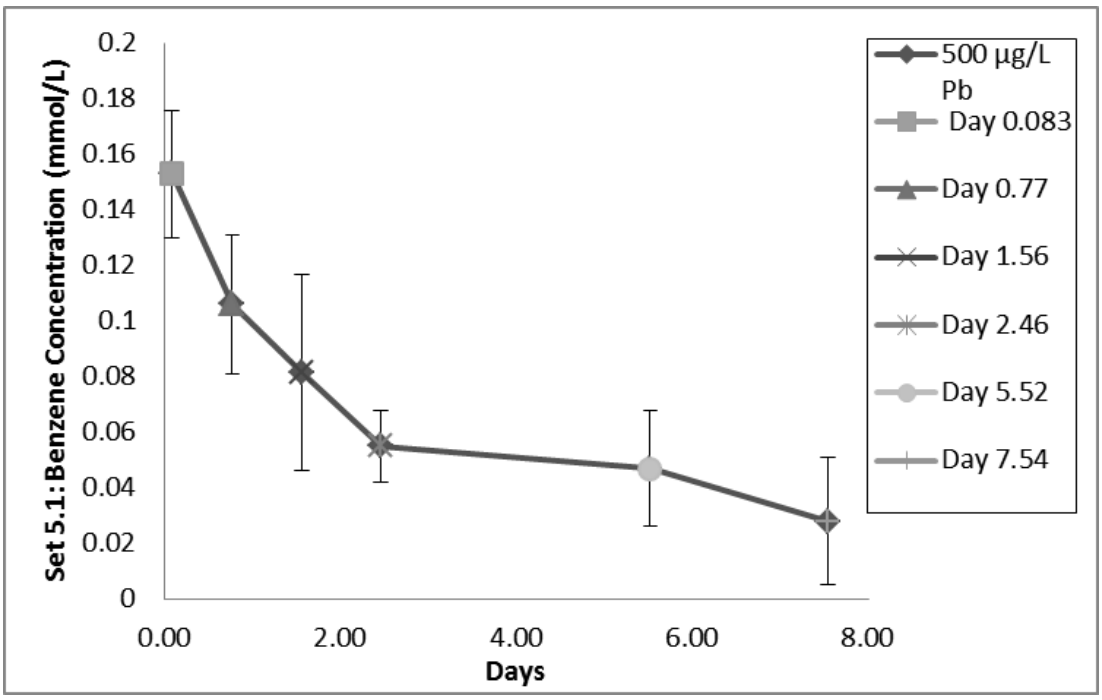

Figure 64: The figure shows the set 5.1 benzene degradation curve for the 500 µg/L Pb microcosms. The degradation of benzene is linear. Starting benzene concentration was 0.2244 mM. Due to the immediate drop in concentration there was no real lag time observed. As shown in the previous tables the degradation is a result of biological activity due to a lack of degradation in the sterile controls. The degradation of benzene has a slower rate than toluene. Complete degradation was not observed.

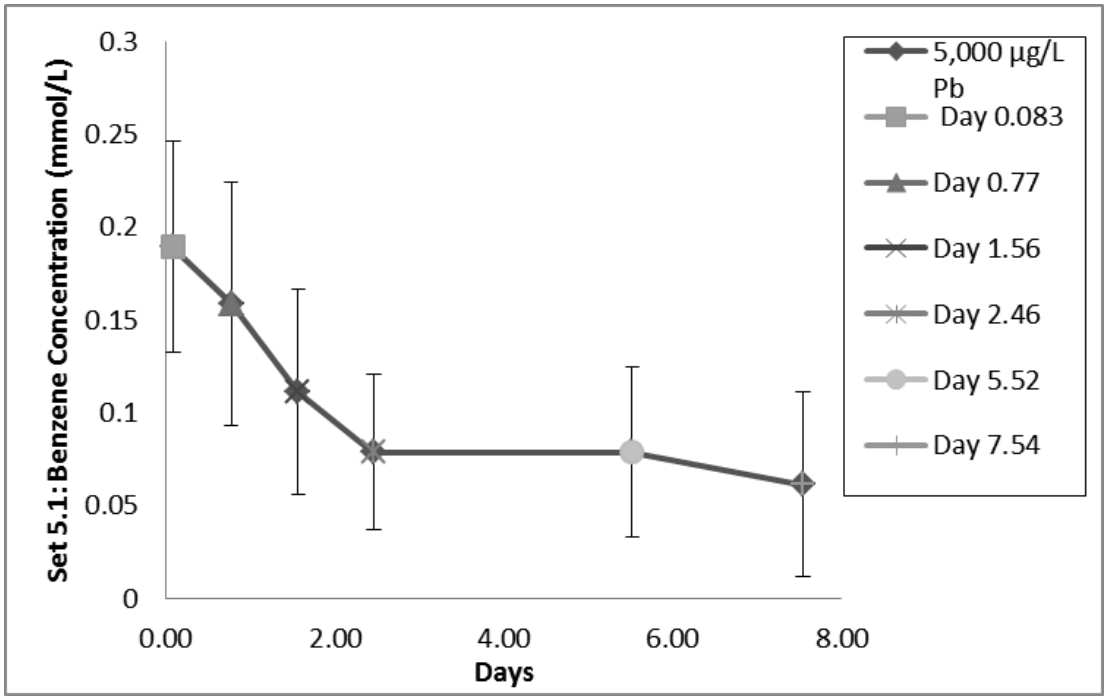

Figure 65: The figure shows the set 5.1 benzene degradation curve for the 5,000 µg/L Pb microcosms. The degradation of benzene is linear. Starting benzene concentration was 0.2244 mM. Due to the immediate drop in concentration there was no real lag time observed. As shown in the previous tables the degradation is a result of biological activity due to a lack of degradation in the sterile controls. The degradation of benzene has a slower rate than toluene. Complete degradation was not observed.

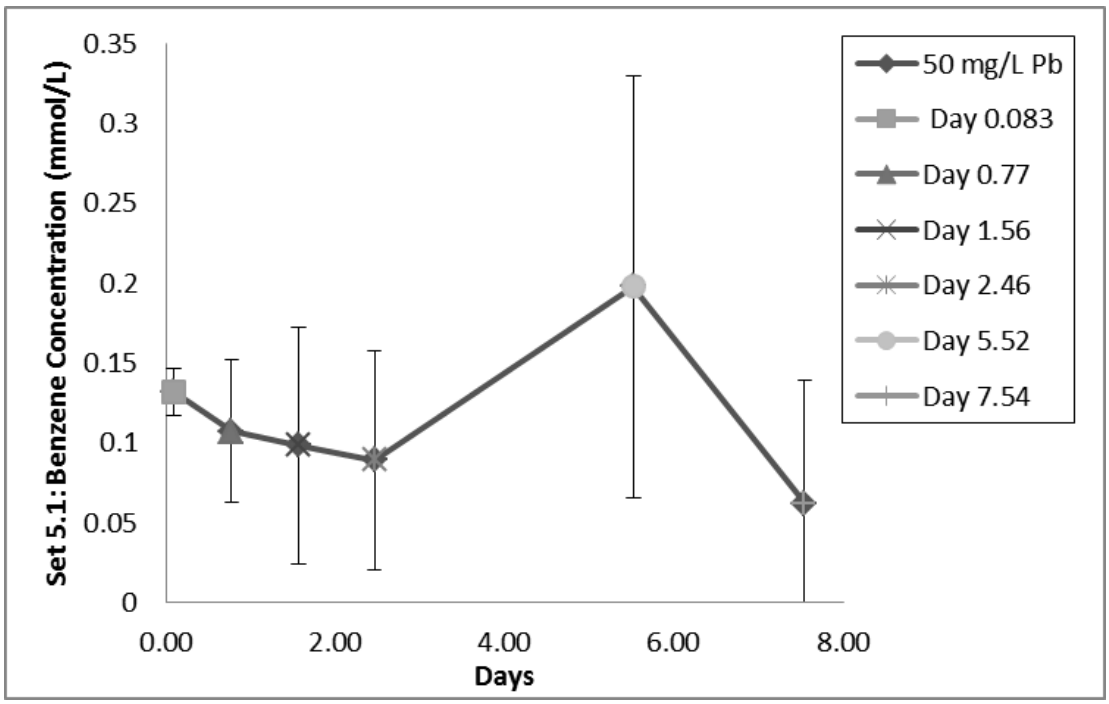

Figure 66: The figure shows the set 5.1 benzene degradation curve for the 50 mg/L Pb microcosms. Starting benzene concentration was 0.2244 mM. Due to the immediate drop in concentration there was no real lag time observed. As shown in the previous tables the degradation is a result of biological activity due to a lack of degradation in the sterile controls. Though there was a high variance in the data, the overall slope of the line shows degradation. The degradation of benzene has a slower rate than toluene. Complete degradation was not observed.

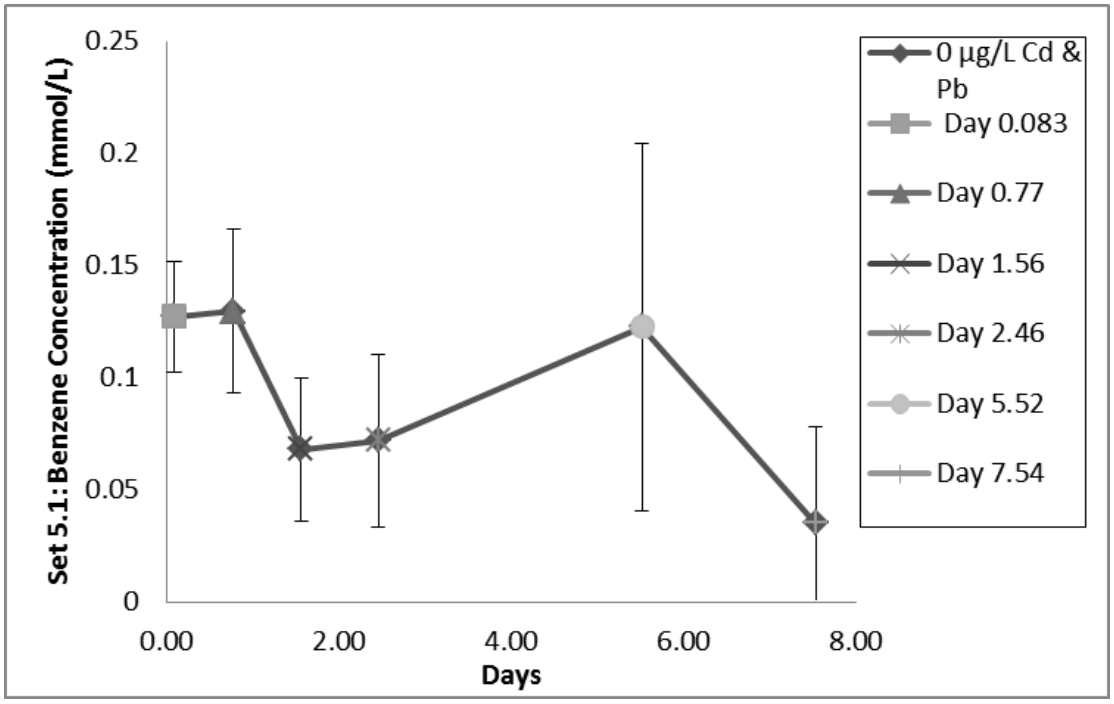

Figure 67: The figure shows the set 5.1 benzene degradation curve for the 0 µg/L Cd and Pb microcosms. The degradation of benzene is linear. Starting benzene concentration was 0.2244 mM. Due to the immediate drop in concentration there was no real lag time observed. As shown in the previous tables the degradation is a result of biological activity due to a lack of degradation in the sterile controls. Though there was a high variance in the data, the overall slope of the line shows degradation. The degradation of benzene has a slower rate than toluene. Complete degradation was not observed.

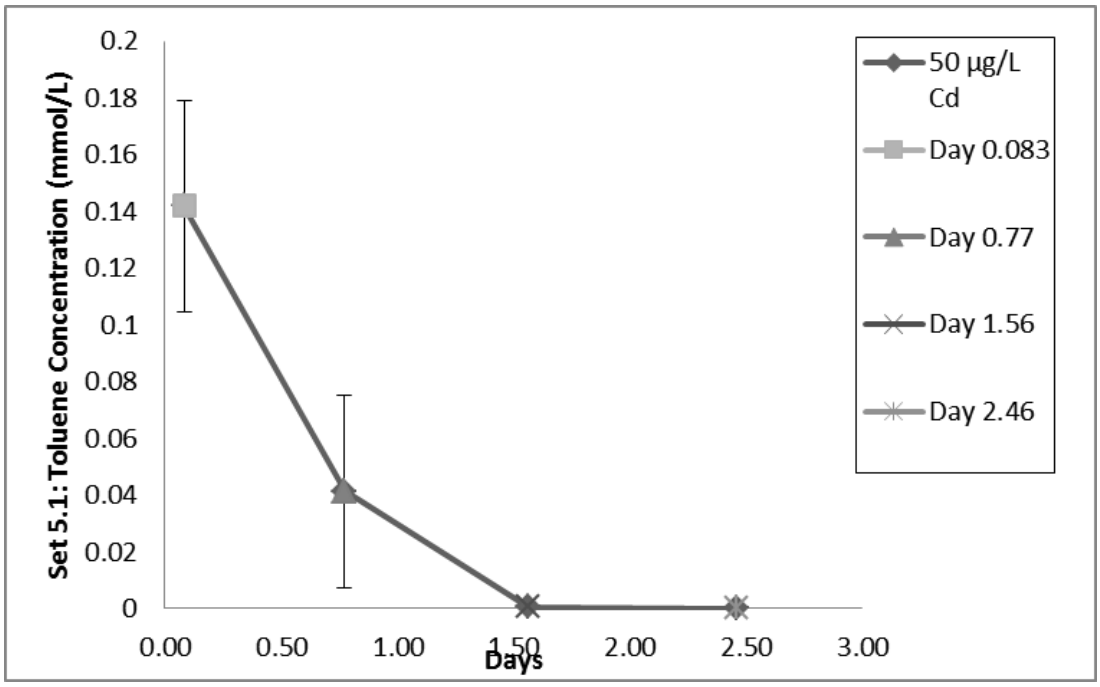

Figure 68: The figure shows the set 5.1 toluene degradation curve for the 50 µg/L Cd microcosms. The degradation of toluene is linear. Starting toluene concentration was 0.1888 mM. Due to the immediate drop in concentration there was no real lag time observed. As shown in the previous tables the degradation is a result of biological activity due to a lack of degradation in the sterile controls. The degradation of toluene has a faster rate than benzene. Complete degradation occurred on day 1.5.

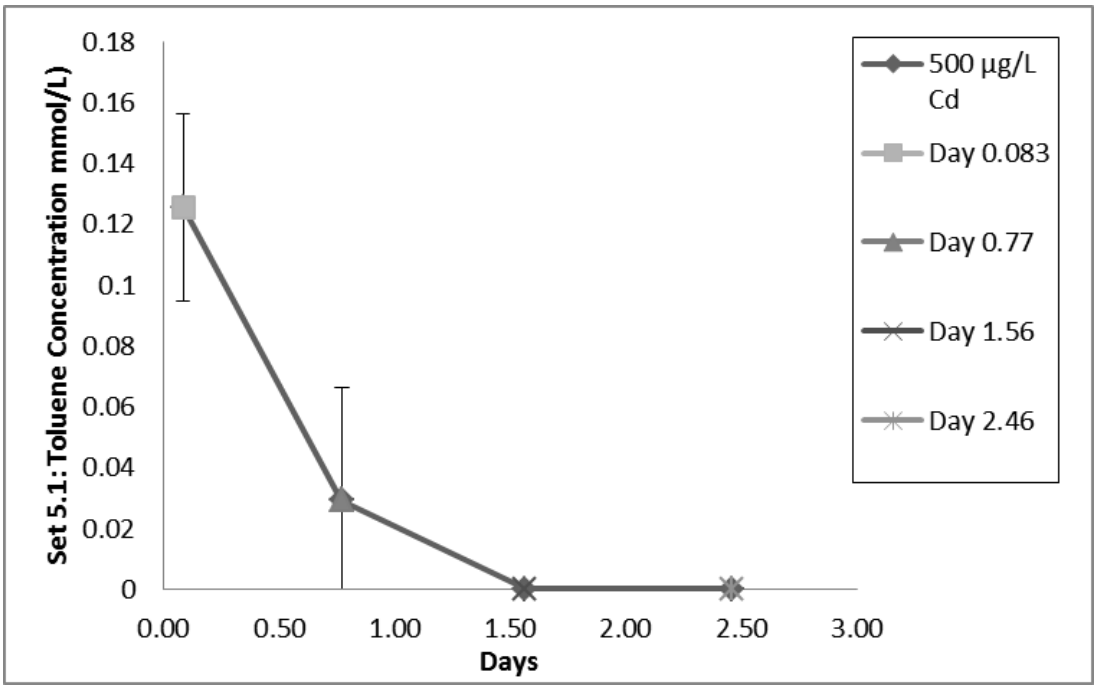

Figure 69: The figure shows the set 5.1 toluene degradation curve for the 500 µg/L Cd microcosms. The degradation of toluene is linear. Starting toluene concentration was 0.1888 mM. Due to the immediate drop in concentration there was no real lag time observed. As shown in the previous tables the degradation is a result of biological activity due to a lack of degradation in the sterile controls. The degradation of toluene has a faster rate than benzene. Complete degradation occurred on day 1.5.

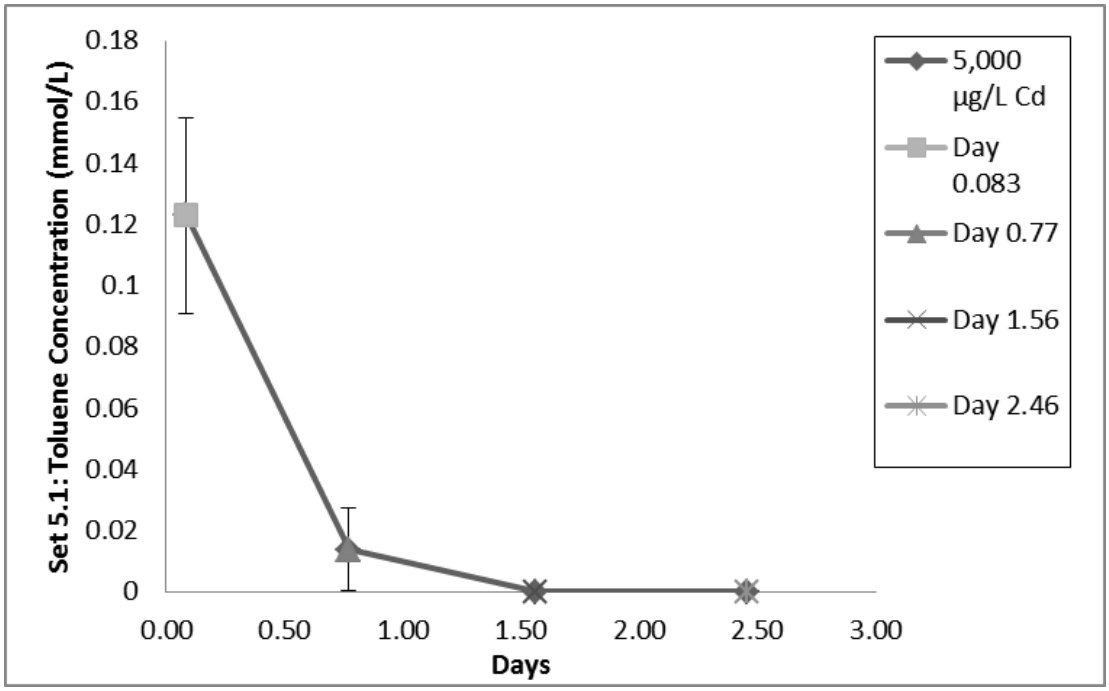

Figure 70: The figure shows the set 5.1 toluene degradation curve for the 5,000 µg/L Cd microcosms. The degradation of toluene is linear. Starting toluene concentration was 0.1888 mM. Due to the immediate drop in concentration there was no real lag time observed. As shown in the previous tables the degradation is a result of biological activity due to a lack of degradation in the sterile controls. The degradation of toluene has a faster rate than benzene. Complete degradation occurred on day 1.5.

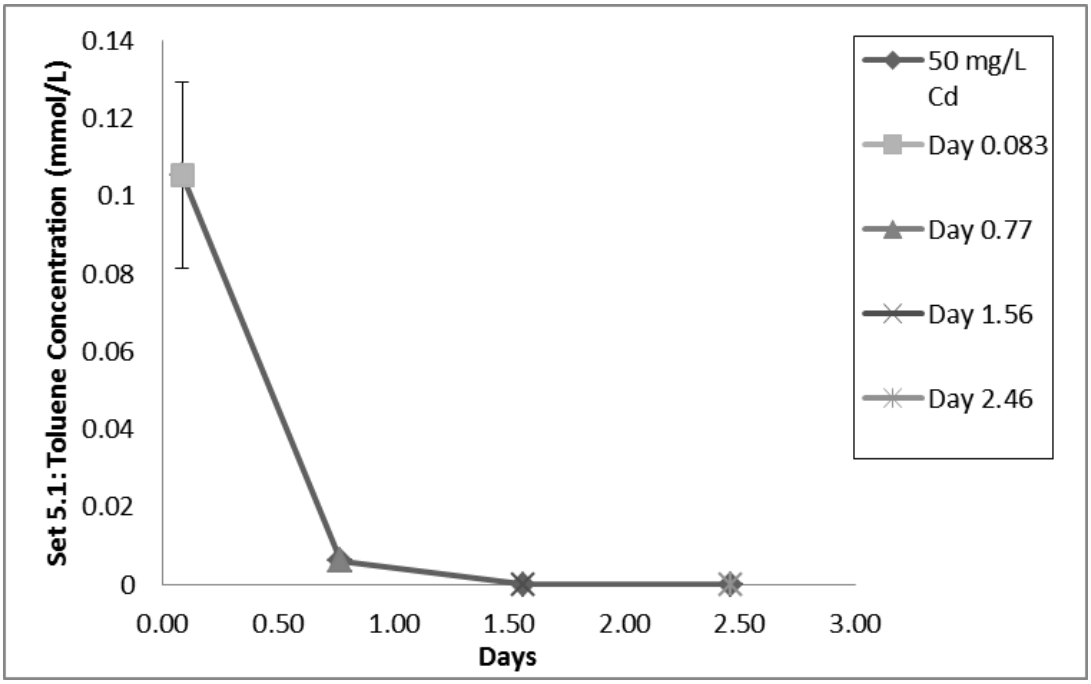

Figure 71: The figure shows the set 5.1 toluene degradation curve for the 50 mg/L Cd microcosms. The degradation of toluene is linear. Starting toluene concentration was 0.1888 mM. Due to the immediate drop in concentration there was no real lag time observed. As shown in the previous tables the degradation is a result of biological activity due to a lack of degradation in the sterile controls. The degradation of toluene has a faster rate than benzene. Complete degradation occurred on day 1.5.

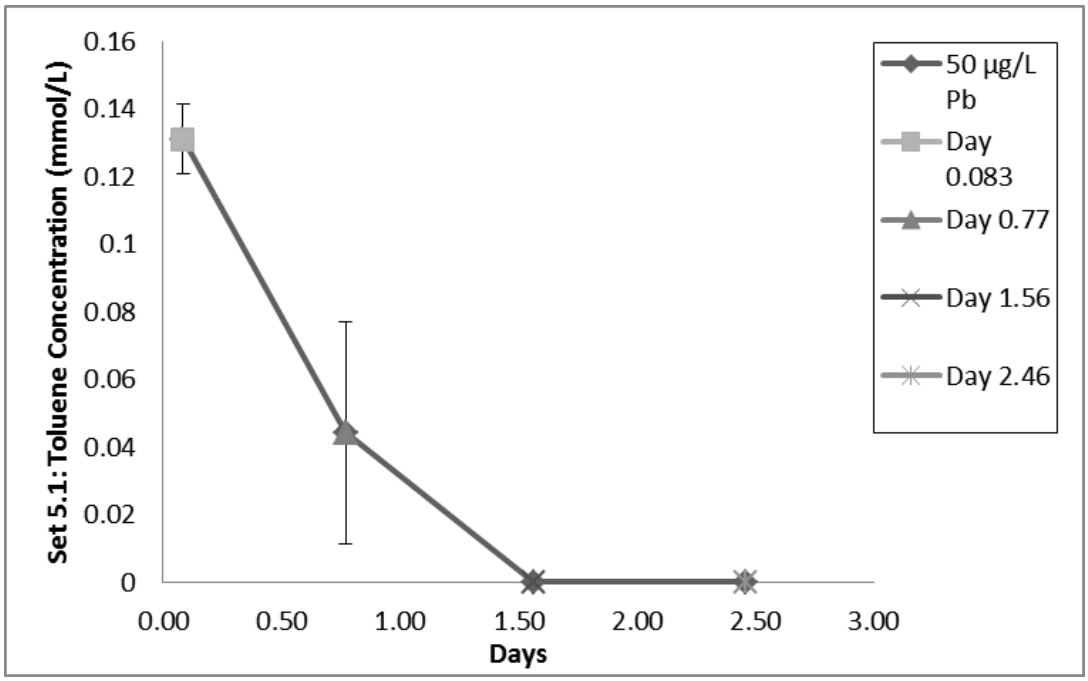

Figure 72: The figure shows the set 5.1 toluene degradation curve for the 50 µg/L Pb microcosms. The degradation of toluene is linear. Starting toluene concentration was 0.1888 mM. Due to the immediate drop in concentration there was no real lag time observed. As shown in the previous tables the degradation is a result of biological activity due to a lack of degradation in the sterile controls. The degradation of toluene has a faster rate than benzene. Complete degradation occurred on day 1.5.

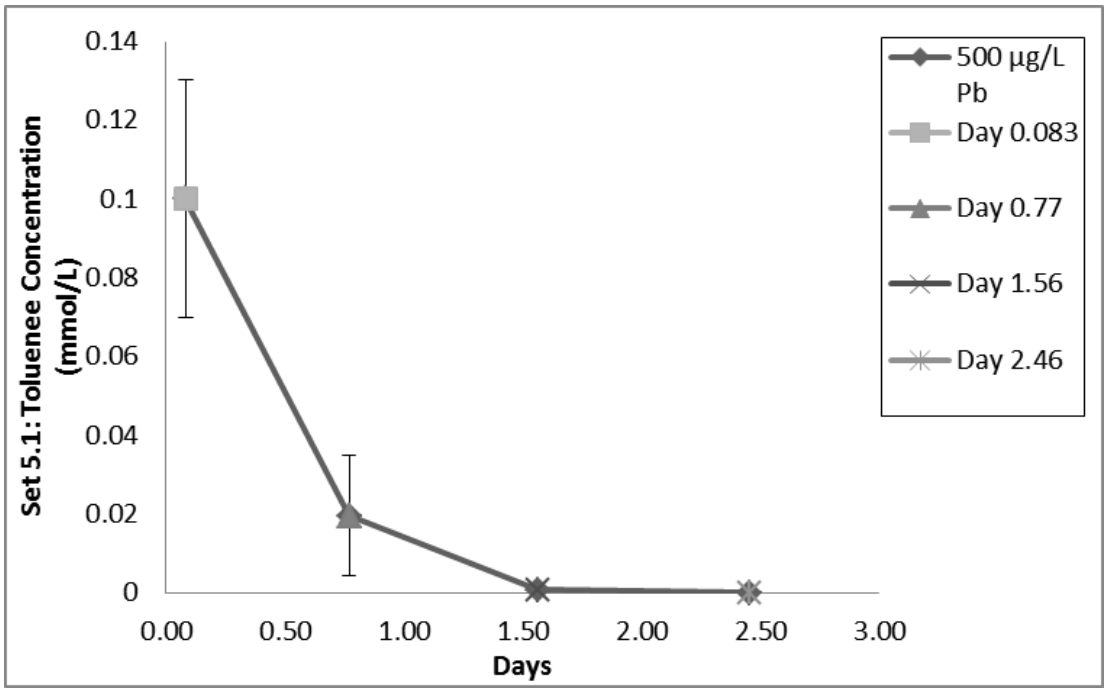

Figure 73: The figure shows the set 5.1 toluene degradation curve for the 500 µg/L Pb microcosms. The degradation of toluene is linear. Starting toluene concentration was 0.1888 mM. Due to the immediate drop in concentration there was no real lag time observed. As shown in the previous tables the degradation is a result of biological activity due to a lack of degradation in the sterile controls. The degradation of toluene has a faster rate than benzene. Complete degradation occurred on day 1.5.

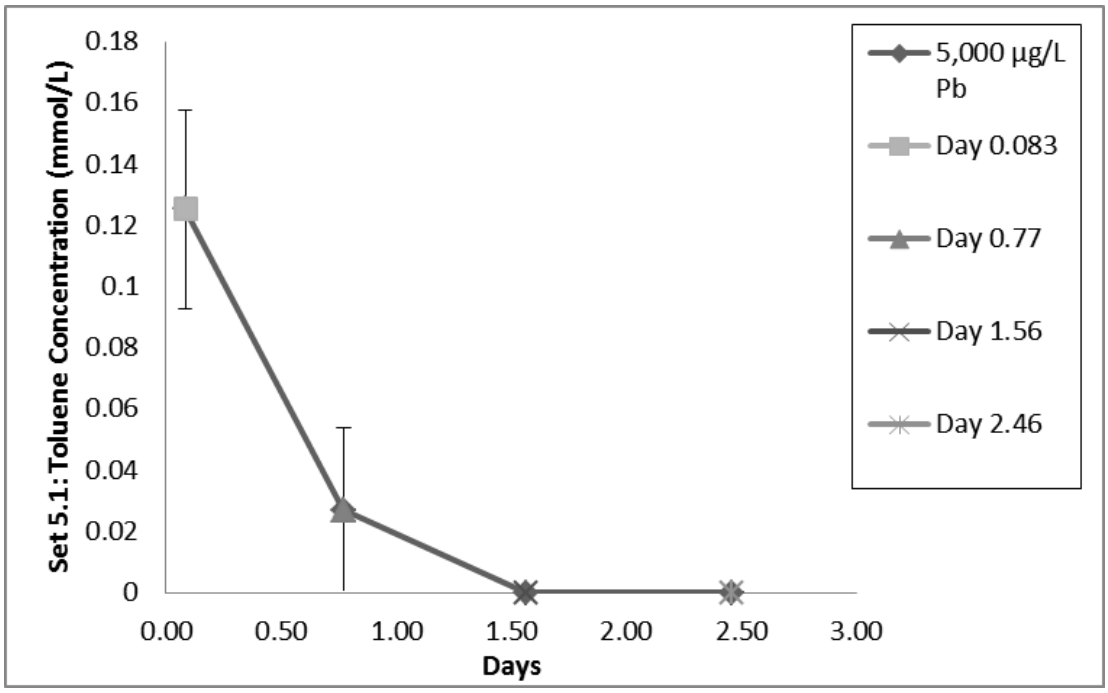

Figure 74: The figure shows the set 5.1 toluene degradation curve for the 5,000 µg/L Pb microcosms. The degradation of toluene is linear. Starting toluene concentration was 0.1888 mM. Due to the immediate drop in concentration there was no real lag time observed. As shown in the previous tables the degradation is a result of biological activity due to a lack of degradation in the sterile controls. The degradation of toluene has a faster rate than benzene. Complete degradation occurred on day 1.5.

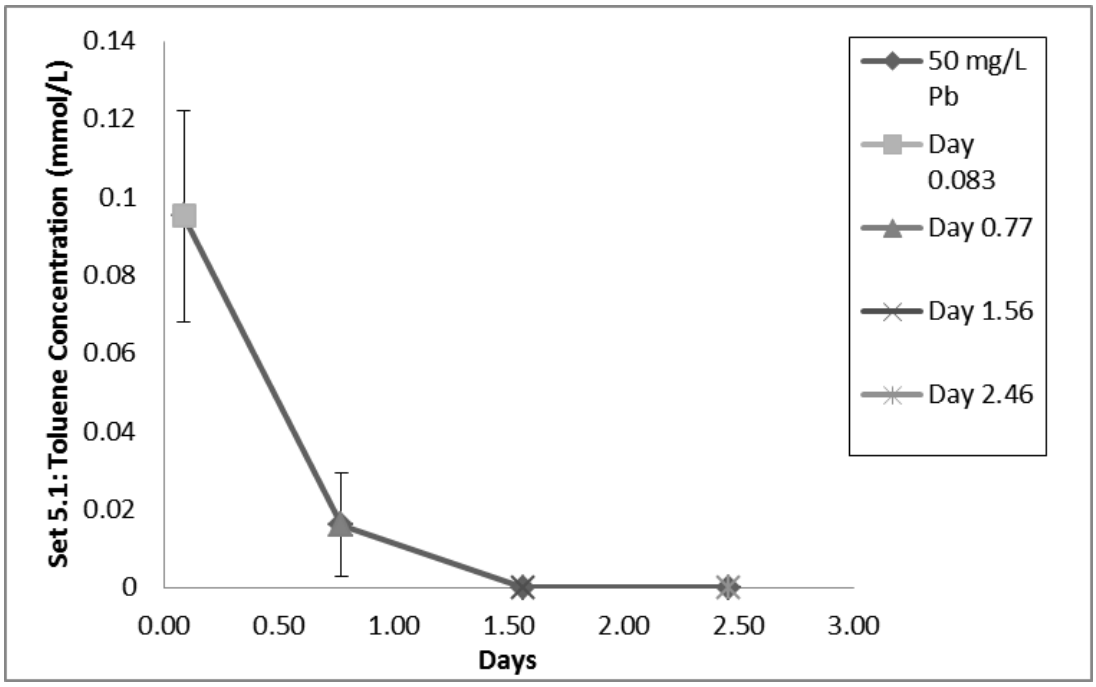

Figure 75: The figure shows the set 5.1 toluene degradation curve for the 50 mg/L Pb microcosms. The degradation of toluene is linear. Starting toluene concentration was 0.1888 mM. Due to the immediate drop in concentration there was no real lag time observed. As shown in the previous tables the degradation is a result of biological activity due to a lack of degradation in the sterile controls. The degradation of toluene has a faster rate than benzene. Complete degradation occurred on day 1.5.

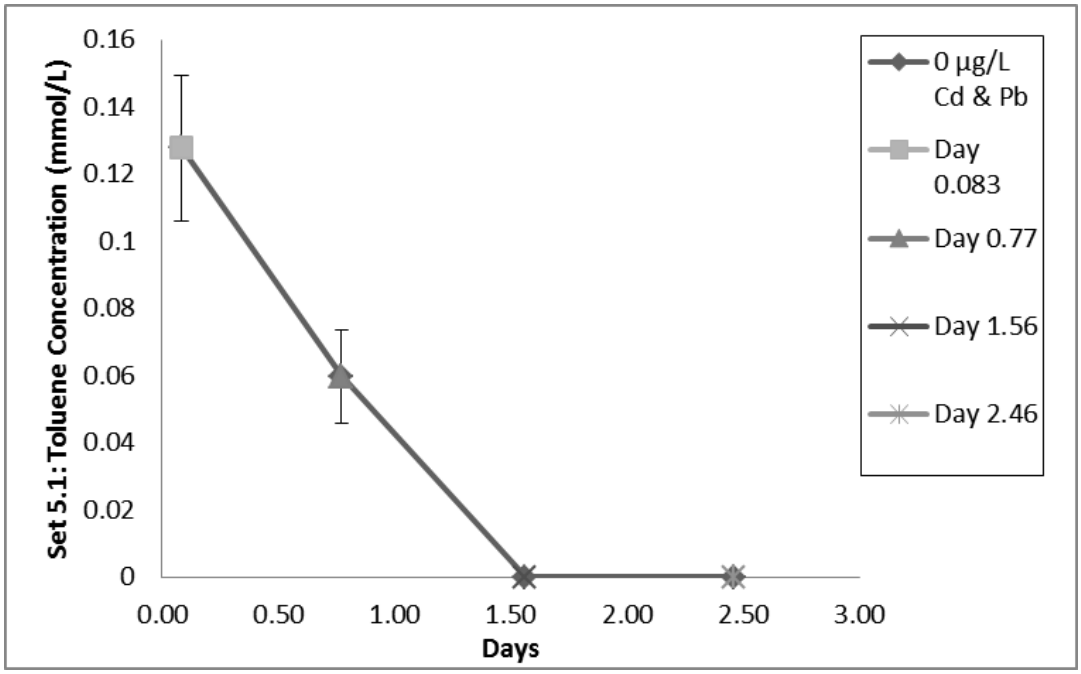

Figure 76: The figure shows the set 5.1 toluene degradation curve for the 0 µg/L Cd and Pb microcosms. The degradation of toluene is linear. Starting toluene concentration was 0.1888 mM. Due to the immediate drop in concentration there was no real lag time observed. As shown in the previous tables the degradation is a result of biological activity due to a lack of degradation in the sterile controls. The degradation of toluene has a faster rate than benzene. Complete degradation occurred on day 1.5.

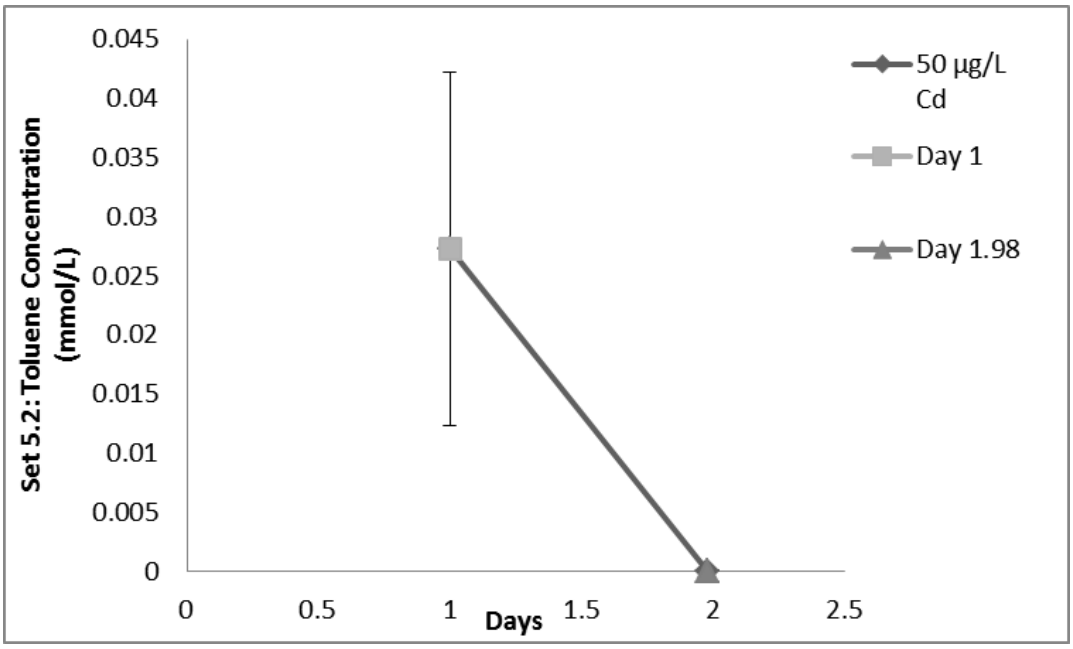

Figure 77: The figure shows the set 5.2 toluene degradation curve for the 50 µg/L Cd microcosms. Starting toluene concentration was 0.1888 mM. Due to the immediate drop in concentration there was no real lag time observed. As shown in the previous tables the degradation is a result of biological activity due to a lack of degradation in the sterile controls. The degradation of toluene has a faster rate than benzene. Complete degradation occurred on day 2. The degradation rate has clearly been increasing with every re-spike.

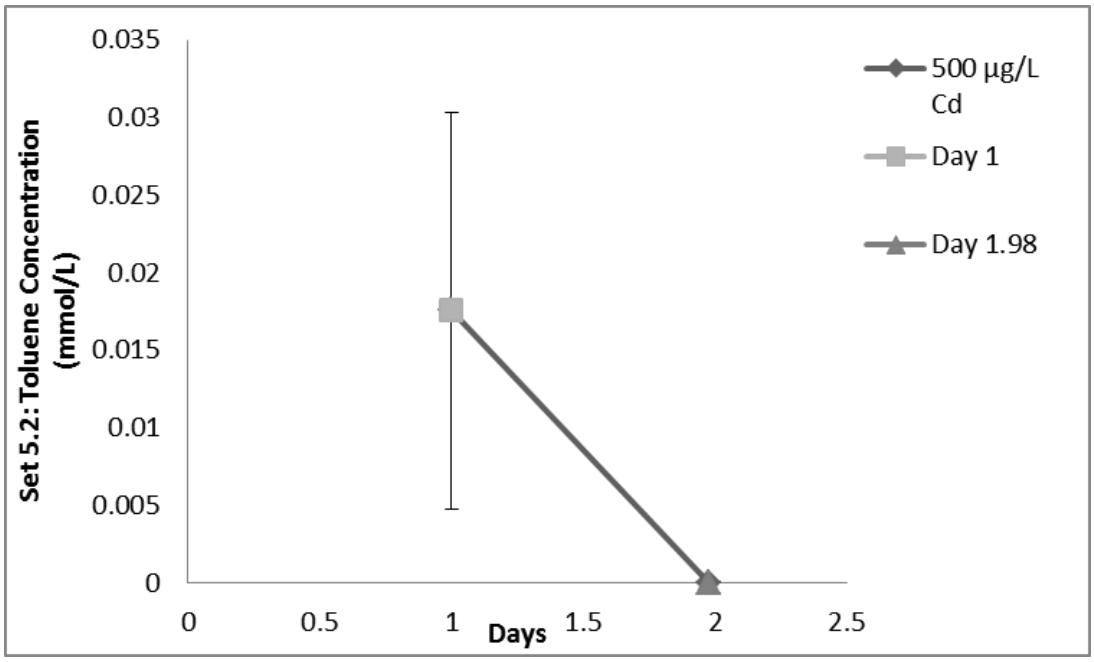

Figure 78: The figure shows the set 5.2 toluene degradation curve for the 500 µg/L Cd microcosms. Starting toluene concentration was 0.1888 mM. Due to the immediate drop in concentration there was no real lag time observed. As shown in the previous tables the degradation is a result of biological activity due to a lack of degradation in the sterile controls. The degradation of toluene has a faster rate than benzene. Complete degradation occurred on day 2. The degradation rate has clearly been increasing with every re-spike.

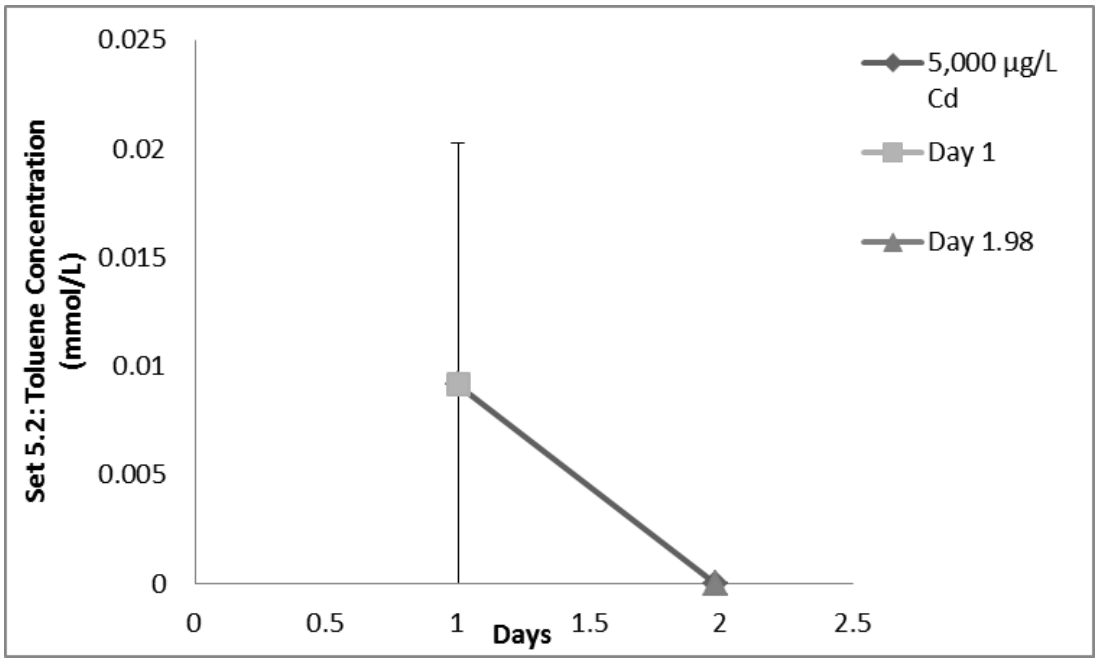

Figure 79: The figure shows the set 5.2 toluene degradation curve for the 5,000 µg/L Cd microcosms. Starting toluene concentration was 0.1888 mM. Due to the immediate drop in concentration there was no real lag time observed. As shown in the previous tables the degradation is a result of biological activity due to a lack of degradation in the sterile controls. The degradation of toluene has a faster rate than benzene. Complete degradation occurred on day 2. The degradation rate has clearly been increasing with every re-spike.

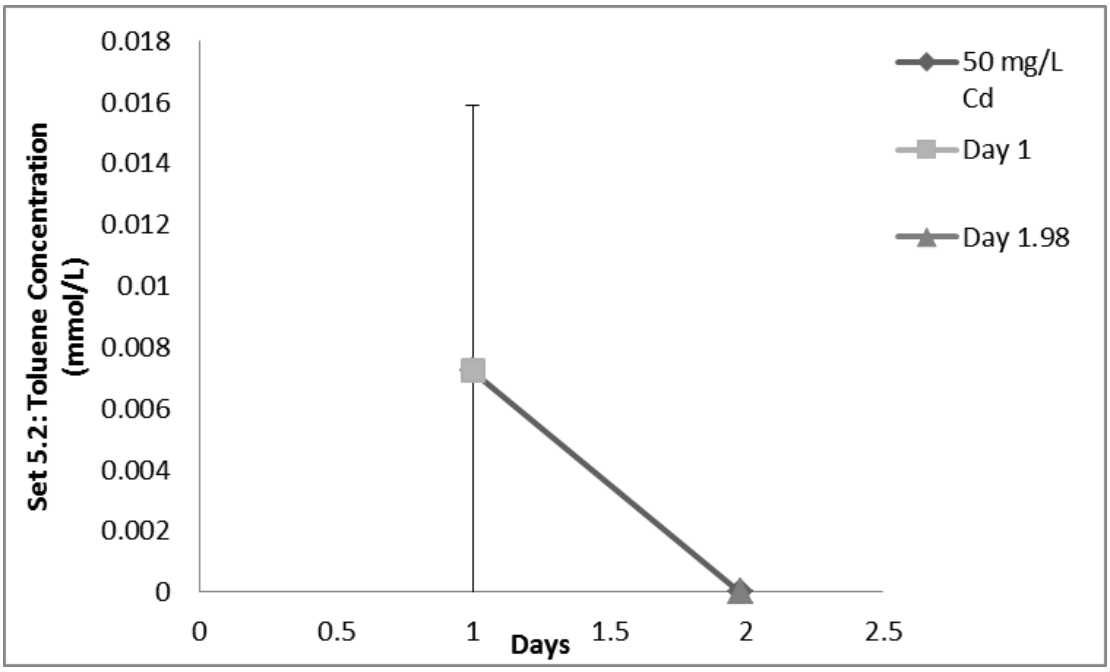

Figure 80: The figure shows the set 5.2 toluene degradation curve for the 50 mg/L Cd microcosms. Starting toluene concentration was 0.1888 mM. Due to the immediate drop in concentration there was no real lag time observed. As shown in the previous tables the degradation is a result of biological activity due to a lack of degradation in the sterile controls. The degradation of toluene has a faster rate than benzene. Complete degradation occurred on day 2. The degradation rate has clearly been increasing with every re-spike.

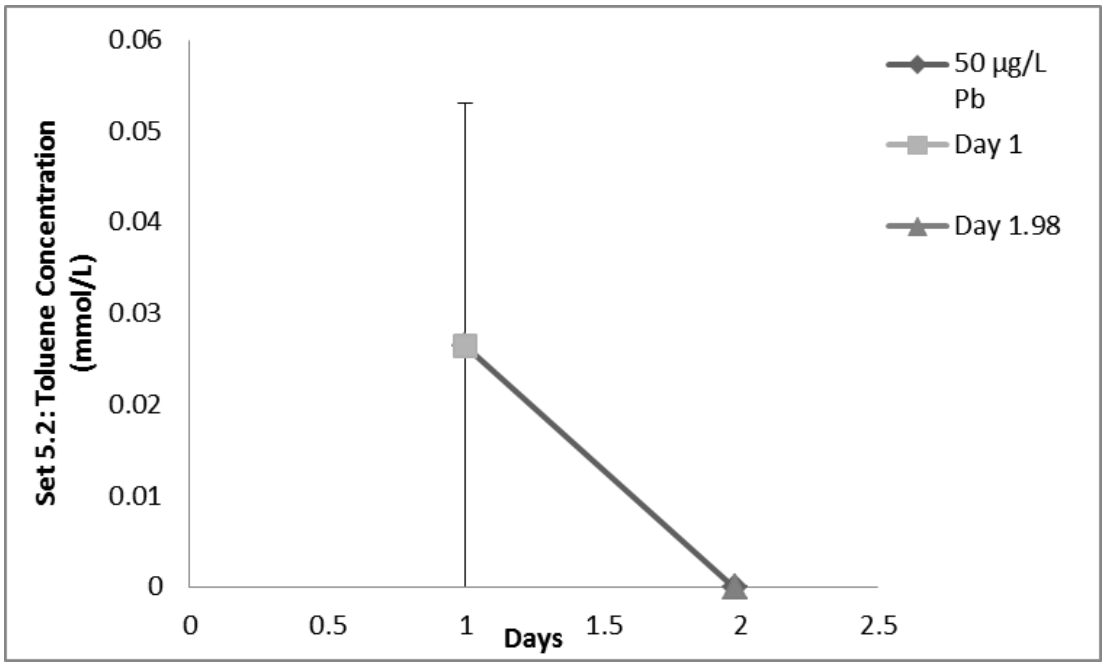

Figure 81: The figure shows the set 5.2 toluene degradation curve for the 50 µg/L Pb microcosms. Starting toluene concentration was 0.1888 mM. Due to the immediate drop in concentration there was no real lag time observed. As shown in the previous tables the degradation is a result of biological activity due to a lack of degradation in the sterile controls. The degradation of toluene has a faster rate than benzene. Complete degradation occurred on day 2. The degradation rate has clearly been increasing with every re-spike.

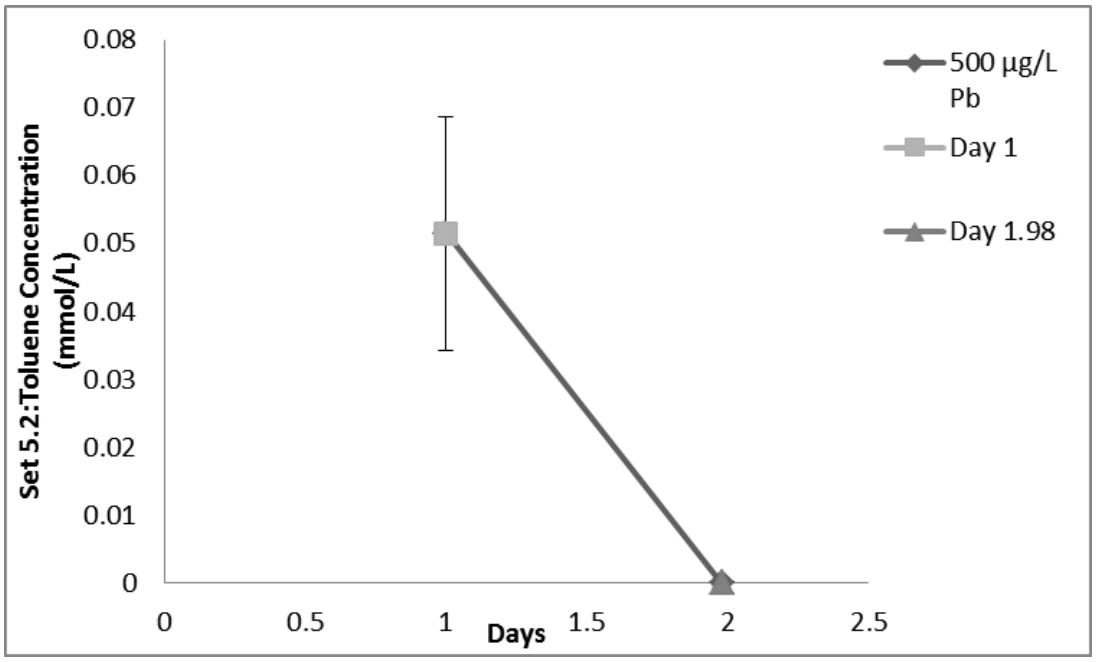

Figure 82: The figure shows the set 5.2 toluene degradation curve for the 500 µg/L Pb microcosms. Starting toluene concentration was 0.1888 mM. Due to the immediate drop in concentration there was no real lag time observed. As shown in the previous tables the degradation is a result of biological activity due to a lack of degradation in the sterile controls. The degradation of toluene has a faster rate than benzene. Complete degradation occurred on day 2. The degradation rate has clearly been increasing with every re-spike.

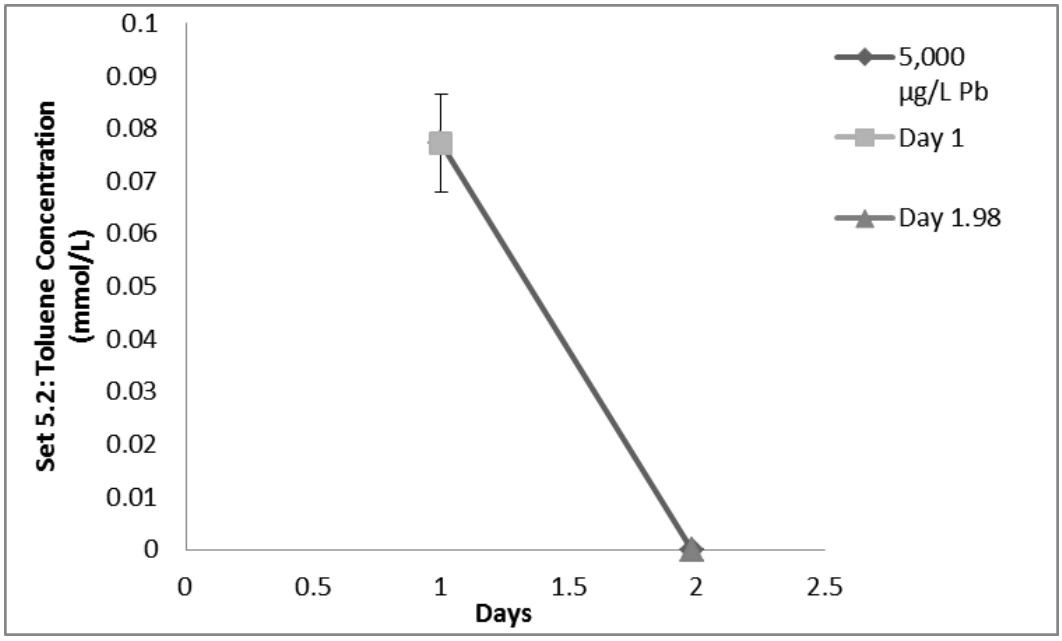

Figure 83: The figure shows the set 5.2 toluene degradation curve for the 5,000 µg/L Pb microcosms. Starting toluene concentration was 0.1888 mM. Due to the immediate drop in concentration there was no real lag time observed. As shown in the previous tables the degradation is a result of biological activity due to a lack of degradation in the sterile controls. The degradation of toluene has a faster rate than benzene. Complete degradation occurred on day 2. The degradation rate has clearly been increasing with every re-spike.

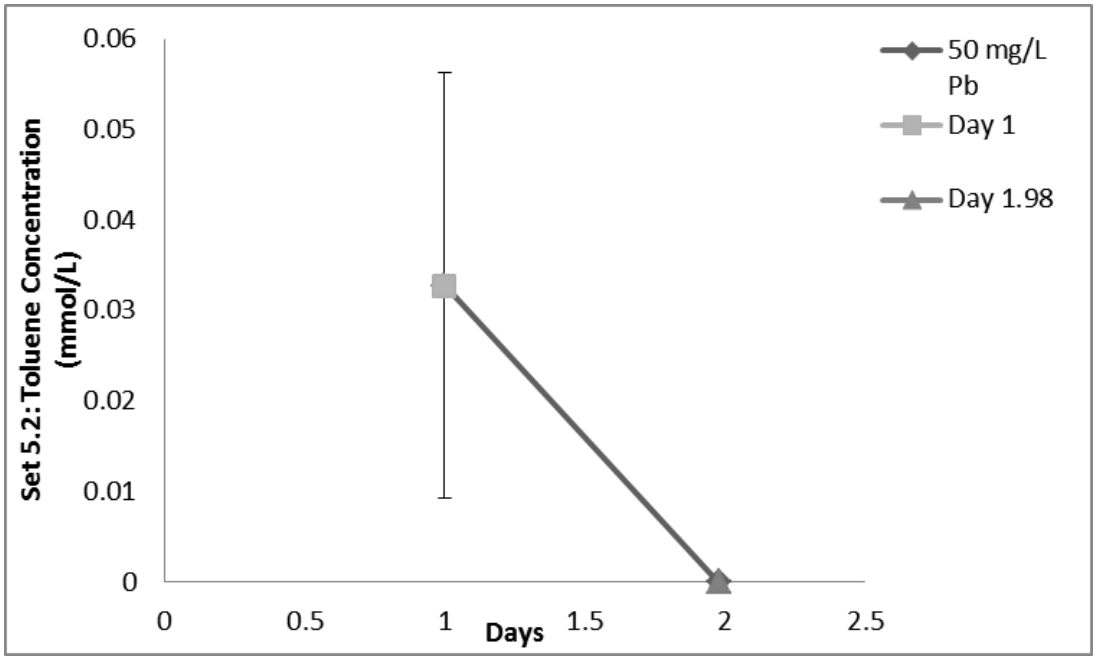

Figure 84: The figure shows the set 5.2 toluene degradation curve for the 50 mg/L Pb microcosms. Starting toluene concentration was 0.1888 mM. Due to the immediate drop in concentration there was no real lag time observed. As shown in the previous tables the degradation is a result of biological activity due to a lack of degradation in the sterile controls. The degradation of toluene has a faster rate than benzene. Complete degradation occurred on day 2. The degradation rate has clearly been increasing with every re-spike.

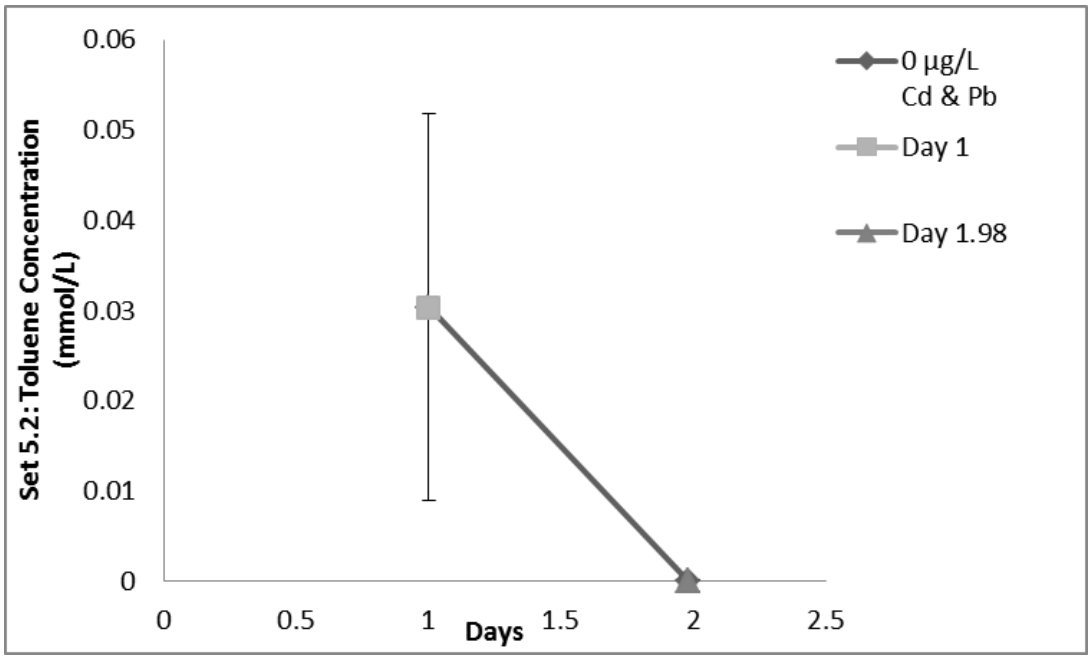

Figure 85: The figure shows the set 5.2 toluene degradation curve for the 0 µg/L Cd and Pb microcosms. Starting toluene concentration was 0.1888 mM. Due to the immediate drop in concentration there was no real lag time observed. As shown in the previous tables the degradation is a result of biological activity due to a lack of degradation in the sterile controls. The degradation of toluene has a faster rate than benzene. Complete degradation occurred on day 2. The degradation rate has clearly been increasing with every re-spike.

Table 16: The toluene microcosms set for one day in an incubator before measurements are taken in order to avoid false reading. After the 7th re-spike, the microbial population is very large and active. This is why the degradation of toluene is almost immediate.

Set 5.7: Toluene Percent Degradation Data		
Concentration Metal	Sample	Day 1.00 Degradation (%)
50 µg/L Cd	A-1	100.0
	A-2	100.0
	A-3	100.0
500 µg/L Cd	B-1	100.0
	B-2	100.0
	B-3	100.0
5,000 µg/L Cd	C-1	100.0
	C-2	95.5
	C-3	100.0
50 mg/L Cd	D-1	100.0
	D-2	100.0
	D-3	90.5
50 µg/L Pb	E-1	100.0
	E-2	100.0
	E-3	100.0
500 µg/L Pb	F-1	100.0
	F-2	100.0
	F-3	100.0
5,000 µg/L Pb	G-1	100.0
	G-2	100.0
	G-3	90.5
50 mg/L Pb	H-1	100.0
	H-2	100.0
	H-3	100.0
0 µg/L Cd & Pb	I-1	100.0
	I-2	100.0
	I-3	94.6

The toluene microcosms still degraded toluene after the 7^{th} re-spike. The re-spikes created a strong microbial population, actively degrading toluene. The microcosms with the largest degradation rate in each heavy metal concentration set were diluted by factors of 10 down to 10^{-8} of the original microcosm. The microcosms for Cd, had degradation even at the most diluted microcosms. The Cd microcosms seemed to have had a higher toluene degrading population at higher concentrations of Cd. The lead microcosms also showed degradation at extremely dilute concentrations. However, unlike Cd, the biodegrading microbial population seemed to be inhibited at higher Pb concentrations (Table 17 and Figure 86 – Figure 94).

The anaerobic microcosms showed little to no degradation after a 20 day period. The only microcosms that showed any signs of degradation were the 0 µg/L of Cd and Pb. The amount of toluene that degraded in the microcosms was 38%, with a 30% standard deviation. This could be a sign of heavy metals affecting bio degradation of toluene in anaerobic conditions; however, further observation is required. All of the microcosms will continue to be observed on a regular basis. If degradation does not occur, the microcosms will be re-inoculated with soil from the original obtainment site in Stillwater, Oklahoma.

Table 17: The data displayed in the table are all of the individual data points for degradation in all of the diluted toluene microcosms. The data is representing degradation percentage. Complete degradation is represented by 100%.

Dilution: Toluene Percent Degradation Data					
Concentration Metal	Sample	Day 0.00 Degradation (%)	Concentration Metal	Sample	Day 0.00 Degradation (%)
50 µL Cd	A-1	100.0	50 µL Pb	E-1	100.0
	A-2	100.0		E-2	100.0
	A-3	100.0		E-3	100.0
	A-4	100.0		E-4	100.0
50 µL Cd	A-5	40.4	50 µL Pb	E-5	100.0
	A-6	29.3		E-6	100.0
	A-7	26.7		E-7	100.0
	A-8	30.0		E-8	100.0
500 µL Cd	B-1	100.0	500 µL Pb	F-1	100.0
	B-2	100.0		F-2	100.0
	B-3	100.0		F-3	100.0
	B-4	100.0		F-4	100.0
500 µL Cd	B-5	36.0	500 µL Pb	F-5	100.0
	B-6	100.0		F-6	97.5
	B-7	82.0		F-7	100.0
	B-8	38.4		F-8	100.0
5,000 µL Cd	C-1	100.0	5,000 µL Pb	G-1	100.0
	C-2	100.0		G-2	100.0
	C-3	100.0		G-3	100.0
	C-4	37.6		G-4	100.0
5,000 µL Cd	C-5	39.4	5,000 µL Pb	G-5	27.7
	C-6	35.5		G-6	37.3
	C-7	34.8		G-7	30.0
	C-8	35.3		G-8	68.9
50 mL Cd	D-1	100.0	50 mL Pb	H-1	95.2
	D-2	100.0		H-2	24.1
	D-3	100.0		H-3	24.0
	D-4	100.0		H-4	21.5
50 mL Cd	D-5	100.0	50 mL Pb	H-5	24.3
	D-6	39.3		H-6	22.0
	D-7	100.0		H-7	26.0
	D-8	100.0		H-8	32.7
			0 µL Cd & Pb	I-1	100.0
				I-2	100.0
				I-3	100.0
				I-4	100.0
			0 µL Cd & Pb	I-5	31.0
				I-6	43.4
				I-7	54.8
				I-8	100.0

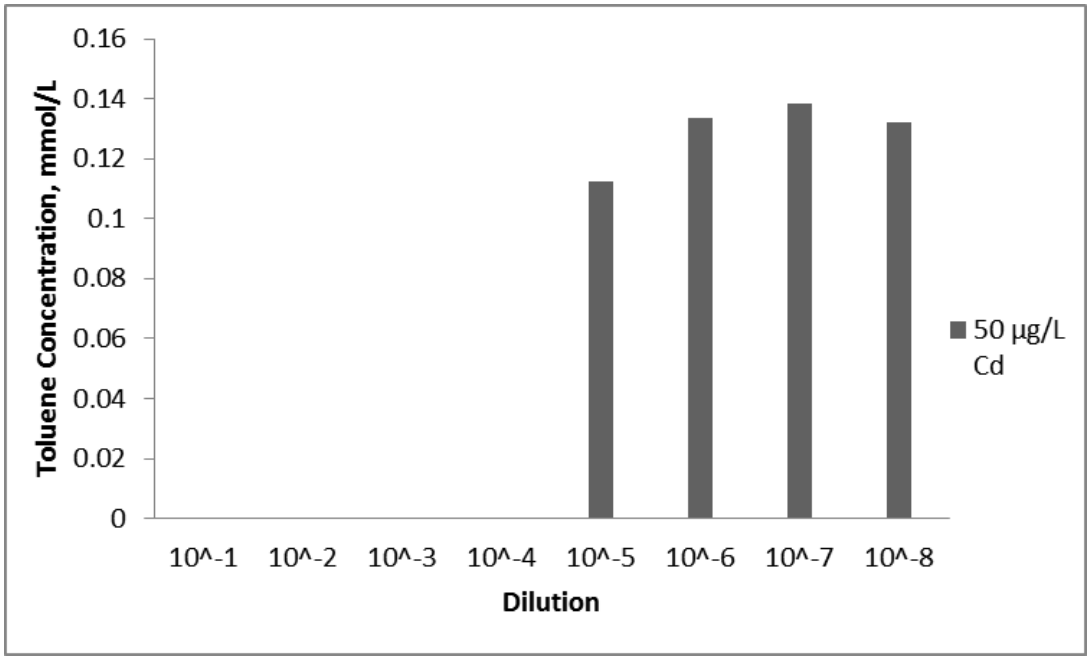

Figure 86: The figure shows the toluene dilution degradation bar graph for the 50 µg/L Cd microcosms. The results from the dilution degradation of toluene show that degradation was able to occur at a dilution of 10^{-4} of the original microcosm. The degradation at 10^{-4} of the original microcosm was a complete degradation. The degradation was observed at day 11.

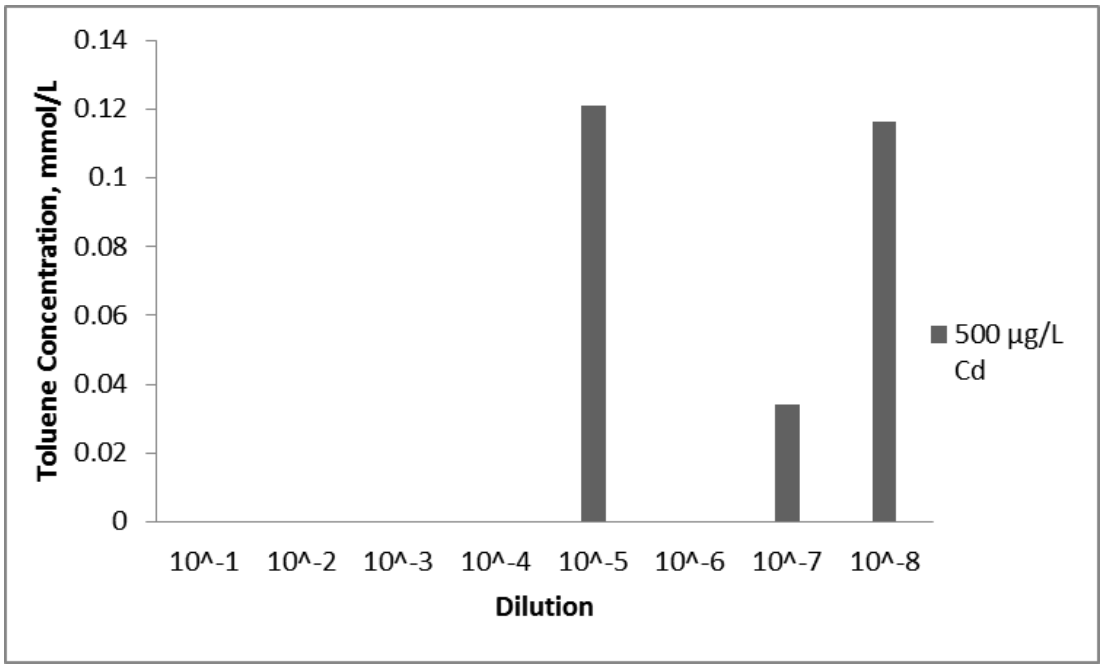

Figure 87: The figure shows the toluene dilution degradation bar graph for the 500 µg/L Cd microcosms. The results from the dilution degradation of toluene show that degradation was able to occur at a dilution of 10^{-4} of the original microcosm. The degradation at 10^{-4} of the original microcosm was a complete degradation. The degradation was observed at day 11.

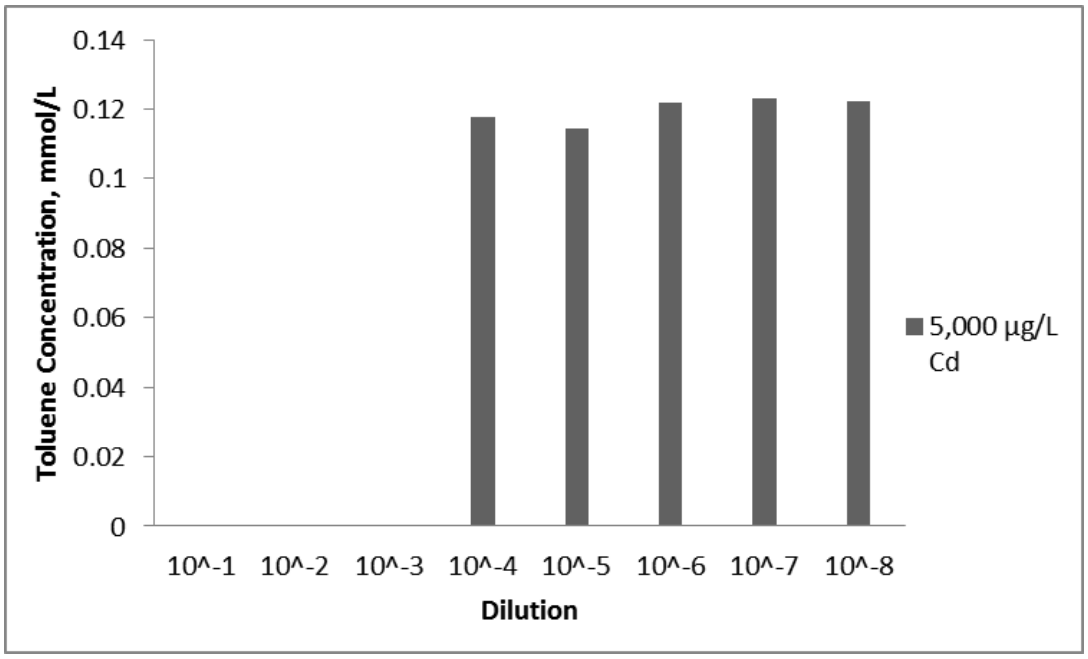

Figure 88: The figure shows the toluene dilution degradation bar graph for the 5,000 µg/L Cd microcosms. The results from the dilution degradation of toluene show that degradation was able to occur at a dilution of 10^{-3} of the original microcosm. The degradation at 10^{-3} of the original microcosm was a complete degradation. The degradation was observed at day 11.

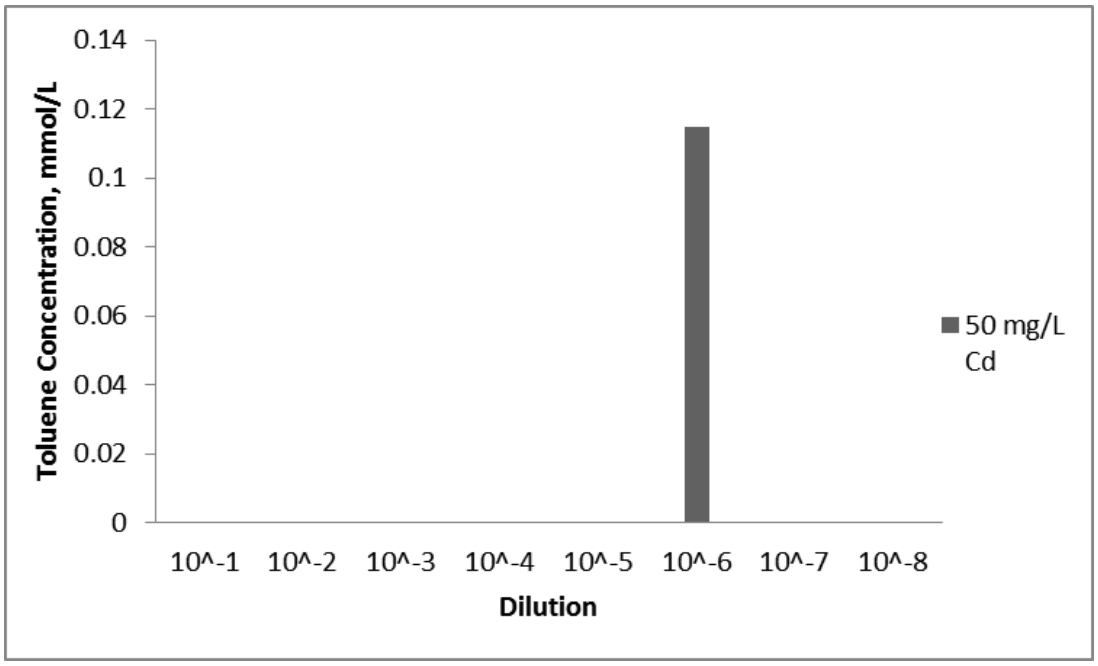

Figure 89: The figure shows the toluene dilution degradation bar graph for the 50 mg/L Cd microcosms. The results from the dilution degradation of toluene show that degradation was able to occur at a dilution of 10^{-5} of the original microcosm. The degradation at 10^{-5} of the original microcosm was a complete degradation. The degradation was observed at day 11.

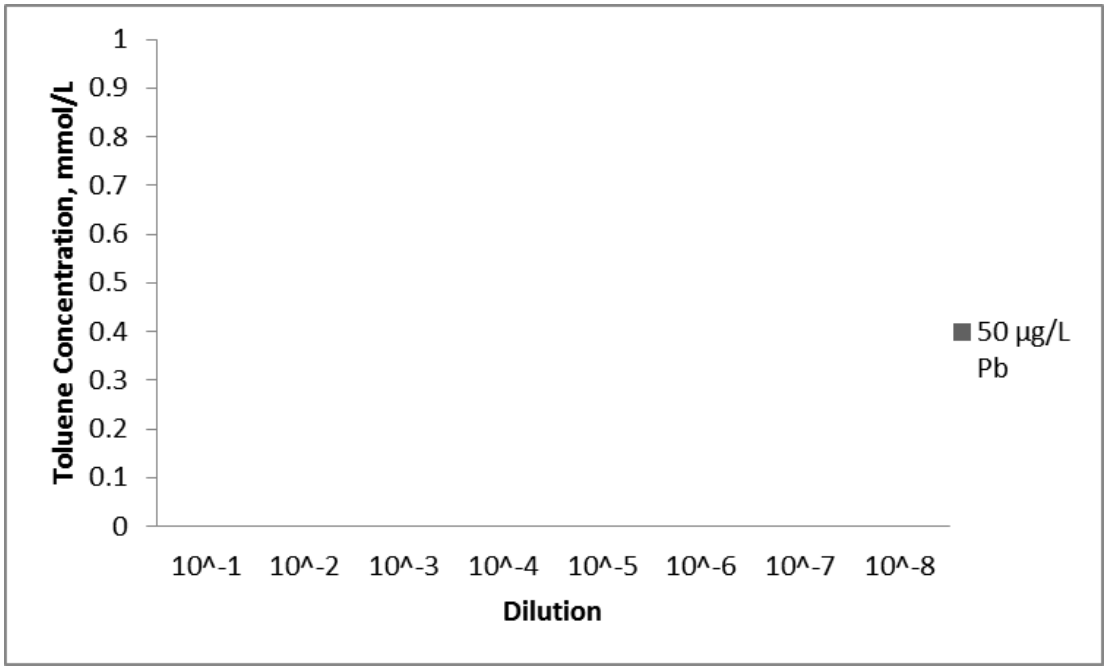

Figure 90: The figure shows the toluene dilution degradation bar graph for the 50 µg/L Pb microcosms. The results from the dilution degradation of toluene show that degradation was able to occur at a dilution of 10^{-8} of the original microcosm. The degradation at 10^{-8} of the original microcosm was a complete degradation. The higher the concentration of lead, the more difficult it was for the bacterial population to degrade toluene. This is shown by the degradation of toluene occurring at lower dilutions as concentration of lead increases. The lack of degradation is the result of lower microbial population and diversity due to a mixture of dilution and heavy metal toxicity. The degradation was observed at day 11.

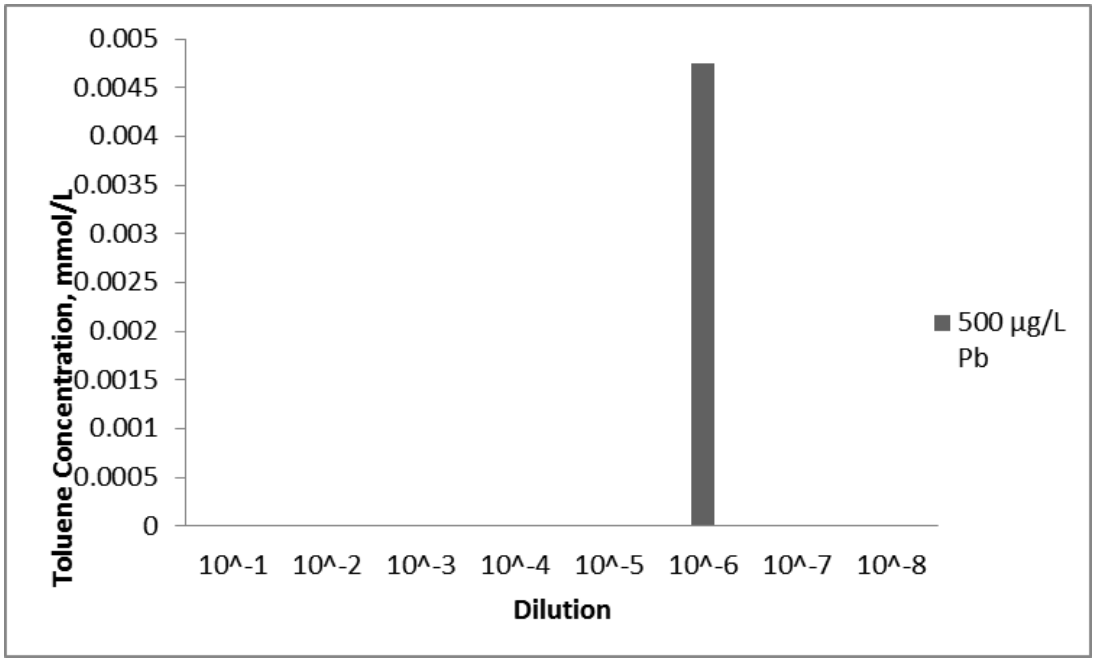

Figure 91: The figure shows the toluene dilution degradation bar graph for the 500 µg/L Pb microcosms. The results from the dilution degradation of toluene show that degradation was able to occur at a dilution of 10^{-5} of the original microcosm. The degradation at 10^{-5} of the original microcosm was a complete degradation. The higher the concentration of lead, the more difficult it was for the bacterial population to degrade toluene. This is shown by the degradation of toluene occurring at lower dilutions as concentration of lead increases. The lack of degradation is the result of lower microbial population and diversity due to a mixture of dilution and heavy metal toxicity. The degradation was observed at day 11.

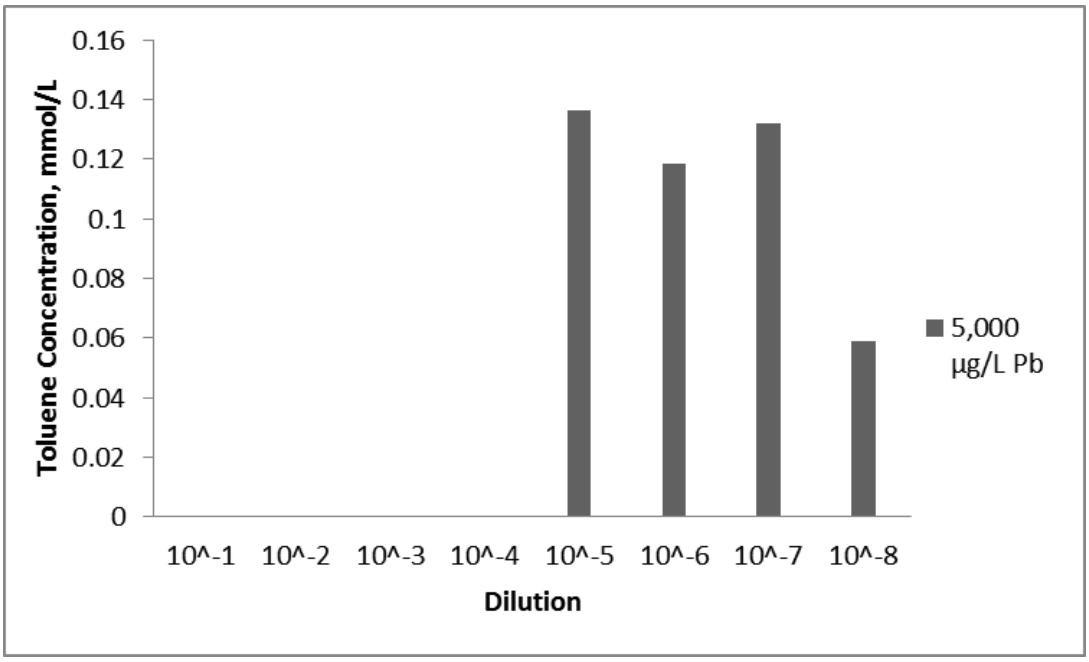

Figure 92: The figure shows the toluene dilution degradation bar graph for the 5,000 µg/L Pb microcosms. The results from the dilution degradation of toluene show that degradation was able to occur at a dilution of 10^{-4} of the original microcosm. The degradation at 10^{-4} of the original microcosm was a complete degradation. The higher the concentration of lead, the more difficult it was for the bacterial population to degrade toluene. This is shown by the degradation of toluene occurring at lower dilutions as concentration of lead increases. The lack of degradation is the result of lower microbial population and diversity due to a mixture of dilution and heavy metal toxicity. The degradation was observed at day 11.

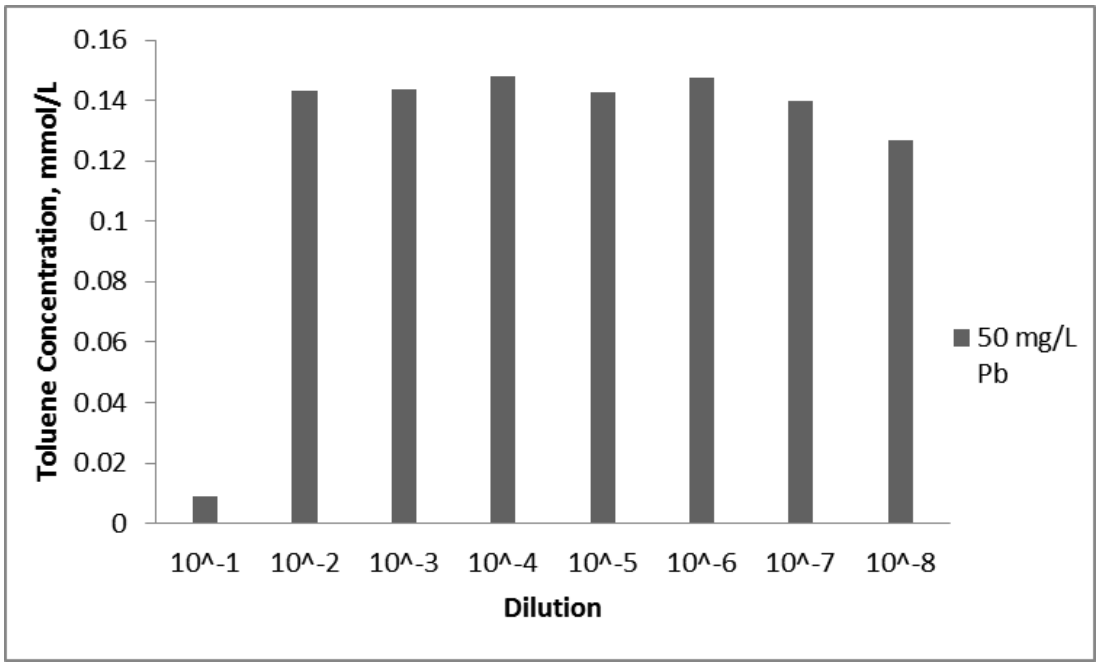

Figure 93: The figure shows the toluene dilution degradation bar graph for the 50 mg/L Pb microcosms. The results from the dilution degradation of toluene show that degradation was able to occur at a dilution of 10^{-2} of the original microcosm. The degradation at 10^{-1} of the original microcosm was a complete degradation. The higher the concentration of lead, the more difficult it was for the bacterial population to degrade toluene. This is shown by the degradation of toluene occurring at lower dilutions as concentration of lead increases. The lack of degradation is the result of lower microbial population and diversity due to a mixture of dilution and heavy metal toxicity. The degradation was observed at day 11.

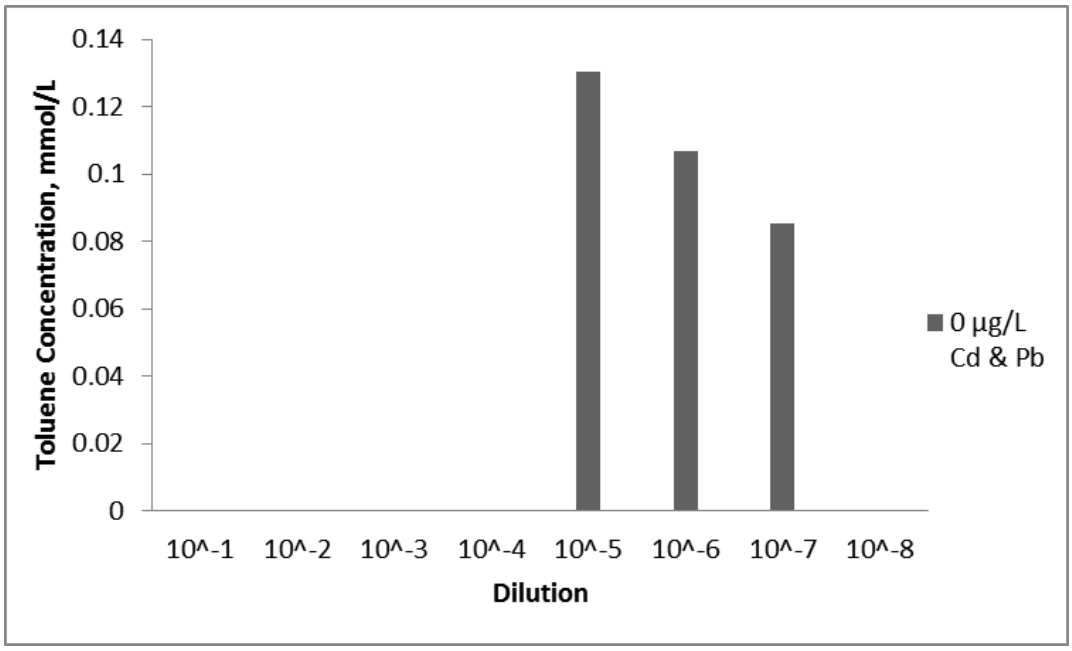

Figure 94: The figure shows the toluene dilution degradation bar graph for the 0 µg/L Cd and Pb microcosms. The results from the dilution degradation of toluene show that degradation was able to occur at a dilution of 10^{-4} of the original microcosm. The degradation at 10^{-4} of the original microcosm was a complete degradation. The degradation was observed at day 11.

CHAPTER V

CONCLUSION

Sites co-contaminated with benzene or toluene and heavy metals are difficult to remediate. Contacts with these pollutants are a serious health concern and their presence in the environment can lead to less diverse and stunted populations of organisms. These contaminants are very mobile and can travel through a wide variety of mediums. Finding microbes that are resistant to heavy metal toxicity and can degrade benzene or toluene is essential to remediation efforts of co-contaminated sites. Both aerobic and anaerobic microbes have shown the ability to degrade benzene or toluene, with aerobic degradation being the more efficient degradation pathway. The genes shown to allow microbes to degrade benzene and toluene are the tmoA-like gene and the xylM gene.

Microcosms were created for both aerobic and anaerobic microbes. Headspace measurements were taken on a GC-FID. Degradation was observed and re-spikes were performed in order to build the microbial population. Dilutions were created for toluene to isolate specific microbes able to degrade toluene in the presence of heavy metals. Microcosms were re-spiked and stored in an incubator for future use.

This research has found that there are naturally occurring bacteria in the soil with the ability to degrade benzene or toluene in the presence of heavy metals. Microcosms were created

and sterile controls confirmed that degradation was biological. The active microcosm degraded benzene and toluene while the sterile controls did not, proving that the degradation of benzene and toluene was due to biological activity. There was little to no effect to the degradation of benzene or toluene due to the increased concentration of heavy metals. After re-spikes the microbial population in the toluene microcosms had an increased degradation rate due to a stronger microbial population. The average degradation time for toluene was three days, while for benzene it was ten days.

Toluene degrading microcosms were then diluted by factors of ten to a dilution factor of 10^{-8} of the original microcosm which then inoculated new microcosms with toluene or lead and the heavy metal. Microbes in the presence of Cd degrade toluene similarly, while the microbes in the presence of Pb degraded toluene less as the concentration of Pb increased. This shows that the heavy metals do have a negative effect on microbial degradation if the population is smaller or less diverse. This research shows that there are microbes that are resistant to heavy metal concentrations that are able to use benzene or toluene as a carbon source. These microbes in a diverse and populated environment are less affected by heavy metal toxicity. In the presence of lead, the microbes degrade toluene at a slower rated if the population is smaller and less diverse. The presence of cadmium has little to no effect on the degradation of benzene or toluene. This information is vital to the initial steps in co-contaminated site bio-remediation.

REFERENCES

1. Abd-Allah, A. R., Al Bakheet, S. A., Asiri, Y. A., Attafi, I. M., Korashy, H. M., Maayah, Z. H., (2013). "Effect of long-term human exposure to environmental heavy metals on the expression of detoxification and DNA repair genes" *Environmental Pollution,* 181, 226-232.

2. Agency for Toxic Substances and Disease Registry, (2007) "Public Health Statement Lead CAS#: 7439-92-1."

3. Agency for Toxic Substances and Disease Registry, (2008) "Public Health Statement Cadmium CAS # 7440-43-9."

4. Alfreider, A., Vogt, C., (2007). "Bacterial Diversity and Aerobic Biodegradation Potential in a BTEX-Contaminated Aquifer." *Water Air Soil Pollution,* 183, 415–426.

5. Alisi, C., Chiavarini, S., Cremisini, C., Marconi, P., Pinto, V., Sciullo, A., Sprocati, A. R., Tasso, F., Ubaldi, C., (2012)."Effectiveness of a microbial formula, as a bioaugmentation agent, tailored for bioremediation of diesel oil and heavy metal co-contaminated soil." *Process Biochemistry*, 47(11), 1649-1655.

6. Alvarez , P. J. J., Deng, Y., Ma, J., Yuan, T., Zhou, J., (2015). "Succession of microbial functional communities in response to a pilotscale ethanol-blended fuel release throughout the plume life cycle." *Environmental Pollution*, 198, 154-160.

7. An, S., Cui, C., Li. H., Lin, K., Xiong, B., Zhang, M., Zhang, W., (2012). "Ecotoxicological effects of decabromodiphenyl ether and cadmium contamination on soil microbes and enzymes." *Ecotoxicology and Environmental Safety*, 82, 71–79.

8. Arjoon, A., Olaniran A. O., Pillay, B. (2015). "Kinetics of heavy metal inhibition of 1,2-dichloroethanebiodegradation in co-contaminated water." *Journal of Basic Microbiology*,55(3), 277-284.

9. Bae, S., Choi, K., Lee, W., (2014) "Degradation of off-gas toluene in continuous pyrite Fenton system." *Journal of Hazardous Materials*, 280(15), 31–37.

10. Barker, J., Molson, J., Raeisi, E., Vaezihir, A., Zare, M., (2012). "Field-Scale Modeling of Benzene, Toluene, Ethylbenzene, and Xylenes (BTEX) Released from Multiple Source Zones." *Bioremediation Journal*, 16(3), 156–176.

11. Barua, S., Barry, K., Deng, Y., Fields M. W., Gentry, T. J., Green-Tringe, S., Hazen, T. C., He, Z., Hemme, C. L., Rubin, E. M., Tiedje, J. M., Watson, D. B., Wu, L., Zhou, J., (2010). "Metagenomic Insights into Evolution of a Heavy Metal-Contaminated Groundwater 2 Microbial Community." *The ISME Journal*, 4, 660–672.

12. Begonia, M. F. T., Sobolev, D., (2008). "Effects of Heavy Metal Contamination upon Soil Microbes: Lead-induced Changes in General and Denitrifying Microbial Communities as Evidenced by Molecular Markers." *International Journal of Environmental Research and Public Health*, 5(5), 450-456.

13. Berry, C., Brigmon, R. L., Płaza, G. A., Wypych, J., (2006). "Utilization of Monocyclic Aromatic Hydrocarbons Individually and in Mixture by Bacteria Isolated from Petroleum-Contaminated Soil." *U.S. Department of Energy*.

14. Boberg, E., Lessner, L., Carpenter, D. O., (2011), "The role of residence near hazardous waste sites containing benzene in the development of hematologic cancers in upstate New York." *International Journal of Occupational Medicine and Environmental Health*, 24(4), 327-338.

15. Bolden, A. L., Colborn, T., Kwiatkowski, C. F., (2015). "New Look at BTEX: Are Ambient Levels a Problem?" *Environmental Science & Technology*, 49(9), 5261-5276.

16. Bulsara, M., Denison, L., Edwards, J. W., Eiseri, C., Farrar, D., Galbally, I., Gillett, R. W., Glass, D., Hinwood, A. L., Horton, Lawson, S., A., Powell, J., Murray, F., Rodriguez, C., Runnion, T., Sheppeard, V., Weeks, I., Whitworth, T., (2007). "Risk factors for increased BTEX exposure in four Australian cities." *Chemosphere*, 66, 533–541.

17. Burken, J. G., Tsao, D., Weishaar, J. A., (2009). "Phytoremediation Of Btex Hydrocarbons: Potential Impacts Of Diurnal Groundwater Fluctuation On Microbial Degradation." *International Journal of Phytoremediation*, 11, 509–523.

18. Chen, B. C., Chen, T. C., Guo, H. Y., Hseu, Z.Y., Lai, H. Y. (2010), "Health Risk-Based Assessment and Management of Heavy Metals-Contaminated Soil Sites in Taiwan." *International Journal of Environmental Research and Public Health*, 7(10), 3595-614.

19. Chen, J., Gu, Q., Liang, C., Li, F., Sang, Y., (2008). "Heavy metal-contaminated groundwater treatment by a novel nanofiber." *Desalination*, 223(1–3), 349–360.

20. Chen, X., Hu, S., Tang, J., Yang, R., (2007). "Effects of coexisting plant species on soil microbes and soil enzymes in metal lead contaminated soils." *Applied Soil Ecology*, 37, 240–246.

21. Conley, N. L., Luttrell, W. E., (2011). “Benzene.” *Journal of Chemical Health and Safety*, 18(4), 32–33.

22. Dang, Z.,Yi, X. Y., Zhang H., Zheng, L. C., (2009). “Remediation of soil co-contaminated with pyrene and cadmium by growing maize (Zea mays L.).” *International Journal of Environment Science and Technology*, 6(2), 249-258.

23. Daugulis, A. J., McLellan, P. J., Nielsen, D. R., (2006). “Direct estimation of the oxygen requirements of Achromobacter xylosoxidans for aerobic degradation of monoaromatic hydrocarbons (BTEX) in a bioscrubber.” *Biotechnol Letters*, 28, 1293–1298.

24. Deng, D., Dou, J., Liu, X., Hu, Z., (2008). “Anaerobic BTEX biodegradation linked to nitrate and sulfate reduction.” *Journal of Hazardous Materials*, 151, 720–729.

25. Dou, J., Hu, Z., Liu, X., (2008). “Anaerobic BTEX degradation in soil bioaugmented with mixed consortia under nitrate reducing conditions.” *Journal of Environmental Sciences*, 20(5), 585-592.

26. Drake, D. K., Hu, S. C., Jim, R., Neuberger, J. S. (2009). “Potential health impacts of heavy-metal exposure at the Tar Creek Superfund site, Ottawa County, Oklahoma.” *Environmental Geochemistry and Health*, 31(1), 47-59.

27. Duarte, S., Ferreira, V., Guerold, F., Koricheva, J., Niyogi, D. K., (2016). “Effects of anthropogenic heavy metal contamination on litter decomposition in streams e A meta-analysis.” *Environmental Pollution*, 210, 261-270.

28. Duruibe, J. O, Ogwuegbu, M. O. C., Egwurugwu, J. N., (2007). “Heavy metal pollution and human biotoxic effects.” *International Journal of Physical Sciences*, 2(5), 112-118.

29. Escher, B. I., Fenner, K., Gunten, U. V., Hofstetter, T. B., Johnson, C. A., Schwarzenbach, R. P, Wehrli, B., (2006). "The Challenge of Micropollutants in Aquatic Systems." *Science*, 313(5790), 1072-1077.

30. Fowler, S. J., Gieg L., Gutierrez-Zamora, M., Manefield, M., (2014). "Identification of toluene degraders in a methanogenic enrichment culture." *FEMS Microbiology Ecology*, 89(3), 625–636.

31. Gidarakos, E., Simantiraki, F., (2015). "Comparative assessment of compost and zeolite utilisation for the simultaneous removal of BTEX, Cd and Zn from the aqueous phase: Batch and continuous flow study." *Journal of Environmental Management*, 159, 218-226.

32. Giller, K. E., McGrath, S. P., Witter E., (2009). "Heavy metals and soil microbes." *Soil Biology and Biochemistry*, 41(10), 2031–2037.

33. Guignet, D., (2014). "To Sell Or Not To Sell: The Impacts of Pollution on Home Transactions." *NCEE Working Paper Series*, 14-01.

34. Haquea, F., Visschera, A. D., Sena, A., (2012). "Biofiltration for BTEX Removal Biofiltration for BTEX Removal." *Critical Reviews in Environmental Science and Technology*, 42(24), 2648-2692.

35. Hendrickx, B., Junca, H., Vosahlova, J., Lindner, A., Rüegg, I., Bucheel-Witschel, M., Faber, F., Egli, T., Mau, M., Schlömann, M., Brennerova, M., Brenner, V., Pieper, D. H., Top, E. M., Dejonghe, W., Bastiaens, L., Springael, D., (2006). "Alternative primer sets for PCR detection of genotypes involved in bacterial aerobic BTEX degradation: Distribution of the genes in BTEX degrading isolates and in subsurface soils of a BTEX contaminated industrial site." Journal of Microbiological Methods, 64(2), 250-265.

36. Hong, H. B., Nam, I. H., Kim, Y. M., Change, Y. S., Schmidt, S. (2007). "Effect of heavy metals on the biodegradation of dibenzofuran in liquid medium." *Journal of Hazardous Materials*, 140(1-2), 145-148.

37. Junjib, C., Peixuana, D. Posmentier, E. S., Yongminga, H., (2006). "Multivariate analysis of heavy metal contamination in urban dusts of Xi'an, Central China." *Science of the Total Environment*, 355, 176–186.

38. Kang, H., Kim, I., Lee, M., Lee, S., Paik, I. S., (2007). "Remediation of heavy metal contaminated groundwater originated from abandoned mine using lime and calcium carbonate." *Journal of Hazardous Materials*, 144(1–2), 208–214.

39. Kasi, M., Khan, E., McEvoy, J., Padmanabhan, G., Wadhawan, T., (2013). "Effect of carbon source during enrichment on BTEX degradation by anaerobic mixed bacterial cultures." *Biodegradation*, 24, 279–293.

40. Klimiuk, E., Kulikowska D., (2008). "The effect of landfill age on municipal leachate composition." *Bioresource Technology*, 99, 5981–5985.

41. Lin, C. W., Wu, C. H., Yeha, C. H., (2010), "A permeable reactive barrier for the bioremediation of BTEX-contaminated groundwater: Microbial community distribution and removal efficiencies." *Journal of Hazardous Materials*, 178(1–3), 74–80.

42. Madhaiyan, M., Poonguzhali, S., Sa, T., (2007). "Metal tolerating methylotrophic bacteria reduces nickel and cadmium toxicity and promotes plant growth of tomato (Lycopersicon esculentum L.)." *Chemosphere*, 69, 220–228.

43. Miller, B., (2016). "Regulatory Impact Analysis of the Final Oil and Natural Gas Sector: Emission Standards for New, Reconstructed, and Modified Sources." *United States Environmental Protection Agency*.

44. Mitra, S., Roy, P., (2011).”BTEX: A Serious Ground-water Contaminant.” *Research Journal of Environmental Sciences,* 5(5), 394-398.

45. Oliveira, A., Pampulha, M. E., (2006). “Effects of Long-Term Heavy Metal Contamination on Soil Microbial Characteristics.” *Journal of Bioscience and Bioengineering*, 102(3), 157–161.

46. Stams., A. J. M., Van Eekert, M. H. A., Weelink, S. A. B., (2010). 385 “Degradation of BTEX by anaerobic bacteria: physiology and application.” *Reviews in Environmental Science and Bio/Technology*, 9(4), 359.

47. Stasik, S., Wendt-Potthoff, K., Wick, L. Y., (2015). “Anaerobic BTEX degradation in oil sands tailings ponds: Impact of labile organic carbon and sulfate-reducing bacteria.” *Chemosphere*, 138, 133–139.

APPENDICES

Appendix A

Rough Draft of Manuscript for Peer Review, pending results of microbial analysis.

Introduction

BTEX compounds are volatile organic compounds, (retrieved during fossil fuel extraction), that are used globally as solvents in many manufacturing and refining processes [19], (37), and [22]. BTEX compounds are some of the most common and hazardous industrial VOC emissions [18], [20], and [22]. These compounds cause public health and ecological issues due to their toxicity and ability to bio-accumulate in the food chain. Benzene is one of the most widely produced chemicals in the United States and is used in the production of other chemicals, rubber, pesticides, dyes, detergents, and it is used as a fuel additive [1], [7], [15], [19], [22], and [23]. BTEX compounds are water soluble and can find their way into water systems [22]. Benzene can reach the soil and groundwater near industrial sites that use or create the chemical [21 and 23]. Accidental spills and storage container leaks can cause serious soil and ground water contamination due to benzene being highly mobile in the soil [1, 5, 16, 20, 22, and 23].

BTEX exposure can be linked to nervous system damage and heavy metals are known to cause human organ failure and nervous system damage. The majority of contaminated sites with BTEX and heavy metals are located on industrial areas and the populations that live near them are nowadays typically small. Local rural populations are still affected by contaminated sites today. Communities living near superfund sites have experienced higher levels of contaminants in drinking water and soil concentration. Benzene can enter the body though inhalation, ingestion, and dermal contact [15]. BTEX compounds cause nervous system damage, endocrine system damage, and can also cause birth defects when contact with the contaminant occurs [19]. Benzene is a known human carcinogen and can cause brain, heart, lung, and liver damage [15],

[22], and [23]. A study in 2011 found that communities living near benzene contaminated hazardous waste sites were found to have an increased risk of hematologic cancers. The study also correlated the demographic of the individuals afflicted by the hematologic cancers. The results showed an increased likelihood of women, African Americans, and people in a higher socioeconomic status being affected by benzene hazardous waste sites [1]. BTEX compounds can spread to the groundwater, affecting irrigation and drinking water if not properly controlled [23] and [24].

Heavy metals are typical contaminants found at hazardous waste sites. The heavy metals cannot be degraded and must be remove by another remediation method, such as phytoremediation. Lead and cadmium are some of the most common heavy metal contaminates at hazardous sites [3] and [6]. Cadmium is the second most common metal found at superfund sites and is one of the "ten high-priority pollutants" [3]. "Lead has been found in at least 1,272 of the 1,684 current or former National Priorities List sites" [13].

Both lead and cadmium can disrupt the metabolic activity of microbes at low concentrations. Lead and cadmium are found in the environment typically as a result of mining waste, industrial wastewater discharges, and fly ash [2], [4], [6], [9], [13], and [14]. The waste disposal sites of these industries can seep into the groundwater causing contamination of both surface and groundwater [8] and [9]. The amount of heavy metals released into the environment increases due to industrial activities and technological development [7].Lead and cadmium can travel through the soil and infiltrate groundwater sources [2] and [4]. "Most heavy metals are adsorbed on soil particles, and some heavy metals such as arsenic and chromium can be oxidized to anionic forms that freely move in the soil environment" [6]. This mobility is influenced by pH and organic content; a low pH and a low organic content increase the mobility of these heavy metals [14]. Public water supply wells near mine discharges have been shown to be contaminated by heavy metals [4].

Discovery of new bacteria and/or new biological treatment methods for sites contaminated with both organics and heavy metals is critical to finally cleaning up many of these sites. Many micro-organisms, such as the symbiotic bacteria Rhizobium [11], are sensitive to higher heavy metal concentrations. This causes a sever reduction in microbial activity [7] and [12]. Metal/organic complexion can also reduce the bio-availability of the organics, making the organics less available to the microbes for degradation [7].

BTEX compounds can also become inhibitory compounds if the concentration becomes greater than 80 mg/L [20]. These effects pose a problem for remediation projects that contain both organic compound and heavy metals. The diversity of the environment, difficult to degrade carbon and energy source, and higher heavy metal concentrations inhibit the growth and degradation rate of the microbes in the co-contaminated sites [6] and [7]. The level of inhibition and the degradation rate and other biological processes are controlled by multiple factors, including the type of metals, the type of media, and the microbial species [6] and [7].

There are many different electron acceptors microbes can use during metabolism of organic compounds; because of this it has been shown that BTEX compounds can be remediated in anaerobic and aerobic conditions [17] and [23]. Aerobic and anaerobic remediation applications must be investigated because benzene and toluene can contaminated surface water and then leech into the ground water, an anoxic environment [5]. Both conditions must be studied because major differences exist between BTEX degradation under aerobic and anaerobic conditions [22].

The remediation of co-contaminated sites is difficult due to the toxic effect the heavy metals have on the microbial community. Bioremediation is the most widely used remediation technique and is an effective way to remove harmful organics from contaminated sites due to the

ability to restore the soil and preserves its quality [6], [12], and [20]. Bioremediation is an reliable, simple, and cost effective when compare to other forms of remediation [18] and [20].

There have been many different types of bacteria that have shown the ability to degrade BTEX compounds. The micro-organisms use the organic compounds for their carbon and energy source, removing the contaminant from the system [5] and [18]. Degradation can occur down two different pathways: either, "an activation of the aromatic ring by dioxygenation or monooxygenation reactions causing a catalysis of the dioxygenolytic cleavage of the aromatic ring, or by processing the side chains" [20]. "Bacteria that degrade BTEX in the absence of oxygen do not have the ability to employ degradation pathways with mono- or dioxygenases", they instead must use nitrate or sulfate as their electron acceptor [22] and [23]. "The initial oxidative attack of BTEX convert[s] the compound into a catechol structure and the cleavage of the catechol structure are key steps in aerobic BTEX degradation" [5]. In aerobic conditions, oxygen can be the terminal electron acceptor and the initial enzymatic activation of aromatic compounds [22].

In-situ bioremediation has been used for the anaerobic stimulation of BTEX degradation in contaminated aquifers [22]. In-situ bioremediation is the addition of electron acceptors and nutrients to stimulate degradation [21]. Toluene has been shown to be an easier compound to degrade in anaerobic conditions using in-situ bioremediation [21] and [22]. Benzene, however, is a very difficult compound to degrade under anaerobic conditions due to its stability [22].

There are numerous methods for identifying the micro-organisms that can be used for the remediation of co-contaminated sites. Some micro-organisms have already shown the ability to degrade BTEX compounds. These bacteria contain specific genes that allow the degradation of BTEX compounds. The genes shown to aid in the degradation of BTEX have been the tmoA-like

gene and the xylM gene [5]. Gene sequences are typically identified using the PCR gel electrophoresis method [12] and [20].

The bacteria shown to degrade BTEX belong to the phyla Actinobacteria and Proteobacteria, and the genus Pseudomonas, which can use benzene as its only carbon source in aerobic conditions [5], [18], and [22]. Studies have shown that the ability to degrade benzene was largely congruent with the distribution of the tmoA-like genes [5]. However, only a few anaerobic species have been observed to degrade benzene, including Dechloromonas and Azoarcus strains [22].

Using RT-qPCR and RNA stable isotope probing researchers have found many bacteria associated with toluene degradation including: in aerobic conditions Desulfosporosinus sp, species belonging to the Azoarcus or Thauera genus, in anaerobic conditions Syntrophaceae, Desulfovibrionales and Chloroflexi [17] and [22]. The anaerobic pathway to toluene catabolism is the addition of toluene to the double bond of fumarate. The compound is eventually oxidized via reductive ring cleavage to carbon dioxide [22]. Methanogenic toluene degrading bacteria, such as Firmicutes, Chloroflexi, Spirochaetes, and Deltaproteobacteria, have been shown to mineralize toluene to methane [17].

It has been reported that the addition of some metals at low levels increase biodegradation and microbial activity because they are required for certain physiological processes [3], [6], and [7]. The discovery of a micro-organism that is resistant to heavy metal toxicity can be used to bio-remediate BTEX contaminated soils and water sources. There are types of bacteria that exhibit resistance to heavy metal toxicity [11].

Many sites have been shown to be contaminated by both toxic organics and heavy metals. Around 40% of hazardous waste sites are co-contaminated with both heavy metals and organic

compounds [3] and [7]. This co-mingling of organics and heavy metals makes treatment options for these sites difficult for the micro-organisms degrading the organics [7]. The impact the metals have on the biodegradation of organic pollutants is not only due to the metal concentrations and type, but also the type organic pollutants [3] and [6]. Different types of heavy metals at various concentrations affect the soil micro-organisms differently [7] and [11]. Co-contaminated sites are an important for public health issues and remediation efforts. Many bacteria have the ability to degrade BTEX compounds but are also sensitive to heavy metals. Discovery of micro-organisms with the ability to degrade BTEX while under the influence of heavy metals is vital to the remediation of co-contaminated hazardous waste sites.

Materials and Methods

Microcosms. Soil samples were collected from a parking lot runoff in Stillwater, Oklahoma. The samples were collected from a parking lot runoff so that the microbes in the soil would be adjusted to BTEX from the oil in the storm water running off the parking lot. Around 1 L of soil was collected for both aerobic and anaerobic tests. The aerobic soil was taking from the top soil and stored in a Norlake Scientific incubator at 30 ºC, while the anaerobic soil was taken from a depth of 0.5 ft. in water saturated soil. It was assumed that the majority of air voids would be full of water, unable to contain oxygen. The anaerobic soil was then sealed with tin foil, to preserve moisture content and transported to an anaerobic glove box.

The mineral media was created in 1 L and 2 L flasks, then autoclaved to remove any pre-existing bacteria. The anaerobic media's pH was then adjusted, using a 1 M solution of the base sodium hydroxide (NaOH) and 1 M solution of the acid phosphoric acid (H_2PO_3). Minor elements were added in the Coy Lab anaerobic glove box, the aerobic media's pH was adjusted before autoclaving in a Primus Sterilizer Co. Inc. autoclave.

The mineral media was then divided into 160 ml silanized serum bottles at 100 mL per bottle. The salinization processed was perform by placing 3 mL of 10% dichlorodimethylsilane ($Si(CH_3)_2Cl_2$) with toluene as a solvent for one hour in a fume hood. The bottles were then rinsed in hexane, methanol, and water. The process was conducted in order to prevent the compounds from adsorption to the glass by forming a covalent bond between the glass and $Si(CH_3)_2Cl_2$. There were 92 bottles used for the initial aerobic tests (54 standard microcosms and 38 sterile controls) and 52 bottles for the anaerobic tests (48 standard microcosm and 4 sterile controls).

Heavy metal stock was created using cadmium chloride ($CdCl_2$) and lead acetate ($Pb(CH_3COO)_2$). The heavy metal solutions were made at a concentration of 5,000 ppm (5,000 mg/L) and then added to the microcosms at increasing concentrations of 50 µg/L, 500 µg/L, 5,000 µg/L, and 50 mg/L. Triplicates were made for each different heavy metal concentration and duplicates were made for each varied heavy metal concentration for the sterile controls. Then 2 g of soil was added to the microcosms. The anaerobic soil was stored in the anaerobic glove bag for one day, to insure a completely anaerobic medium, before being added to the microcosms. The 42 microcosms used for controls were then autoclave once a day for three straight days in order to insure complete sterilization of the microcosms.

Stock solutions of benzene and toluene were created by filling and sealing 160 mL serum bottle with deionized (DI) water from a Labconco Water Pro PS, then injecting 160 µL of benzene to create a 1 µL/mL stock solution of benzene and injecting 80 µL of toluene to create 0.5 µL/mL stock solution of toluene. The rubber stoppers used to seal the serum bottles were coated with a Teflon layer in order to prevent adsorption to the stopper. Concentrations of the stock solution were determined by the solubility of both benzene and toluene. The aerobic stock solutions were place in an incubator for three days until complete mixing, while the anaerobic solutions were left in the anaerobic glove box until the BTEX compounds had completely

dispersed throughout the water. After complete mixing of the BTEX stock solutions, 2 mL of benzene stock and 4 mL of toluene stock were added bringing both concentrations to 2 µL/L in the microcosm. Twelve bottles were also made for standard curves six for benzene and six for toluene. The standard curve bottles were made by adding 100 mL of DI water, autoclaving and then adding benzene/toluene stock to bring the concentration to 0.1 µL, 0.5 µL, 1 µL, 1.5 µL, 2 µL, and 4 µL of the organic compound. A complete list describing both sets of microcosms are found in Table 3 (aerobic) and Table 4 (anaerobic).

GC Method. The headspace measurements were injected manually. The FID combusts the organics using a hydrogen flame, the gas stream passes through a detector measuring the resulting ions that are specific to each compound. The amount of ions is proportional to the concentration of the organic in the headspace. BTEX compounds are VOCs and, according to Henry's Law, it is assumed there is a relationship between the concentration in the headspace and the concentration in the liquid media. When the detector read a large concentration of ions a peak appears.

There is a correlation between peak area and concentration of the compound. By creating a standard curve based on Peak Area vs. Known Concentration, the unknown concentrations of the microcosms can be found by dividing the area of the peak by slope of the standard curve line. If the 4 µL standard deviated more than 20% of the original value, a new standard was created in order to better represent the microcosms.

The syringe used was a 10 µL gas tight glass syringe with a rounded tip needle. The gas tight syringe had a valve that could be closed in order to prevent air from escaping. The rounded tip needle was used in order to prevent tearing of the rubber stopper on the microcosms and the GC septa. In order to prevent cross contamination between bottles, after every measurement, the air tight syringe was rinsed with hexane and then placed in a Hamilton Company syringe cleaner

to sterilize the needle with heat and vacuum out any remaining hexane. There was residual hexane in the syringe, test were ran in order to pinpoint the hexane readings on the GC. The difference in time between injection of benzene, toluene, and hexane were found. This allowed for proper interpretations of peak sequences.

Enrichment. Degradation was observed and analyzed. Once there was complete degradation of BTEX in the microcosms, a 1 mL sample of mixed media was taken and stored in a Frigidaire Commercial freezer at -3 ºC for later research. Then the microcosms were re-spiked with benzene and toluene in order to build a strong microbial population. This cycle was repeated seven times. After the seventh re-spike, the toluene microcosms with the greatest rate of degradation were diluted into eight new microcosms, each microcosm was diluted by factors of 10 with each new microcosm. The diluted microcosms were then re-spiked to determine the most dilute microcosm that still degraded toluene. This would contain the media with the least diverse microbial population, making it easier to identify the specific microbe responsible for the biodegradation of toluene while still being resistant to the heavy metal toxicity. Once the most dilute microcosm that was still able to degrade toluene was identified, those microcosms were re-spiked.

Microbial Analysis. Enriched cultures of microbes were analyzed with Illumina sequencing technology… (*future work*).

Results

Results from the GC-FID found that, across the concentrations of both lead and cadmium, BTEX compounds can be bio-degraded naturally by indigenous aerobic bacteria. All concentrations of heavy metals, ranging from 50 µg/L to 50 mg/L, had little to no effect of the aerobic biodegradation.

This shows that there are bacteria commonly found in soils that are resistant to heavy metal toxicity. Data showed that the sterile controls containing soil did not degrade over a ten day period, the time period that the longest microcosm degraded. This proves that the degradation of BTEX in the microcosms was caused by biological activity.

The toluene microcosms dilutions still degraded toluene. The microcosms for Cd, had degradation even at the most diluted microcosms. The Cd microcosm seem to have had a higher toluene degrading population at higher concentrations of Cd. The lead microcosms also showed degradation at extremely dilute concentrations. However, unlike Cd, the biodegrading microbial population seemed to be inhibited at higher Pb concentrations.

Appendix B

Equipment

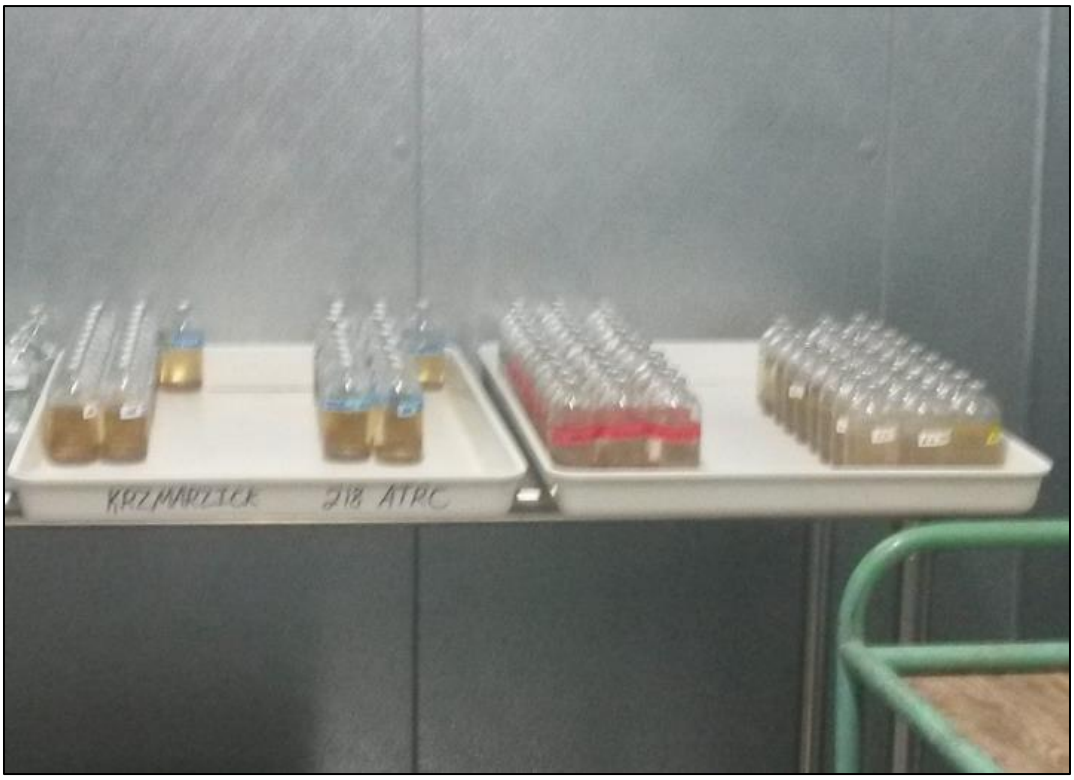

Figure 95: Microcosms were stored in a Norlake Scientific incubator. The incubator was used to maintain an optimal temperature and humidity for microbial growth. The incubators temperature was set to 30 ºC.

Figure 96: The Coy Labs glove box is a sealed container used to create a separate atmospheric environment for specific microbial growth. The microcosms are place in a separate vacuum box, in order to remove the oxygen containing air and replace it with an anaerobic nitrogen air mixture. This glove box is used to grow anaerobic microbial cultures.

Figure 97: The Primus Sterilizer Co. Inc. autoclave is a chamber that raises the temperature and pressure in order to sterilize its contents. The autoclave runs cycles reaching temperatures of 250 ºF and 18 psig. Microcosms were placed in an autoclave cycle once a day, three days in a row to ensure the removal of microbial activity. These controls allow conclusions to be made about how the benzene and toluene are being removed from the microcosm system.

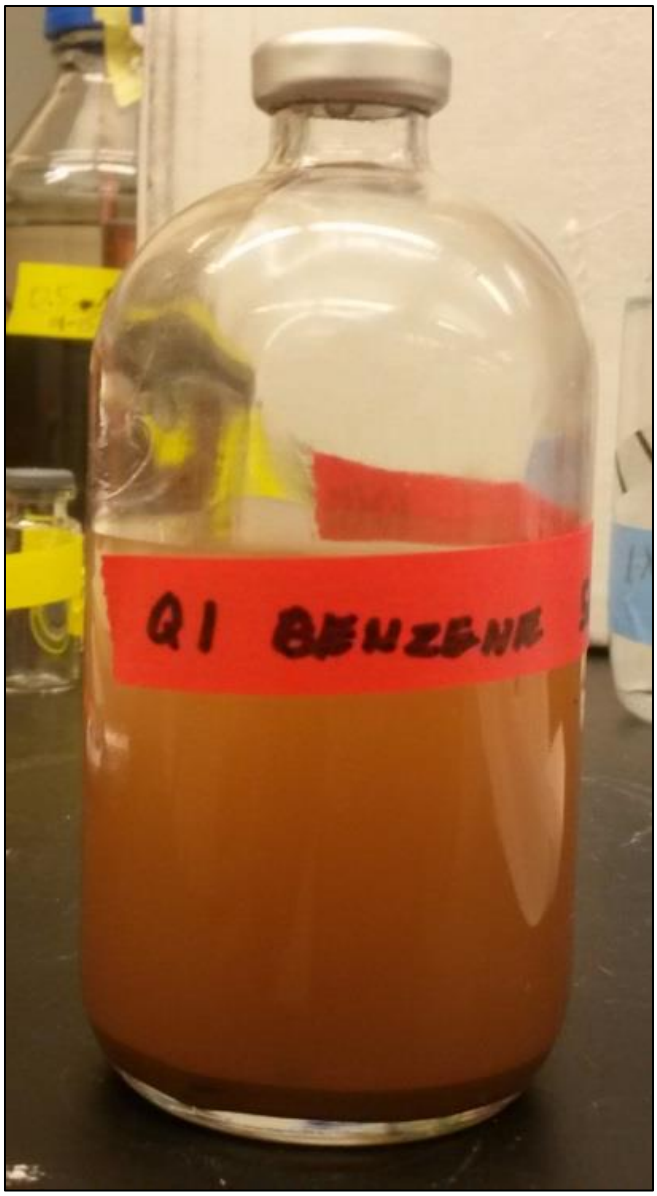

Figure 98: The 160 mL bottles are used to contain, store, and transport the microcosms. The bottles were capped in order to prevent the volatile benzene or toluene from escaping the media. This creates the headspace require for the GC-FID process and measurements. The bottles were salinized and capped with Teflon lined stoppers in order to prevent benzene and toluene adsorption. Microcosms contained a soil sample, 0.2244 mM of benzene and 0.1888 mM of toluene in the respective microcosm sets, varying concentrations of heavy metals, and mineral media.

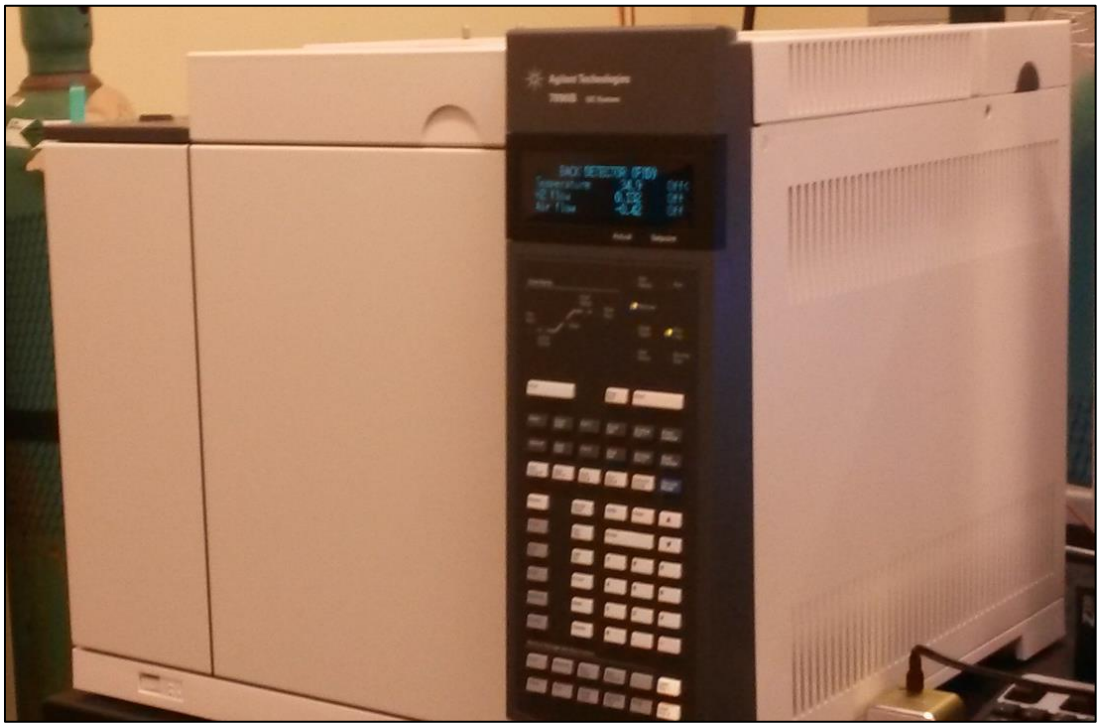

Figure 99: The Agilent Technologies gas chromatograph flame ionization detector (GC-FID) is used to measure an organic compound's concentration in a gas stream. The compound travels through the GC, with the inert gas helium, and is measured by a detector. A headspace sample is taken from the microcosm bottles and injected in the machine. The detector measures the concentration of the compound and plots the data. Benzene and toluene are very volatile compounds. There is a relationship between the concentrations of benzene and toluene in the headspace and the concentrations in the microcosm's media.

VITA

Brice Allen Fiddler

Candidate for the Degree of

Master of Science

Thesis: BIOREMEDIATION OF SITES CO-CONTAMINATED WITH BENZENE OR TOLUENE AND HEAVY METALS

Major Field: Environmental Engineering

Biographical:

Education:

Completed the requirements for the Master of Science in your major at Oklahoma State University, Stillwater, Oklahoma in July, 2016.

Completed the requirements for the Bachelor of Science in your major at Oklahoma State University, Stillwater, Oklahoma in May, 2014.
Experience: Grand River Dam Authority, Langley, OK, July 2014 - Aug. 2014

Professional Engineering Consultants P.A., Tulsa. OK, May 2013 - Aug. 2013

Circuit Engineering District 8 Intern, Enid, OK, May 2012 - Aug. 2012

Professional Memberships: Chi Epsilon, Civil Engineering Honor Society, Feb. 2012 – present

American Society of Civil Engineers, Civil Engineering Professional Society, Aug. 2011 - present

HONORS

Bridge to the Doctorate Fellow, Aug. 2014 – present

Oklahoma Louis Stokes Alliance for Minority Participation in Science, Technology, Engineering, and Mathematics Program Research Scholar, Sept. 2011 - May 2014